INSTITUTO SUPERIOR TÉCNICO
Universidade Técnica de Lisboa

Modelling of Linear Coverage in UMTS applied to Tunnels and Bridges

Vikash Mukesh Laxmidas

Dissertation submitted for obtaining the degree of Master in Electrical and Computer Engineering

Jury

Supervisor: Prof. Luis M. Correia

Co-Supervisor: Mr. Sérgio Pires

President: Prof. António L. C. Topa

Members: Prof. Carlos C. Fernandes

September 2008

To my parents and brother

“The idea that cannot be converted into words is a bad idea, and the word that cannot be converted into action is a bad word”

(Chesterton)

Acknowledgements

First of all, I would like to thank Professor Luis Correia for giving me the opportunity to perform this thesis and for the constant knowledge and experience sharing. It was a pleasure to participate in all the meetings performed during the thesis, since in all of them I learned something useful to the development of the work as well as to my professional future. I am thankful to all the time he spent with explanations and orientations, for his availability, guidelines, advising and constant support, which were essential to this work.

To Celfinet, especially to Sérgio Pires, for all the suggestions, constructive critics, technical support and for the patience and availability shown to answer all my doubts. His experience and knowledge have been very helpful to improve this work. I also would like to thank Rúben Ferreira for his availability and time spent in the measurements performance and for all the information supplied.

To all GROW members, for the opinions and suggestions given during the presentations performed, as well as for all the support given during the development of this work. Being part of this group was very important, since I had the chance to learn and meet many people working in the mobile communications area.

A special thank to Professor António Topa, for all the availability and for the explanations given that allowed me to better understand some concepts.

I also would like to thank Mr. Pedro Fernandes, for his contribution to this work, namely for his availability and for the information supplied regarding some antennas characteristics.

I also want to thank my colleagues for their friendship, good company and contribution for this work. More specifically, I would like to thank Ricardo Preguiça, Filipe Leonardo and Sara Duarte for all of the above, as well as for the useful suggestions and different points of view that have been important to improve this thesis. A special thank to Armando Marques for all his contribution, namely regarding the important discussions and advising that allowed me to better understand several concepts, as well as for all the availability and patience shown.

I would like to thank all my friends for their support, patience and good company given. Their contribution has been important especially to lighten up the stress and to provide good leisure moments.

At last but not least, I would like to thank my family, especially my parents and brother, for all the support, understanding, patience and love which helped me in the development of this thesis. Their contribution was essential to perform this work.

Abstract

The main purpose of this thesis was to study and analyse the coverage, the capacity and the interference in linear environments, such as the tunnels and the bridges. For this purpose, a model that accounts for different environmental and system parameters was developed and implemented in a simulator. For validation purposes, the results obtained in both scenarios were compared with measurements performed in a real network in the Lisbon Underground and in the 25 de Abril Bridge. Results show that, in tunnels, no coverage or capacity problems are expected, even considering a high number of users or the most demanding services, since the powers obtained are below the maximums allowed and the carrier-to-interference ratios are clearly above 0 dB for both DL and UL. In bridges, for the parameters considered, there might be some capacity problems since the maximum number of users served simultaneously is in the order of 15. Furthermore, if some of the users are performing the most demanding services, more capacity problems are expected. The developed model has proven to be very useful for radio planning in UMTS, since, in general, a good agreement was obtained with the measurements performed.

Keywords

UMTS, Coverage, Interference, Tunnels, Bridges.

Resumo

O objectivo principal desta tese foi estudar e analisar a cobertura, capacidade e interferência em ambientes lineares, como os túneis e as pontes. Para isso, um modelo que tem em conta diferentes parâmetros relacionados com o ambiente e com o sistema foi desenvolvido e implementado num simulador. Com o propósito da sua validação, os resultados obtidos em ambos os cenários foram comparados com medidas efectuadas na rede real no Metropolitano de Lisboa e na Ponte 25 de Abril. Os resultados mostram que, em túneis, não são esperados problemas de cobertura nem de capacidade, já que as potências obtidas estão abaixo dos valores máximos permitidos e a razão portadora-interferência está claramente acima dos 0 dB tanto em DL como em UL. Nas pontes, para os parâmetros considerados, alguns problemas de capacidade poderão existir dado que o número máximo de utilizadores servidos simultaneamente é da ordem de 15. Além disso, se alguns dos utilizadores estiveram a utilizar os serviços mais exigentes, mais problemas de capacidade são esperados. O modelo desenvolvido provou ser bastante útil no planeamento de rádio em UMTS, já que, em geral, uma boa concordância foi obtida com as medidas realizadas.

Palavras-chave

UMTS, Cobertura, Interferência, Túneis, Pontes.

Table of Contents

List of Figures

List of Tables

List of Acronyms

3GPP	3rd Generation Partnership Project
BPSK	Binary Phase Shift Keying
BS	Base Station
CDF	Cumulative Distribution Function
CDMA	Code Division Multiple Access
CS	Circuit Switch
DL	Downlink
DS-CDMA	Direct-Sequence Code Division Multiple Access
EIRP	Equivalent Isotropic Radiated Power
ETSI	European Telecommunications Standard Institute
FDD	Frequency Division Duplex
GSM	Global System for Mobile Communications
HSDPA	High-Speed Downlink Packet Access
HSUPA	High-Speed Uplink Packet Access
IMT-2000	International Mobile Telephony 2000
L1	Layer 1 (Physical Layer)
LoS	Line-of-Sight
LTE	Long Term Evolution
MIMO	Multiple Input Multiple Output
MMS	Multimedia Message Service
MT	Mobile Terminal
NLoS	Non-Line-of-Sight
PS	Packet Switch
QAM	Quadrature Amplitude Modulation
QoS	Quality of Service
QPSK	Quaternary Phase Shift Keying
SF	Spreading factor
SIR	Signal-to-interference Ratio
SMS	Short Message Service
SNR	Signal to Noise Ratio
TDD	Time Division Duplex
UL	Uplink
UMTS	Universal Mobile Telecommunications System
UTRA	UMTS Terrestrial Radio Access

WCDMA	Wideband Code Division Multiple Access

List of Symbols

α	Orthogonality factor
α_{3dB}	Half power beam width of an array
α_j	DL orthogonality factor of user j
δ	Angle used to indicate the position of the interfering BS
ε_r	Permittivity
φ_1	Grasing angle of incidence
η	Load factor
η_{arr}	Efficiency of the array
η_{DL}	DL load factor
$\overline{\eta_{DL}}$	Average DL load factor value across the cell
η_{hel}	Efficiency of the helical antenna
η_{UL}	UL load factor
λ	Wavelength
ρ	Roughness of the walls
Δf	Signal bandwidth
ΔP	Margin used in the received power calculation
$\Gamma_{1,2}$	Reflection coefficient of the vertical/horizontal walls
$\Gamma_{v,h}$	Reflection coefficient for the vertical/horizontal polarisation
a	Path loss exponent
A	Parameter used in the UL inter-cell interference calculation
C	Carrier
C_t	Perimeter of the circular projection of the turn
d	Distance between the BS and the MT
d_a	Distance between consecutive antennas
D_{arr}	Directivity of the array
D_{hel}	Directivity of the helical antenna
$\bar{e}$	Relative mean error
E_b	Energy per user bit
$EIRP^{DL}$	Equivalent isotropic radiated power in DL

$EIRP^{UL}$	Equivalent isotropic radiated power in UL
f	Frequency
F	Load factor
G_{arr}	Gain of the array
G_{hel}	Gain of the helical antenna
G_P	Processing gain
G_{Pj}	Processing gain of user j
G_{SH}	Soft handover gain
$G_{t,r}$	Gain of the transmitting/receiving antenna
h	Tunnel height
h_{BS}	Height of the BS, in the plane earth model
h_{MT}	Height of the MT, in the plane earth model
i	Inter-cell to intra-cell interference ratio
i_j	Inter-cell to intra-cell interference ratio for user j
I	Total interference
$I_{Inter,i}^{DL}$	Inter-cell interference in DL
$I_{Inter,j}^{UL}$	Inter-cell interference in UL
$I_{Intra,i}^{DL}$	Intra-cell interference in DL
$I_{Intra,j}^{UL}$	Intra-cell interference in UL
k	Propagation constant
k_r	Parameter used in the Rice distribution
K	Parameter of the Rice distribution
$L_{ant\ t,r}$	Coupling loss of the transmitting/receiving antenna
L_c	Losses in the cable between transmitter and antenna
L_{curv}	Path loss the curve
L_{fe}	Path loss of the flat earth propagation
L_{fr}	Path loss in the far region
L_{fs}	Path loss of the free space propagation model
L_{nr}	Path loss in the near region
L_p	Path loss
L_{pind}	Losses due to indoor penetration
L_{ptotal}	Total path loss
L_u	Losses due to user

M_I	Interference margin
M_{FF}	Fast fading margin
M_{SF}	Slow fading margin
M_p	Parameter accounting for the margins
N	Total noise power
N_0	Noise spectral density
$N_{1,2}$	Number of reflections in the vertical/horizontal walls
N_{1c}	Number of reflections, per metre, in the vertical walls
N_a	Number of elements in the array
N_{BS}	Number of interfering BSs
$N_{j,g}$	Number of MTs using service g on the cell of BS j
$N_{q,g}$	Number of users using service g in interfering cell q
N_{rf}	Noise spectral density of MT receiver
N_s	Number of turns of the helical antenna
N_{serv}	Total number of services used
N_{users}	Number of users in the sector studied and in the interfering sectors
P	Power allocated by the BS
P_0	Initial power of the ray
$P_{1,2}$	Power allocated from BS_1/ BS_2
$P_{BS \to MT_i}$	Power transmitted by the BS to the MT in which interference is being calculated
$P_{BS_j \leftarrow MT}$	Power received in the BS j from a MT
$P_{BS_j \leftarrow MT_{n_u}}$	BS j received power from MT n_u being covered by an adjacent cell q
P_{FF}	Fast fading probability for the Rice distribution
P_r	Power available at the receiving antenna
P_{ref}	Power after a certain number of reflections
$P_{Rx}^{DL,UL}$	Power at the receiver, in DL/UL
$P_{Rx\min}$	Receiver sensitivity
P_t	Power fed to the transmitting antenna
P_{Tx}	Power at the transmitter
P_{TX}^{BS}	Total transmission power of Node B
P_{TX}^{BSj}	BS j total transmitted power, including antennas gains
$r_{j,n}$	Distance from MT n using service g to BS j

$r_{q,n}$	Distance from MT n using service g to BS q
R_b	Bit rate
R_{bj}	Bit rate of user j
R_c	Chip rate
R_{curv}	Radius of the curve
S	Spacing between turns
v_g	Activity factor of service g
v_j	Activity factor of user j
v_{n_u}	Activity factor of user n_u
w	Tunnel width
x_{curv}	Distance between the external wall of the tunnel and the ray launched along the tunnel width
$x_{t,r}$	Position of the transmitted/receiver antenna in the *x* axis
$y_{t,r}$	Position of the transmitted/receiver antenna in the *y* axis
y_{curv}	Parameter related to the length of the reflected ray in a curve
z'	Length of the curve
z_i	Sample i
z_r	Reference value

List of Software

Borland C++ Builder	ANSI C++ Integrated Development Environment
Google Earth	Virtual globe visualisation tool
Matlab	Computational math tool
Microsoft Excel	Calculation tool
Microsoft Visio	Design tool
Microsoft Word	Text Editor tool
Nemo Outdoor V.4.24	Measurements storage and analysis tool

Chapter 1

Introduction

This chapter gives a brief overview of the work. The scope and the motivations of the thesis are presented. At the end of the chapter, the work structure is provided.

1.1 Overview and Motivations

Mobile communications systems have experienced a rapid growth in the last decades, being essential nowadays, joining together communications and mobility. In fact, wireless communications are the only way to provide the exchange of information anywhere and anytime, a significant increase in the quality and in the speed at which these exchanges are allowed being observed. Achieving such versatile communication services implies a good knowledge of the radio-wave propagation, in order to achieve optimally designed networks.

Global Systems for Mobile Communications (GSM) technology has been at the leading edge of the wireless revolution [Cast01]. The first GSM network was launched in Finland in July 1991 [HoTo04]. At the end of 2007 the number of GSM subscribers was over 3 billion, more than 80% of the world's population being covered by GSM networks. The fast evolution of the number of GSM users is confirmed by the fact that it took 12 years to get to 1 billion GSM connections and only 30 months to get to 2 billion [GSMW08]. However, this technology is limited, in the sense that it allows for only voice communications and data communications at low rate, 14.4 kbps.

In January 1998, the European Telecommunications Standard Institute (ETSI) selected the Wideband Code Division Multiple Access (WCDMA) as the third-generation air interface [HoTo04]. The first version of the common specification, called Release 99, was completed at the end of 1999. According to the regulatory authorities, the first Universal Mobile Telecommunications System (UMTS) networks should have started operating in 2002. However, the real start of operation has been delayed due to technical problems and the fact that the market for mobile high data rate applications had to be developed first. With the end and the start of 2003 and 2004, respectively, the major mobile providers in Europe started to offer subscriptions to UMTS and the appropriate devices [Moli05]. The deployment of this technology started in Europe and Asia, including Japan and Korea, in the frequency bands around 2 GHz. While 2nd generation systems, as GSM, were originally designed for delivery of voice services, UMTS networks are designed from the beginning for flexible delivery of any type of service [HoTo04]. Regarding this technology, the latest figures confirm that global subscriptions to 3G/UMTS networks have passed the 200 million milestone [UMTS08]. This system is operational anywhere, indoors and outdoors, in stationary and mobile environments [Shan02]. Theoretical bit rates up to 2 Mbps are enabled in Release 99, although, the practical bit rates achieved are up to 384 kbps [HoTo04]. The exponential growth of data communications over mobile phones forced a further development of systems that would be capable of offering higher capacity, throughput and enhanced multimedia services, available to consumers 'anywhere, anytime' [LaWN06].

High Speed Downlink Packet Access (HSDPA) was standardised as part of 3rd Generation Partnership Project (3GPP) Release 5 the first specifications being available in March 2002. The first commercial HSDPA networks were available at the end of 2005, with initial peak data rate of 1.8 Mbps, increased to 3.6 Mbps during 2006, and to 7.2 Mbps in 2007, being now provided by some operators a peak data rate of 14.4 Mbps. The same approach was taken for the Uplink (UL) case, being launched, in

December 2004, by 3GPP Release 6 the High Speed Uplink Packet Access (HSUPA). HSUPA started to be deployed at the end of 2007, with data rates up to 1.45 Mbps, and around 3-4 Mbps in later releases [HoTo06].

Future developments are being studied, namely regarding the Long Term Evolution (LTE). 3GPP LTE, an evolution of the GSM/UMTS family, provides Downlink (DL) peak data rates up to 300 Mbps using advanced antenna techniques, such as Multiple Input Multiple Output (MIMO). The radio technology is optimised enabling significant new high capacity mobile broadband applications. The specifications of this technology have been approved in January 2008, being included in Release 8 [UMTS08].

As already mentioned, mobile phones are part of everyday life. Nowadays, users expect that good coverage exists wherever they are, thus, this is a key factor to maintain them satisfied. In fact, engineering does not happen in a vacuum – the demands of people change what engineers develop, and the products of their labour influences how people behave [Moli05]. Therefore, since the performance of a mobile radio communication system depends on the radio propagation environment, besides the traditional urban, suburban and rural areas widely studied in the literature, a good coverage is also desired in other environments, such as the tunnels and the bridges. With the new and more demanding services, mobility is becoming more important and the number of users in trains and in cars is growing, thus, these cases must be carefully studied and analysed. In fact, the ability to move around while communicating is one of the main charms of wireless communication for the user [Moli05].

Railway and road tunnels are very common nowadays in metropolitan cities, therefore, radio coverage is needed for personal and emergency communications [ZhHw98]. As a result, radio wave propagation in tunnels has been widely studied for years. A detailed study of the technical literature reveals that some work relevant to the problem has been published, namely some propagation models and experimental results mainly to describe the path loss behaviour, in [BrCA07], [DLMD07], [KiJL03], [NiSB98] and [Zhan03]; extensive references to other works are provided in all the mentioned works.

Wireless communications in a bridge are not extensively studied in the literature, although a good coverage is also required in this type of environment. The main reason should be that the free space propagation model provides a good approximation to the real behaviour of radio propagation in bridges; however, some characteristics must be taken into account in order to optimise the system and the available resources.

As mentioned, the propagation models used in the environments being studied are more or less defined. However, although UMTS is already implemented in many parts of the world, a complete model, to study the path loss, the coverage, the capacity and the interference in such environments, is steel needed in order to improve the radio network planning and optimisation. In fact, such a tool can be an important contribution to a more efficient exploitation of the resources available, allowing the companies operating in these areas to significantly reduce their costs with the equipments required in the networks, which is very important nowadays. It is well known that the design of wireless systems

does not only aim to optimise performance for specific application, but also to do that at reasonable cost [Moli05]. Actually, the general target of radio network planning and optimisation is to find a network configuration with minimal costs that fulfils the service specific network requirements in terms of coverage, capacity and QoS [Stae05].

The main purpose of this thesis is the study of coverage, capacity and interference in UMTS in linear environments, namely in tunnels and in bridges. These objectives were accomplished through the development and implementation of a complete model that allows the study of the propagation in both environments as well as the estimation of the parameters referred. The methods and the expressions used in the calculation of the parameters are presented. The study of these parameters in different scenarios, varying, e.g., the environmental characteristics, the number of users and the services used, is performed. The characteristics of the scenarios were carefully chosen to approximate the environments to the real tunnels and bridges studied. The results obtained with the simulator are compared with the measurements performed in the real network, in order to validate and evaluate the simulator. Measurements have been conducted in the Lisbon Underground and in the 25 de Abril Bridge.

This thesis was made in collaboration with Celfinet, a mobile communications consulting company. The measurements performed were carried out with both equipment and human resources supplied by the company.

The main contribution of this thesis is the study performed regarding the coverage and the capacity aspects, as well as the tool developed for that analysis. In fact, the developed simulator supplies an important practical application, since it can be used in the planning and optimisation of a network in the referred environments. As mentioned before, many propagation and interference models exist in the literature, however, a solution and a tool to study the coverage, capacity and interference in such environments was required. Therefore, this thesis contributes to fill in this gap. Moreover, several important results and conclusions were obtained, regarding the influence of many parameters, in both environments studied.

1.2 Structure of the Dissertation

This work is composed by 6 Chapters, including the present one, followed by a set of annexes.

In Chapter 2, an introduction to UMTS is performed. UMTS basic aspects are presented, namely concerning the radio interface, coverage, capacity and interference concepts, and the services and applications allowed by this system. A brief introduction to the antennas' main characteristics and to the propagation models is also presented.

In Chapter 3, all the models studied in this work are presented. First, the antenna models and main characteristics are presented. Afterwards, the propagation models considered for the tunnel are described, all the assumptions taken being presented. The propagation models used for the bridge case are presented next. In the last section of the chapter, the interference models used are described.

Chapter 4 is entirely dedicated to the implementation of the models in the simulator developed. The simulator overview is given, the different modules being then presented in detail, namely regarding the functionalities, the assumptions taken, the interaction between the modules, and the input and output parameters. This chapter ends with the simulator assessment.

Chapter 5 begins with the description of the scenarios considered in the simulations. Afterwards, the analysis of the results obtained for those scenarios, for both the tunnel and the bridge, are presented and analysed, and the study of some parameters' influence is also presented. The results obtained in these studies are compared with those observed in the default scenarios, in order to be possible to evaluate the parameters influence. In the following sections, the results obtained for the simulations performed for some particular scenarios are presented. The chapter concludes with the analysis of the results obtained in the measurements performed in a tunnel and in a bridge, being a comparison with the simulations done.

The thesis concludes with Chapter 6, where the main conclusions of the work are drawn and suggestions for future work are pointed out.

A set of annexes with auxiliary information and results is also included. In Annex A, the link budget used throughout the thesis is presented. Annex B presents the expressions used for the reflection coefficients. In Annex C, the model used to predict the attenuation in curves is presented. In Annex D, the simulator user's manual is presented. Annex E presents the *K* parameters and the fast fading margins used for the Rice distribution. Annex F contains the radiation pattern of the Base Station (BS) antenna used in this thesis, as well as the characteristics of other antennas normally used. In Annex G, the additional results obtained for the tunnel case are presented, while Annex H contains the same information but concerning the bridge. In Annex I, the additional results obtained for the analysis of the Rossio Tunnel are presented. Annex J contains some additional results concerning the Vasco da Gama Bridge analysis. Annex K and Annex L present the tracks considered in the measurements for the Lisbon Underground and for the 25 de Abril Bridge, respectively. Finally, in Annex M, additional results regarding the measurements performed in the Lisbon Underground are presented.

Chapter 2

Basic Aspects of UMTS

This chapter provides an overview of the UMTS, focussing on the radio interface, interference, capacity, coverage and services and applications. Some important aspects about antennas and radio wave propagation are also presented.

2.1 Radio Interface

In this section, UMTS (Release 99) basic concepts are presented, based on [HoTo04], regarding the radio interface.

UMTS uses WCDMA as the underlying air interface, which is a Direct-Sequence Code Division Multiple Access (DS-CDMA) system. It provides a few advantages for the operator in that it enables data but also improves basic voice. The main parameters in WCDMA are summarised in Table 2.1.

Table 2.1. Main WCDMA parameters (adapted from [HoTo04]).

Duplexing Method	FDD / TDD
Modulation	UL: Binary Phase Shift Keying (BPSK) DL: Quaternary Phase Shift Keying (QPSK)
Chip Rate	3.84 Mcps
Frame length	10 ms

WCDMA supports two basic modes of operation: FDD (Frequency Division Duplex) and TDD (Time Division Duplex). In the FDD mode, separate 5 MHz carrier frequencies are used for UL and DL respectively, whereas in TDD only one 5 MHz carrier is timeshared between UL and DL. Only the FDD mode is in use nowadays.

UMTS uses spreading to separate the physical data and control channels from the same mobile terminal (MT) in UL, and to distinguish different users in DL. In addition, on top of spreading, scrambling is used to separate MTs or BSs from each other. Scrambling does not change the signal bandwidth nor does it affect symbol rate. Due to spreading and despreading, the wideband Signal-to-Interference Ratio (SIR) can be lower in UMTS than in GSM.

UMTS can support bit rates up to 2 Mbps in DL and up to 384 kbps in UL, depending on the type of cell and on the users' velocity, using a variable spreading factor (SF) and multi-code links. However, these data rates can be improved using HSDPA and HSUPA. Highly variable user data rates are supported by UMTS, through the allocation of 10 ms frames. The chip rate in UMTS is 3.84 Mcps, which allows the actual carrier spacing to be selected on a 200 kHz grid between 4.4 and 5 MHz. The maximum bit rates achievable for different environments are presented in Table 2.2. As expected, the higher data rates are achieved for low speeds and in small indoor areas.

One of the most important aspects in UMTS is power control. Without it, a single overpowered MT could block a whole cell. UMTS uses two types of power control: closed loop to avoid the use of excessive power, thus, to keep interference levels at minimum and outer loop to keep the quality of the communication at the required level. Soft and softer handovers are also key features in UMTS,

since without soft/softer handover there would be near-far scenarios of an MT penetrating from one cell deeply into an adjacent cell without being power-controlled.

Table 2.2. Range of transmission rates (extracted from [Cast01]).

High level description	Maximal bit rates [kbps]	Maximal speed [km/h]
Rural outdoor	144	500
Suburban outdoor	384	120
Indoor/Low range outdoor	2048	10

Processing gain is also fundamental in UMTS. It consists in raising the user signal by the SF from the interference. Processing gain is what gives Code Division Multiple Access (CDMA) systems the robustness against self-interference and, together with the wideband nature, suggests a frequency reuse of one between different cells.

In UMTS Terrestrial Radio Access (UTRA) three types of channels can be defined:

- Logical – used to exchange of specific information between the user and the network;
- Transport – to transport signal and traffic information;
- Physical – used to map transport channels and to carry information of physical layer procedures.

The frequencies around 2 GHz were identified as those available for use by third generation systems. In Europe and in most of Asia the International Mobile Telephony 2000 (IMT-2000) bands used for FDD are: [1920, 1980] MHz for UL and [2110, 2170] MHz for DL.

As previously mentioned, HSDPA is used to improve the achievable bit rates. The idea of the HSDPA concept is to increase DL packet data throughput by means of fast physical layer (L1) retransmission and transmission combining, as well as fast link adaptation controlled by the Node B. All these methods have the aim of improving DL packet data performance both in terms of capacity and practical bit rates [HoTo06]. In what concerns modulation, while UMTS only uses QPSK, HSDPA may additionally use the higher order modulation: 16 Quadrature Amplitude Modulation (QAM). This modulation allows higher data rates, but can only be used under good radio signal quality, due to additional decision boundaries [HoTo06].

HSDPA performance depends on the network algorithms, deployment scenarios, traffic generated, Quality of Service (QoS) and MT receiver performance and capability. It uses a fixed spreading factor of 16; from these 16 available codes, only 15 can be allocated for data transmission, as one code is needed for the transmission information. From the BS point of view, all the 15 codes can be allocated. However, for the MT, the allocated codes can vary, depending on the MT category. Terminals supporting HSDPA are divided into 12 categories with different maximum DL bit rates, between 0.9

and 14.4 Mbps [HoTo06].

In HSUPA, similarly to HSDPA, performance depends on network algorithms, deployment scenarios, traffic generated, Quality of Service (QoS) and MT receiver performance and capability. There are six MT categories, with UL bit rates between 69 kbps and above 4 Mbps [HoTo06].

2.2 Interference, Capacity and Coverage

This section presents important aspects related to interference, capacity and coverage in UMTS, based on [HoTo04].

Since in WCDMA all users share the same frequency, they are interfering with each other, meaning that UMTS capacity and interference are user dependent, being different than in GSM. There are three main parameters limiting capacity:

- Number of available codes,
- Node B transmission power,
- System load.

The number of available channelisation codes imposes the maximum number of active users in a cell. The maximum number of orthogonal codes depends on the SF. As data rate increases, the SF must decrease to allow for higher data rates, leading to a decrease of the number of users allowed in the network. The maximum value for the SF is limited to assure a minimum QoS, since high SF values increase the interference. The SF values used in UMTS are presented in Table A.3 in Annex A.

To estimate the amount of supported traffic per BS, the load factor (η) is used. It depends on the link and on the type of service. The load factors for UL and for DL are:

$$\eta_{\mathrm{UL}} = (1+i)\sum_{j=1}^{N}\frac{1}{1+\dfrac{G_{Pj}}{(E_b/N_0)v_j}}; \qquad (2.\ 1)$$

$$\eta_{\mathrm{DL}} = \sum_{j=1}^{N} v_j \frac{(E_b/N_0)_j}{G_{Pj}}\left[\alpha_j + i_j\right] \qquad (2.\ 2)$$

where:

- N : number of users per cell;
- G_{Pj} : processing gain of user j, defined as R_c/R_{bj};
- i : ratio of inter- to intra-cells interference;
- E_b : energy per user bit;
- N_0 : noise spectral density;

- v_j : activity factor of user j (typically 0.67 for speech and 1.0 for data);
- R_c : Chip rate (equal to 3.84 Mcps);
- R_{bj} : bit rate of user j ;
- α_j : DL channel orthogonality of user j (where 0 corresponds to complete orthogonal codes);
- i_j : ratio of inter- to intra-cells interference for user j .

As the load increases, a larger interference margin is needed, leading to a decrease of the cell coverage area. The DL load factor exhibits very similar behaviour to the UL load factor, in the sense that, when approaching unity the system reaches its pole capacity. However, in DL, the maximum transmission power does not vary with the number of active users. The BS transmitting power is shared among all users, and it is bounded, thus, this is a limiting factor in cell capacity. The total transmission power of the BS can be expressed as

$$P_{TX\,[\mathrm{W}]}^{BS} = \frac{N_{rf} R_c L_p \sum_{j=1}^{N} v_j \frac{\left(E_b/N_0\right)_j}{G_{Pj}}}{1-\overline{\eta_{DL}}} ; \qquad (2.\ 3)$$

where:

- $\overline{\eta_{DL}}$: average DL load factor value across the cell;
- L_p : path loss between BS and MT;
- N_{rf} : noise spectral density of MT receiver.

However, it is important to note that the total transmission power has two components: one related to the traffic and other related to signalling and control information, meaning that the effective power, used for traffic, is reduced, being lower than the total transmission power of the BS.

In both UL and DL, the air interface load affects coverage, however, in DL, it depends more on the load than in UL. The reason is that in DL the power is shared among users, thus as the number of users increase, the power per user decreases. Capacity and coverage are closely related in UMTS networks, thus, both must be analysed simultaneously when these networks are dimensioned.

2.3 Services and Applications

This section presents the most relevant aspects related to the services and applications provided by UMTS, based on [HoTo04] and on [KALN05].

UMTS offers not only mobile services supported by 2nd generation systems, such as GSM, but also expands these services to higher rates and greater flexibility and introduces new services.

There are four classes of UMTS traffic which differ in their characteristics and applications, as summarised in Table 2.3. The main distinction factor is traffic delay's sensitivity, although the bit rates required, the files dimensions and the switching methods are also different in each class.

Table 2.3. UMTS classes and their main parameters (adapted from [HoTo04], [3GPP01] and [Cast01]).

Class	Conversational	Streaming	Interactive	Background
Transfer Delay	80 ms	250 ms	-	-
Guaranteed bit rate [Mbps]	≤ 2	≤ 2	-	-
Switching	Circuit Switch (CS)	Circuit Switch (CS)	Packet Switch (PS)	Packet Switch (PS)
Examples	Voice	Multimedia	Internet	e-mail

The conversational class applies to speech and to any application that involves person-to-person communication in real-time, such as voice, videoconferencing and interactive video games. This class is characterised by low end-to-end delay – the maximum end-to-end delay (400 ms) is given by the human perception – and symmetric traffic between UL and DL in person-to-person communications.

The streaming class requires bandwidth to be maintained like conversational class, but it tolerates some delay variations. Video-on-demand and news streams are examples in this class.

The interactive class is characterised by the request response pattern of the end user. At the message destination there is an entity expecting the message within a certain time. Examples of this include games and the Internet.

The background class covers all applications that either receive data passively or actively request it, but without any immediate need to handle the data. Examples of this are e-mail, Short Message Service (SMS), Multimedia Message Service (MMS) and file transfers.

It is also important to know the usual bit rates and the typical file dimensions required for the different services. Table 2.4 presents these values. As already mentioned, the theoretical bit rates in UMTS can reach 2 Mbps, although the practical bit rates achieved are up to 384 kbps.

Table 2.4. Bit Rates and applications of different services (adapted from [Corr07]).

Service	Bit Rate [kbps]	Size [kB]	Applications
Speech	12.2	-	Voice, Voice mail
Simple Messaging	14.4	10 – 40	SMS, e-mail
High Interactive Multimedia	128	$\leq$10 000	Video-telephony, Video-conference
Medium Multimedia	384	$\leq$10 000	Internet access, Interactive gaming
High Multimedia	2 000	$\leq$10 000	Fast Internet, Video Clips on Demand

2.4 Antennas and Propagation

To implement a mobile communications system, it is necessary to study the characteristics of the antennas and also to study the radio wave propagation, therefore propagation models must be carefully analysed.

The antennas used in a mobile communications system are one of the key aspects to achieve a good coverage and to provide a good QoS. The antennas performance depend also on the interaction between them and the radio environment, meaning that it is essential to study the different types of antennas in order to obtain the best solution for each environment. Small size, low power consumption, low prices, frequency gain and radiation pattern are some important characteristics of the antennas to consider when the system is being designed. Additionally, there are some important parameters that need to be considered. The half power beam width of the antenna is one of the main parameters studied, since it provides an estimation of the antenna directivity, being useful in the dimensioning of the system. In linear environments, such as the tunnels and the bridges, directive antennas, thus, with low values of half power beam width, are normally used, since they provide a more efficient coverage.

In what concerns tunnels and bridges, two different approaches regarding the antennas are taken: the collinear arrays and the helical antennas. These solutions are considered since it is necessary to ensure the coverage in these environments and not outside, thus, the usage of omnidirectional antennas is not a good approach. For this purpose, the usage of antennas with higher directivity is more efficient, a good solution being the usage of collinear arrays or helical antennas. With arrays, it is possible to change the radiation pattern and increase the directivity, in comparison with that achieved, for example, with simple dipoles or omnidirectional antennas, according to the desired requirements. The helical antenna constitutes a basic, simple, and practical configuration of an electromagnetic

radiator, being normally used in terrestrial mobile communications systems and in satellite communications systems. Usually, two modes are operated by helical antennas: the normal and the axial. The axial mode is more efficient and practical, since circular polarisation is achievable over a wider bandwidth [Bala97].

In what concerns radio wave propagation, there are four basic mechanisms to describe it: reflection, diffraction, scattering and penetration. The guided wave is also a propagation mechanism, used to describe the propagation in corridors and in tunnels [DaCo99].

In the literature, there are different cell type definitions. Table 2.5 presents the cell types and their main characteristics, namely the cell radius, the characteristic environments and the position of the BS antennas, defined in [DaCo99].

Table 2.5. Definition of cell types (extracted from [DaCo99]).

Cell type	Typical cell radius [km]	Environment Classification	Typical position of BS antennas
Macro-cell	1 to 30	Outdoor	Mounted above medium roof-top level; heights of all surrounding buildings are below BS antenna height
Small macro-cell	0.5 to 3	Outdoor	Mounted above medium roof-top level; heights of some surrounding buildings are above BS antenna height
Micro-cell	Up to 1	Outdoor	Mounted below medium roof top level
Pico-cell	Up to 0.5	Indoor or outdoor	Mounted below roof top level

To establish propagation models, two complementary approaches can be used: experimental and theoretical. Experimental investigation is based on measurements, thus, it is closer to the reality, accounting for all factors influencing propagation. However, this approach has also disadvantages, such as the difficulties in the design of the experiments and the interpretation of the results due to several propagation phenomena involved [DaCo99], [Corr07]. In a theoretical investigation, the environment can easily be described and modified. One disadvantage of this approach is that the results obtained are valid only for the particular case analysed [DaCo99]. The theoretical approach can be divided into two categories:

- Simulation of wave propagation – consists in analysing the electromagnetic propagation theoretically or by simulations;
- Ray theory – consists in observing that the radio wave interacts with the propagation environment through the four basic mechanisms already presented [DaCo99].

In what concerns fading, two types can be distinguished: the slow and the fast fading. The slow fading, also known as long term fading, depends essentially on distance and follows a log-normal distribution [Corr07]. On the other hand, fast fading, or short term fading, is associated to both MT and propagation environment movements. For Line-of-Sight (LoS) conditions, fast fading follows the Rice

distribution, while for Non-Line-of-Sight (NLoS) it follows the Rayleigh one [Corr07]. Fading must be taken into account when a mobile communications network is designed, since it can influence the QoS obtained [Corr07], [DaCo99].

The propagation of electromagnetic waves in tunnels and in bridges cannot be studied as in other environments. Inside a tunnel, in most cases, the power loss is lower than in free space propagation due to guidance by the walls, and it decreases with increasing frequency, for frequencies up to 17 GHz [DaCo99]. It is important to note that the classic solution for radio coverage inside tunnels is the usage of leaky feeders. With this approach a good coverage can be obtained, however, leaky feeders are difficult to maintain and install, providing a high path loss and being too expensive especially in long tunnels. Therefore, the usage of antennas seems to be the more interesting approach [BrCA07].

Considering the tunnel as a waveguide, only the modes with frequency higher than the tunnel's cut-off frequency can propagate. Since the cross-sectional dimensions in tunnels are, normally, large compared to the wavelength, as it happens in UMTS, the propagation is strongly multi-modal, thus, a wide range of hybrid modes can propagate inside the tunnel [BrCA07]. The modes usually travel at different phase velocities, leading to strong and quite rapid variations in signal along the propagation path. Inside a tunnel, normally fast fading is present due to the movements of the vehicles or trains, causing changes on the environment [DLMD07]. When a straight tunnel is considered, there is usually LoS between the BS and the MT, thus, fast fading follows the Rice distribution. Otherwise, if the tunnel has curves, a LoS situation cannot be considered along the entire tunnel, meaning that the Rayleigh distribution is used.

There are several factors that influence radio coverage in a tunnel, such as the frequency used, the tunnel section, the existence of curves, some characteristics of the walls and also characteristics of the antennas. Moreover, it is well known that two propagation regions separated by a break point are observed along a LoS path in a tunnel [Zhan03]. Briso-Rodriguez et al. [BrCA07] have presented a propagation model for railway tunnels that considers the modes' attenuation, the permittivities, the roughness and the tilt of the walls. This model has been experimentally verified in one tunnel. Dudley et al. [DLMD07] have presented and experimentally verified a propagation model for circular and rectangular tunnels, both straight and gently curved. Kim et al. [KiJL03] have also presented a model to analyse radio wave propagation in tunnels using simulations by ray-tracing method and measurements in a tunnel in Korea. Nilsson et al. [NiSB98] have presented a model to predict the path loss in rectangular tunnels, based on a simple Geometrical Optics extension to the standard waveguide solution. This model considers the tunnel dimensions and the permittivity of the tunnel walls. Zhang [Zhan03] has presented a propagation model for tunnels, based on both the single and the ray optical models, that considers the tunnel dimensions, the reflection coefficients and the transmitting and receiving antennas' coupling losses, among other parameters. This model has been successfully tested in many tunnels, being also used and referenced by other authors, moreover, it considers all the factors mentioned above, therefore, this is the model used in this thesis. Additionally,

the models for the path loss prediction in curves presented in [NiSB98] and in [BrCA07] have been used, to obtain a more complete and useful model.

Since the model developed is intended to be used in any-shaped tunnels, it is necessary to analyse the behaviour of the polarisation for different section types. The propagation in rectangular tunnels is based on the assumption that, at large distances, waves remain polarised predominantly in the horizontal or vertical directions, depending on the excitation conditions [MLND08]. In circular tunnels, however, the field behaviour is quite different due to the geometry of the tunnel section, being higher the probability for waves depolarisation. Still, Molina-García-Pardo et al. [MLND08] have concluded that, in the frequency range similar to that used in UMTS, the waves remain polarised even if the antennas are placed very near the tunnel walls.

The propagation in bridges has also some characteristics that distinguish it from the propagation observed in normal urban, suburban or rural environments, although it has some common aspects to the propagation discussed in tunnels. In fact, as in tunnels, bridges are also linear environments where the planning is done considering that confined regions, thus the traditional COST231 – Okumura-Hata and the COST231 – Walfisch-Ikegami models [Corr07] are not suitable for propagation prediction, since these models are used in outdoor environments and are not efficient for the study in linear environments. However, opposite to tunnels, in bridges the waveguide phenomenon is not present, since they are open areas. In a bridge, a LoS condition between the BS and the MT is normally observed and the reflections are mainly in the floor and due to other vehicles.

The propagation in bridges has not been widely studied in the literature, since the traditional approach considered to predict the path loss is the usage of the free space propagation model. However, some aspects need to be discussed in order to obtain a more efficient coverage, such as, the differences between the existence or not of traffic in the bridge. In fact, different propagation models must be used in these cases, namely the free space and the flat earth models respectively, to account more accurately for the path loss behaviour, thus, for better predicting coverage, capacity and interference. All these considerations and conditions are not usual in other environments, so they must be carefully analysed to obtain a good and efficient coverage.

Furthermore, other important aspect must be considered in what concerns to the interference in bridges. Even being linear environments, the BSs located outside the bridges, used to cover surrounding areas, are normally causing interference to the communications in the bridge, thus, they need to be taken into account when the planning of the network is being studied.

Chapter 3

Models

This chapter presents the antennas models, as well as the propagation models used in this work. The interference models used are also described.

3.1 Antenna Models

Regarding the antennas, there are some parameters that must be studied. The half power beam width of the BS antenna is an important parameter that must be carefully chosen, especially in the environments being studied, as well as the BS antenna radiation pattern, since the antenna gain influences strongly the covered area. For a very high-gain antenna, the half power beam width is a narrow angle, therefore, outside this beam width, the signal typically drops off fairly quickly [Gast05]. For an array, the half power beam width is given by [Corr07]

$$\alpha_{3\mathrm{dB[rad]}} \cong \frac{0.886}{N_a d_a / \lambda}, \tag{3. 1}$$

for

$$N_a d_a / \lambda >> 1, \tag{3. 2}$$

where:

- N_a : number of elements on the array;
- d_a : distance between consecutive antennas;
- λ : wavelength.

The total gain of the array is given by [Corr07]

$$G_{arr} = \eta_{\mathrm{arr}} D_{arr}, \tag{3. 3}$$

where:

- η_{arr} : efficiency of the array;
- D_{arr} : directivity of the array.

The efficiency of the array depends on the type of antennas used. For dipoles, the efficiency is around 100%, while for patch antennas it is around 30%. The directivity of the array is dependent on the directivity of their elements and it is inversely proportional to the half power beam width, as expressed in [Corr07].

The half power beam width of the helical antenna is given by [Bala97]

$$\alpha_{3\mathrm{dB[rad]}} \approx \frac{13\pi\lambda^{3/2}}{45 C_t \sqrt{N_s S}}, \tag{3. 4}$$

where:

- N_s : number of turns;
- C_t : perimeter of the circular projection of the turn;
- S : spacing between turns.

The gain of the helical antenna can be obtained as

$$G_{hel} = \eta_{\text{hel}} D_{hel} \,, \tag{3. 5}$$

where:

- η_{hel} : efficiency of the helical antenna;
- D_{hel} : directivity of the helical antenna.

The directivity of the helical antenna is given by [Bala97]

$$D_{hel} \approx 15 N \frac{C_t^2 S}{\lambda^3} \,. \tag{3. 6}$$

3.2 Propagation in Tunnels

Since coverage, capacity and interference are the main parameters being studied in this thesis, it is important to have a good estimation of the path loss observed in a tunnel. In fact, the attenuation is used in the calculation of the transmitted powers required in the BS and in the MT, as shown by (A.1), as well as in the interference estimation, therefore, it influences the parameters mentioned. The model used in this thesis and described in the next paragraphs is based in [Zhan03], since it accounts for most of the factors analysed in Section 2.4, therefore, a good prediction of the propagation attenuation can be obtained. Furthermore, it can be used in both railway and road tunnels, thus, providing a complete and useful model.

In this model, two regions are considered: near and far ones. In the near region, the propagation loss is larger due to the interaction of many modes, and propagation takes place as if it were in free space, being approximated by a single ray optical model as

$$L_{nr[\text{dB}]} = L_{fs[\text{dB}]} = 32.44 + 20\log_{10}\left(f_{[\text{MHz}]}\right) + 20\log_{10}\left(d_{[\text{km}]}\right); \tag{3. 7}$$

where:

- f : frequency;
- d : distance between the BS and the MT.

Experiments, detailed in [Zhan03], have shown that the free space model is a good approximation to predict the propagation loss in the region near the transmitting antenna.

In the far region, the attenuation increase with distance is smaller, since it can be assumed that only one mode, namely the E_{11}^h one, is propagating. Propagation takes place as if it were in a waveguide, the analytical ray optical model being used as

$$L_{fr\ [\text{dB}]} = 5\lambda d \left[\frac{1}{w^2}\log_{10}\left(\frac{1}{\Gamma_1^2}\right) + \frac{1}{h^2}\log_{10}\left(\frac{1}{\Gamma_2^2}\right) \right] + L_{ant\ t[\text{dB}]} + L_{ant\ r[\text{dB}]} \,; \tag{3. 8}$$

where:

- $\Gamma_{1,2}$: reflection coefficient of the vertical/horizontal walls, at the grasing angles, obtained as expressed in Annex B;
- $L_{ant\ t,r[\mathrm{dB}]}$: coupling loss of the transmitting/receiving antenna;
- w : width of the tunnel;
- h : height of the tunnel.

The antenna coupling losses depend on the near-field characteristics of the antennas, and can be measured in the laboratory or obtained as [Zhan03]

$$L_{ant\ t,r[\mathrm{dB}]} = 10\log_{10}\left(\frac{2\pi wh}{\lambda^2 G_{t,r}}\cos^{-2}\left(\frac{\pi x_{t,r}}{w}\right)\cos^{-2}\left(\frac{\pi y_{t,r}}{h}\right)\right); \tag{3. 9}$$

where:

- $x_{t,r}$: position of the transmitter/receiver antenna in the *x* axis;
- $y_{t,r}$: position of the transmitter/receiver antenna in the *y* axis;
- $G_{t,r}$: gain of the transmitter/receiver.

It should be noted that, according to [Zhan03], (3.9) does not remain accurate when the antenna is located close to the tunnel walls.

The tunnel section and the coordinates system, with the origin at the centre of the tunnel, are presented in Fig. 3.1. The tunnel section, as previously mentioned, is one of the factors that influence propagation in tunnels. Normally, tunnels have two different section types: rectangular and circular; however, the model can be applied for any tunnel shape. For rectangular tunnels, the dimensions considered are the width w and the height h of the tunnel. For circular or other-shaped tunnels, an equivalent rectangular section is obtained as follows: the cross-sectional area of the equivalent rectangular tunnel is the cross-sectional area of the circular tunnel, and the width of the equivalent rectangular tunnel is the floor width of the circular tunnel. This way, the width and the height of the equivalent rectangular tunnel are obtained and the analysis is done considering this equivalent tunnel.

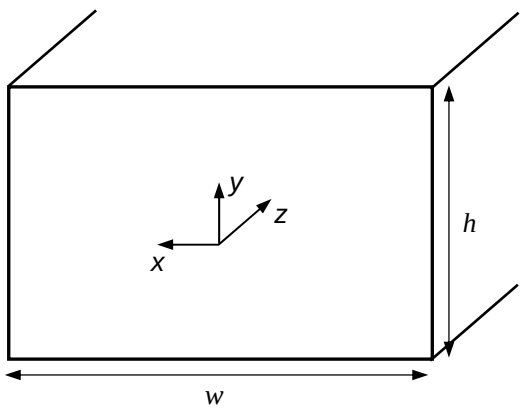

Figure 3.1. Representation of the tunnel section.

The separation of both regions considered is defined by the break point, which can be obtained as the intersection of both curves, where the propagation losses of both models are equal, i.e.,

$$L_{nr\ [\mathrm{dB}]} = L_{fr\ [\mathrm{dB}]}\,. \tag{3. 10}$$

This means that from the transmitter to the break point is the near propagation region where the single ray optical model is used, while after the break point is the far propagation region, the analytical ray model being used.

Another factor that contributes to attenuate the signal is the presence of curves. To account for this factor, shooting and bouncing ray method is used, described in Annex C and based on [NiSB98] and [BrCA07]. This attenuation is obtained as the average of the losses suffered by all the rays, at a certain distance z'. The attenuation depends on the length of the curve, on the reflection coefficient, and on the roughness of the walls. For a curve of length z', the extra attenuation can be obtained as

$$L_{curv}\left(z'\right)_{[\mathrm{dB}]} = 10\log_{10}\left[\left(\rho\left|\Gamma_{\mathrm{v,h}}\right|\right)^{2z'N_{1c}}\right]; \tag{3. 11}$$

where:

- N_{1c} : number of reflections, per metre, in the vertical walls;
- $\Gamma_{\mathrm{v,h}}$: reflection coefficient for vertical/horizontal polarisations;
- ρ : coefficient that considers the roughness of the walls.

When curves exist in a tunnel, this extra attenuation is added to the propagation attenuation previously presented.

It is important to note that the horizontally polarised mode is more affected by the curvature than the vertically polarised one. The reason is that the horizontal electric field is perpendicular to the curved walls, therefore, it is more attenuated [DLMD07]. Another important note is related to fast fading. In straight tunnels, normally there is LoS between the BS and the MT, thus, the Rice distribution is used. However, when there are curves, if the user and the BS are not in a LoS condition, the Rayleigh distribution is considered. For both cases the log-normal distribution is used to predict slow fading. Additionally, the signal shadowing resulting from the blocking effect of two trains passing inside the tunnel must also be analysed. This is an important study since a train stopped inside the tunnel can block the communications of other trains, this being, according to [BrCA07], a problematic situation. Briso-Rodriguez et al. [BrCA07] have studied this phenomenon and concluded that an obstruction up to 20 dB can be observed while the moving train passes the fixed train. In fact, this obstruction can have some impact on communications, especially if the crossing point corresponds to a handover point in between two cells or if the signal margin is very limited [BrCA07].

The received signal inside a vehicle or train, which is the case inside tunnels, is lower in comparison with an outdoor use. Since there is the need to provide reliable in-vehicle coverage, it is necessary to determine and consider the vehicle or train penetration loss. The parameter L_{pind}, presented in Annex A, considers this attenuation. Tanghe et al. [TJVM03] have shown that, for frequencies close to

those used in UMTS, the attenuation caused by a vehicle is normally between 3.8 and 19.9 dB, depending on the MT position in the vehicle and on the relative position of the BS. For railway tunnels, train composition, window size, and the position of the BS antenna with regard to the train wall and the angle of incidence of direct and indirect (reflected, diffracted…) paths influence strongly the penetration loss [VAGH98]. In this case, a value of 9 dB for this parameter is usually assumed.

Considered all parameters, it is now possible to calculate the overall propagation attenuation in a tunnel. For the near region, the path loss is obtained as

$$L_{p[\mathrm{dB}]} = L_{nr[\mathrm{dB}]} + L_{curv}(z')_{[\mathrm{dB}]}; \tag{3. 12}$$

while for the far region it is given by

$$L_{p[\mathrm{dB}]} = L_{fr[\mathrm{dB}]} + L_{curv}(z')_{[\mathrm{dB}]}. \tag{3. 13}$$

Expressions (3.12) and (3.13) are used when there are curves. Otherwise, the parameter L_{curv} is not considered. Additionally, the total power received can be obtained as explained in the Link Budget detailed in Annex A.

It is possible to conclude that the model is easy to use and, according to the experiments shown in [Zhan03], accurate enough to predict the propagation attenuation in a tunnel.

3.3 Propagation in Bridges

The signal attenuation in a bridge, similar to the tunnel case, needs to be carefully studied in order to optimise the network planning, namely the coverage and the capacity obtained. In a bridge, two different cases must be analysed in terms of propagation and fading: the existence or not of traffic.

When there are many vehicles on the bridge, the free space propagation model is used to calculate the propagation loss between the MT and the BS. This model is, in this case, a good approach due to the LoS condition usually verified and due to the obstruction, caused by the vehicles on the bridge, of the reflected ray in the soil, not allowing the usage of the flat earth propagation model. Additionally, fast fading must be taken into account due to the changes in the environment caused especially by the movements of other vehicles, with a Rice distribution due to the LoS condition, while the log-normal distribution is used to account for the slow fading.

For the case of inexistence of traffic, the flat earth propagation model, described in [Corr07], is used, since a direct and a reflected ray are present. This model gives good results for short distances, and considers that there is LoS between the MT and the BS. These conditions are suitable for the propagation in bridges, since the distance between the BS and the MT is normally short enough to allow the consideration of a flat earth situation, and normally a LoS condition is observed. In what

concerns fading, fast fading with Rice distribution and slow fading with log-normal distribution are considered. However, this model has some limitations, in the sense that it is valid for distances between the BS and the MT satisfying

$$d > \frac{5kh_{BS}h_{MT}}{\pi}\ ; \tag{3. 14}$$

where:

- h_{BS} : height of the BS;
- h_{MT} : height of the MT;
- k : propagation constant.

Due to this restriction, when there is no traffic in the bridge, first the free space propagation model is applied up to that minimum distance, then, from the distance from which the free space propagation loss is equal to the flat earth propagation loss, the flat earth model is used. This way, it is guaranteed that there are no discontinuities in the attenuation curve. It is important to note that it has been verified analytically that the intersection of both curves occurs always after the minimum distance of application of the flat earth propagation model.

The propagation attenuation in free space is given by [Corr07]

$$L_{fs[\mathrm{dB}]} = 32.44 + 20\log_{10}\left(d_{[\mathrm{km}]}\right) + 20\log_{10}\left(f_{[\mathrm{MHz}]}\right); \tag{3. 15}$$

while for flat earth the expression used is [Corr07]

$$L_{fe[\mathrm{dB}]} = 120 - 20\log_{10}\left(h_{BS[\mathrm{m}]}\right) - 20\log_{10}\left(h_{MT[\mathrm{m}]}\right) + 40\log_{10}\left(d_{[\mathrm{km}]}\right). \tag{3. 16}$$

The heights of the MT, since MTs are inside vehicles, depend on the type of vehicle considered, the height of 1 m being a typical value for cars.

The additional loss due to vehicles is also considered for propagation in bridges, with the same values presented for the tunnels case.

3.4 Interference Models

Interference is present in every mobile cellular communications systems. Since WCDMA systems are interference-limited, the interference study is fundamental in UMTS. The total interference experienced by an MT is composed of two parts: intra- and inter-cells [Chen03].

In the DL case, as shown in Fig. 3.2 (a), the intra-cell interference is caused by the BS on an MT due to partial loss of orthogonality, caused by multipath, between the codes used for users in the same cell. The inter-cell one, is caused by the power received by the MT from the BSs located in adjacent

cells. Since the BSs are fixed, the DL interference depends on the location of the MT [Chen03].

In UL, the intra-cell interference in the BS is caused by all the other MTs served by the same BS, while the inter-cell interference is due to the signals received from MTs from adjacent cells, as shown in Fig. 3.2 (b). Therefore, the interference in UL is not related to the location of the MT [Chen03].

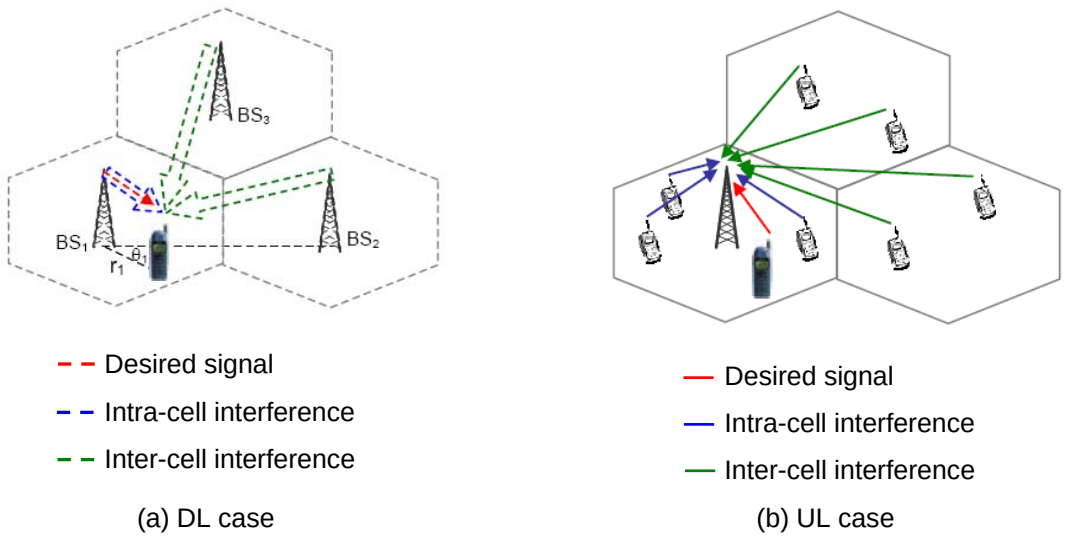

(a) DL case (b) UL case

Figure 3.2. Types of interference (adapted from [Chen03]).

In UMTS-FDD, these are the most important phenomena in what concerns interference, since there is no interference among MTs or among BSs, as it happens in the TDD mode.

Handover is a key aspect in UMTS. Nevertheless, soft and softer handover can also contribute to increase the interference in DL [Chen03]. When the MT is not in soft handover status, as *mobile 1* shown in Fig. 3.3, one DL channel is used for the communication between the BS and the MT and a certain amount of power P is allocated to that channel [Chen03]. However, if the MT is in soft handover, the situation is different. Considering *mobile 1*, in Fig. 3.4, in soft handover, it communicates with BS_1 and BS_2 at the same time, thus, two channels are needed with two amounts of power allocated P_1 and P_2, respectively from BS_1 and BS_2. In this case, P_1 causes intra-cell interference to *mobile 2* and inter-cell interference to *mobile 3*, while P_2 causes inter-cell interference to *mobile 2* and intra-cell interference to *mobile 3* [Chen03].

Comparing the two cases, it is important to understand if the soft handover causes an increase of interference. This is done comparing the power P, needed without soft handover, and the sum of P_1 and P_2, which is the power allocated when the MT is in soft handover. These powers are related to the location of the MT, the radio attenuation and the power division strategy used during soft handover. Anyway, when an MT is in soft handover, all the other active MTs need to adjust their channel power due to the change in the interference caused by that MT [Chen03].

When the MT is in softer handover the situation is similar, but in this case it corresponds to two

sectors from the same cell.

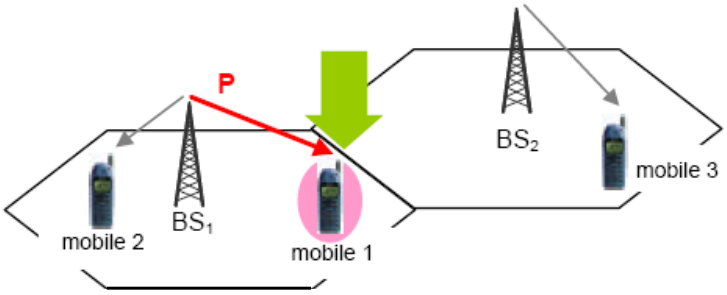

Figure 3.3. Inexistence of soft handover (extracted from [Chen03]).

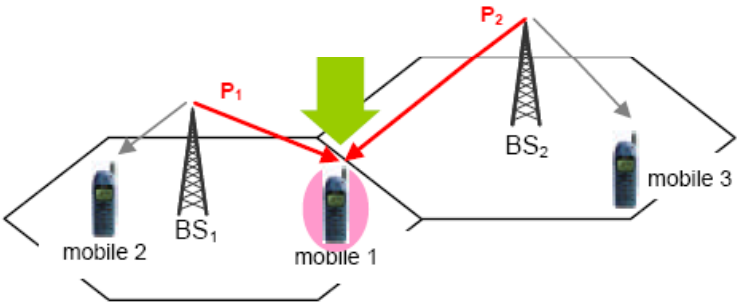

Figure 3.4. MT in soft handover (extracted from [Chen03]).

There are several models in the literature for the calculation of the interference, with different parameters and considerations, some of them mentioned in [EPCC06]. In this thesis, the interference models used are based on the study developed in [EPCC06]. For DL, the total power transmitted by the BS, the orthogonality factor and the propagation losses between BS and MT are considered in the models adapted; while for UL, the number of users, the received signal power and the activity factor, according to the user's service, are considered, as well as perfect power control [EPCC06].

The intra-cell interference in DL, for MT i , is given by

$$I_{Intra,i[\mathrm{W}]}^{DL} = \left(P_{TX}^{BS} - P_{BS \to MT_i}\right) \times \alpha \times L_p \; ; \tag{3. 17}$$

where:

- $P_{BS \to MT_i}$: power transmitted by the BS to the MT in which interference is being calculated;
- α : orthogonality factor.

The intra-cell interference in UL can be obtained as

$$I_{Intra,j[\mathrm{W}]}^{UL} = \sum_{g=1}^{N_{serv}} P_{BS_j \leftarrow MT} \times v_g \times N_{j,g} \; ; \tag{3. 18}$$

where:

- $P_{BS_j \leftarrow MT}$: power received in the BS j from an MT;
- v_g : activity factor of service g ;
- $N_{j,g}$: number of MTs using service g on the cell of BS j ;

- N_{serv} : total number of services used.

The inter-cell interference, in DL, in an MT i , can be obtained as

$$I_{Inter,i[\mathrm{W}]}^{DL} = \sum_{j=1}^{N_{BS}} P_{TX}^{BSj} \times \alpha \times L_p \; ; \tag{3. 19}$$

where:

- P_{TX}^{BSj} : BS j total transmitted power, including antenna gains;
- N_{BS} : number of interfering BSs;

In this case, the orthogonality of the codes is lower than that verified in the intra-cell interference since different BSs use different codes, thus, this value is here considered as half of the orthogonality factor used in the intra-cell interference [EPCC06].

The inter-cell interference in UL is given by

$$I_{Inter,j[\mathrm{W}]}^{UL} = \sum_{q=1}^{N_{BS}} \sum_{n_u=1}^{N_{users}} P_{BS_j \leftarrow MT_{n_u}} \times v_{n_u} \times A \; ; \tag{3. 20}$$

where, for the tunnel case, the A parameter is given by

$$A = \sum_{n=1}^{N_{q,g}} \frac{10^{\left[\frac{5\lambda r_{j,n}}{(wh)^2} \log_{10}\left(\frac{1}{\Gamma_v^2}\right) \log_{10}\left(\frac{1}{\Gamma_h^2}\right) + L_{ant\ t} + L_{ant\ r}\right]}}{10^{\left[\frac{5\lambda r_{q,n}}{(wh)^2} \log_{10}\left(\frac{1}{\Gamma_v^2}\right) \log_{10}\left(\frac{1}{\Gamma_h^2}\right) + L_{ant\ t} + L_{ant\ r}\right]}} \; ; \tag{3. 21}$$

while for the bridge it is obtained as

$$A = \sum_{n=1}^{N_{q,g}} \frac{r_{j,n}^{a}}{r_{q,n}^{a}} \; ; \tag{3. 22}$$

where:

- N_{users} : number of users in the sector studied and in the interfering sectors;
- $P_{BS_j \leftarrow MT_{n_u}}$: BS j received power from MT n_u being covered by an adjacent cell q ;
- $r_{q,n}$: distance from MT n using service g to interfering BS q ;
- $r_{j,n}$: distance from MT n using service g to BS j ;
- $N_{q,g}$: number of users using service g in interfering cell q ;
- v_{n_u} : activity factor of the user n_u ;
- a : path loss exponent.

It is important to mention that, since linear environments are analysed in this work, a BS has only two adjacent cells.

Chapter 4

Simulator Description

This chapter provides the description of the simulator developed on which the models studied are implemented. A brief overview of the simulator is given, as well as a detailed description of the functionalities of each module and the simulator assessment.

4.1 Simulator Overview

In order to help the study of the subject of this thesis, a complete simulator, named “SIMTunBrid” and with the main structure presented in Fig. 4.1, was developed. The main goals underlying the development of the simulator, for both tunnels and bridges, are the study of the influence of many parameters, such as the tunnel and bridge characteristics, the number of users trying to communicate, the data rates used, among others, on the coverage, capacity and interference of the system.

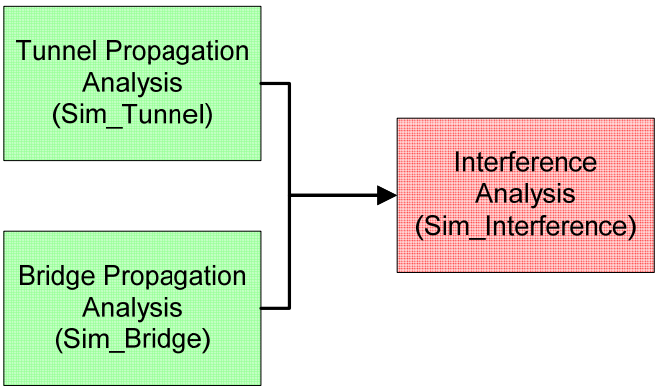

Figure 4.1. Simulator overview.

The Tunnel Propagation Analysis module is responsible for the calculation of the main parameters, such as the powers transmitted and received by the BS and the MT and the propagation attenuation, which are used in the Interference Analysis module, regarding the study of coverage and capacity in a tunnel. The Bridge Propagation Analysis module has the same objective that the previous block, but concerning the analysis in a bridge. The Interference Analysis module makes use of the parameters and results obtained by the previous block and, taking into account other input parameters, estimates the coverage, the capacity and the interference of the system. This module operates in the same way for both tunnels and bridges, although with slight modifications in some parameters, as explained in the following subsections.

The tool is able to analyse the influence of the variation of the tunnel and bridge characteristics, frequencies used in UL and DL, fading characteristics, BS antenna radiation pattern, interfering BSs’ location and other parameters, on coverage, capacity and interference of the system. For that purpose, the simulator uses a snapshot approach.

The simulator has been programmed in C++ programming language, using Borland C++ Builder software [CODE08], enabling an easy upgrade, since each module developed is located in a different unit. The user’s manual, explaining how the simulator must be used, is presented in Annex D.

4.2 Modules Description

This section presents the characteristics, the input parameters and the goals of the three modules constituting the simulator.

4.2.1 Tunnel and Bridge Propagation Analysis Modules

The first module studied is the tunnel propagation analysis module. In this module two different approaches are considered. In the first, the objective is to obtain the transmission power required in the BS to cover a certain number of users within a given distance d. This approach is useful in the sense that when the distance to be covered is known, an optimum solution, i.e., the minimum transmission power required, is obtained. The second approach consists in obtaining the maximum distance covered by a BS with a certain transmitted power.

To perform the network analysis, some parameters are considered in this module:

- Tunnel width and height or section area;
- BS and MT position in the tunnel (in both *x* and *y* axis);
- Permittivity of the tunnel;
- Roughness of the tunnel walls, radius, starting point and length of the curve, if there is one;
- Frequencies used in both UL and DL;
- BS antenna gain (choosing an antenna from a file, which radiation pattern is created to obtain the antenna gain for each distance);
- MT antenna gain;
- User and cable losses;
- Users bit rates;
- Fast fading percentage and *K* parameter for the Rice distribution;
- Fast fading percentage and standard deviation for the Rayleigh distribution, if a curve is considered;
- Slow fading percentage and standard deviation;
- Number of users in the sector;
- Distance of the user being studied and of the other users if the first approach is selected, or the BS transmitted power for the second approach.

For the first approach the simulator operation is shown in Fig. 4.2. If the power transmitted is the parameter to obtain, due to the limited number of codes available, the model initially calculates the number of users that can be served, from all the users in the sector, based on the spreading factor considering a single carrier. After that, another calculation is done to obtain the number of users served based on the load factor. This is done since it is considered that the load factor for UL cannot be higher than 0.75, while for DL the maximum value allowed is 0.5. As explained in Section 2.2, both these calculations are required since they represent the limitations in the capacity in UMTS.

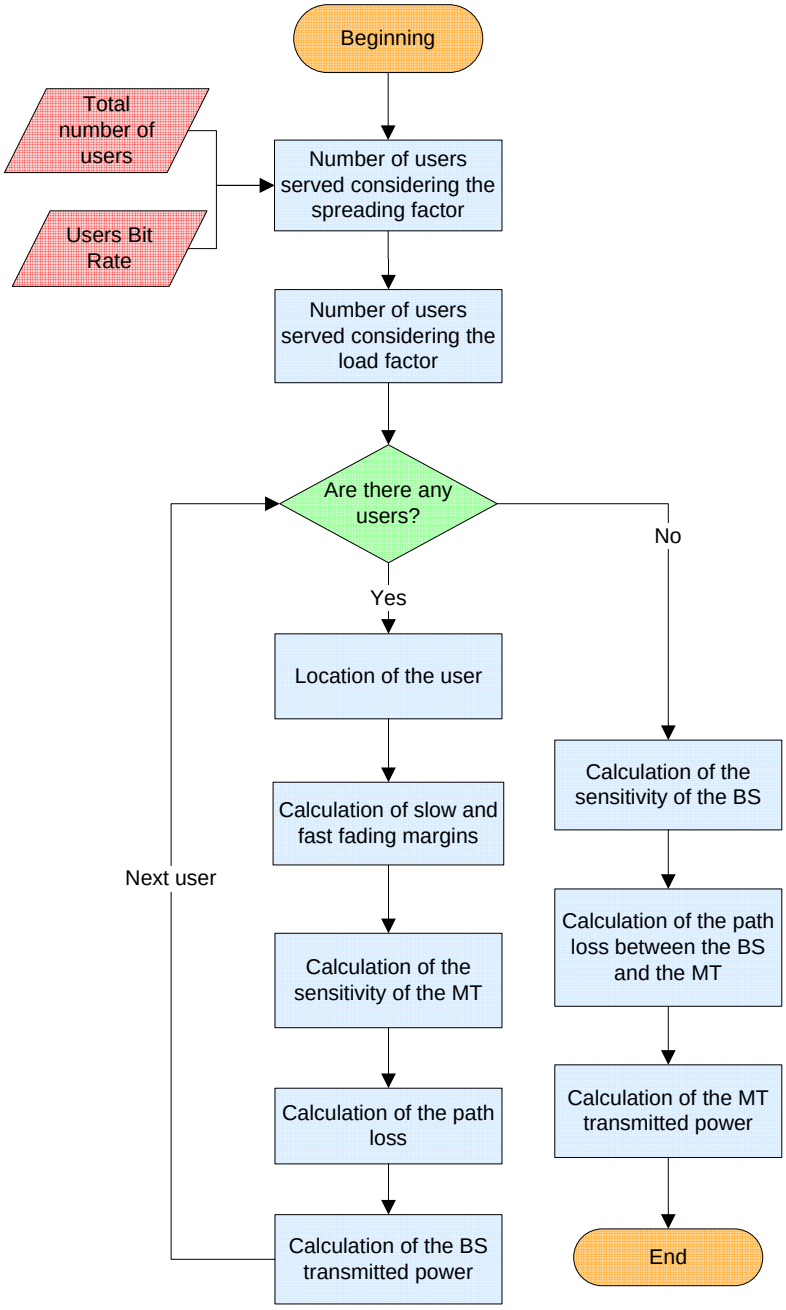

Figure 4.2. Simulator operation for the first approach.

One of the users is chosen to be the one being studied. For that particular user the distance to the BS is defined as well as the position in the *x* axis and the service data rate. For the other users there are some parameters considered: the distances between them can be equal, i.e., they can be distributed in the tunnel with the same distances between each other, or they can be generated at random distances from the BS. Regarding the data rates, they can be the same for all users or be randomly generated for each user. Furthermore, in what concerns their position in the *x* axis, they can be placed in a certain position in the tunnel or be generated with random values of *x*, being these random values restricted to two particular regions in the tunnel, which corresponds to a more realistic situation, one region being between $w/8$ and $3w/8$, and the other region located between $5w/8$ and $7w/8$, as shown in Fig. 4.3, where the grey area represents the locations where the users are generated. These

intervals were chosen, as mentioned, to approximate the model to a real situation in railway and in road tunnels, since users in trains or cars, normally, are not in the centre neither close to the tunnel walls.

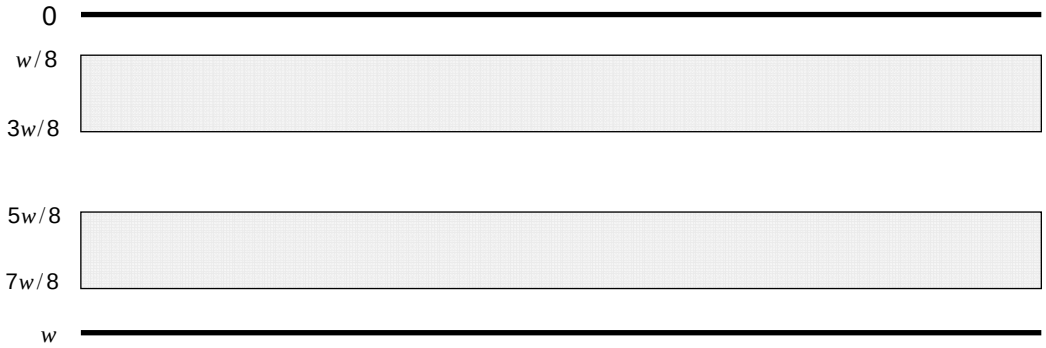

Figure 4.3. Representation of the regions where the users are randomly generated.

As already mentioned, if there are no curves in the tunnel, the Rice Distribution is used to account for fast fading. For that purpose an extrapolation was done to obtain the fast fading margins, using some values for the fading percentage and for the *K* parameter, as described in Annex E. In the simulator, it is possible to choose any combination of those presented in Table E.1. For the Rayleigh distribution (fast fading) and for the log-normal distribution (slow fading) two functions, developed in [Bati08] and [Marq08], that calculate the fading margins given the percentages and the standard deviations, were adapted.

The next step is the calculation of the sensitivity of the receiver, which is the MT in DL and the BS in UL, with (A.6) presented in the Link Budget in Annex A. The sensitivity is obtained considering only noise, since the interference is not yet calculated. Therefore the receiver sensitivity is again estimated after the calculation of the interference, being then considered both the noise and the total interference (intra-cell plus inter-cell). The received power is obtained with (A.10).

With the propagation models used for tunnels presented in Section 3.2 the path loss is obtained. For DL, for each user, whose position in the tunnel is known, the propagation attenuation is calculated. For this purpose, the break point is first obtained being then applied (3.12) or (3.13) according to the distances between the BS and the MT, noting that if there are curves and if the MT is in or after the curve the parameter L_{curv} is used. The path loss considering the fading margins, the indoor penetration and the soft handover gain is then estimated with (A.13). The power transmitted by the BS for each user is obtained with (A.1), taking 25% additional power for signalling and control into account. The total power transmitted by the BS is obtained as the sum of the powers required for each user. In UL, the additional signalling and control power is not considered, since the signalling and control are normally performed by the BS, and the path loss is only calculated for the user being studied as well as the power transmitted.

This module ends with the presentation of the parameters calculated, being also represented in a figure the position of the MTs and of the BS in the tunnel, as well as a graph with the curve of the path

loss and another with the received power variation with the distance. Additionally, an output file is created where the input and output parameters are presented, as well as the path loss and the power received variation for various distances between the BS and the MT being studied.

For the second approach, the simulator operation is described in Fig. 4.4. In this approach some assumptions are taken. The maximum distance is obtained for a single user case, so the number of users served is not calculated since just one user is considered. The sensitivities of the MT and of the BS are calculated with (A.6) according to the service selected for the MT, the received power being obtained with (A.10). In what concerns fading, the same steps explained for the first approach are considered.

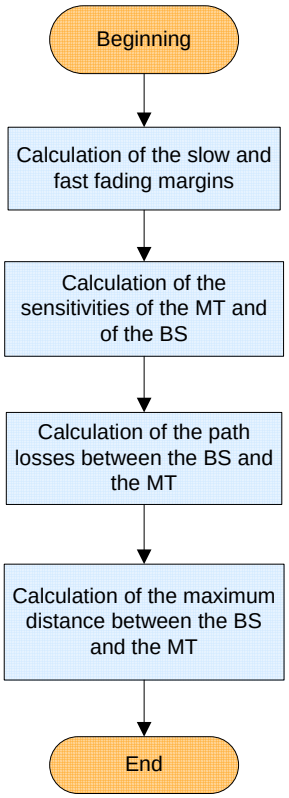

Figure 4.4. Simulator operation for the second approach.

The power transmitted by the BS is an input parameter, thus, the maximum path loss allowed to guarantee that the MT has a power equal to the sensitivity is obtained with (A.1) and (A.13). Knowing this value, the maximum distance can be obtained with (3.12) or (3.13). It is assumed that the MT transmission power is the maximum allowed, i.e., 21 dBm, which can be a limitation to the maximum distance between the BS and the MT, since the distance is not predicted based only on the BS transmission power. It should be noted that there are different values of distance with the same path loss. This happens due to the characteristics of the radiation pattern of the BS antenna, which has an impact on the BS transmission power according to (A.1). Similarly to the first approach, the parameters calculated are presented, and an output file is created with the input and output parameters and the variation of the path loss and of the power received with the distance.

This module includes also an option to study the parameters referred if there are no cars or trains in the tunnel. In this case, the fading margins are considered null, since there are no changes on the environment. This approach is useful to compare with the case where cars or trains are considered.

The second module to be analysed is the bridge propagation analysis module. This module can be compared to the module described for tunnels, since many of the ideas are identical, the propagation models and other aspects that are explained in the next paragraphs being different. The same two approaches used in tunnels are studied here, thus, the model operation can be described by Fig. 4.2 and Fig. 4.4, respectively, for each approach.

The requested parameters for this module are the same considered for the tunnel case, except that the bridge width is required instead of the tunnel characteristics and the Rayleigh distribution is not used. Moreover, an additional parameter is considered to take the down tilt of the BS antenna into account, with the tilt angle as the input parameter, since in bridges the antennas have normally this implementation characteristic.

In this case, the number of users, the sensitivities of the BS and the MT, and the distances between the BS and the MT are estimated as in the tunnel. The position of the users in the *x* axis can be fixed or they can be randomly generated in the bridge, in the same two regions described for the tunnel, and shown in Fig. 4.3.

The next step is the calculation of the path loss for each user. As explained in Chapter 3, two different propagation models are used to predict this parameter. The simulator includes an option to study the cases with or without traffic. The path loss is then obtained with (3.15) or (3.16). Knowing the path loss, the power transmitted for each user is obtained with (A.1), the total power transmitted by the BS and the power transmitted by the MT studied being then calculated.

This module ends with the representation of the location of the users and of the BS in the bridge, being a graph with the variation of the path loss with the distance as well as a graph with the variation of the power received with the distance also presented.

4.2.2 Interference Analysis Module

After the calculation of the power transmitted by the BS and the MT, the interference must be estimated to obtain new and more realistic values for the received and transmitted powers. With this purpose, the interference analysis module was developed, with the operation presented in Fig. 4.5. This module is also responsible for the estimation of the carrier-to-interference ratio (C/I). It works for both tunnels and bridges in the same way and with the same structure. Some of the input parameters required in this module are obtained from the module applied previously, while others are needed:

- Fast and slow fading margins;

- Power transmitted by the BS for each user;
- Distance of the users to the BS being analysed;
- Path loss for each user;
- Service used by each user;
- Number of interfering BSs;
- Distance of each interfering BS;
- Position of each interfering BS;
- Orthogonality factor.

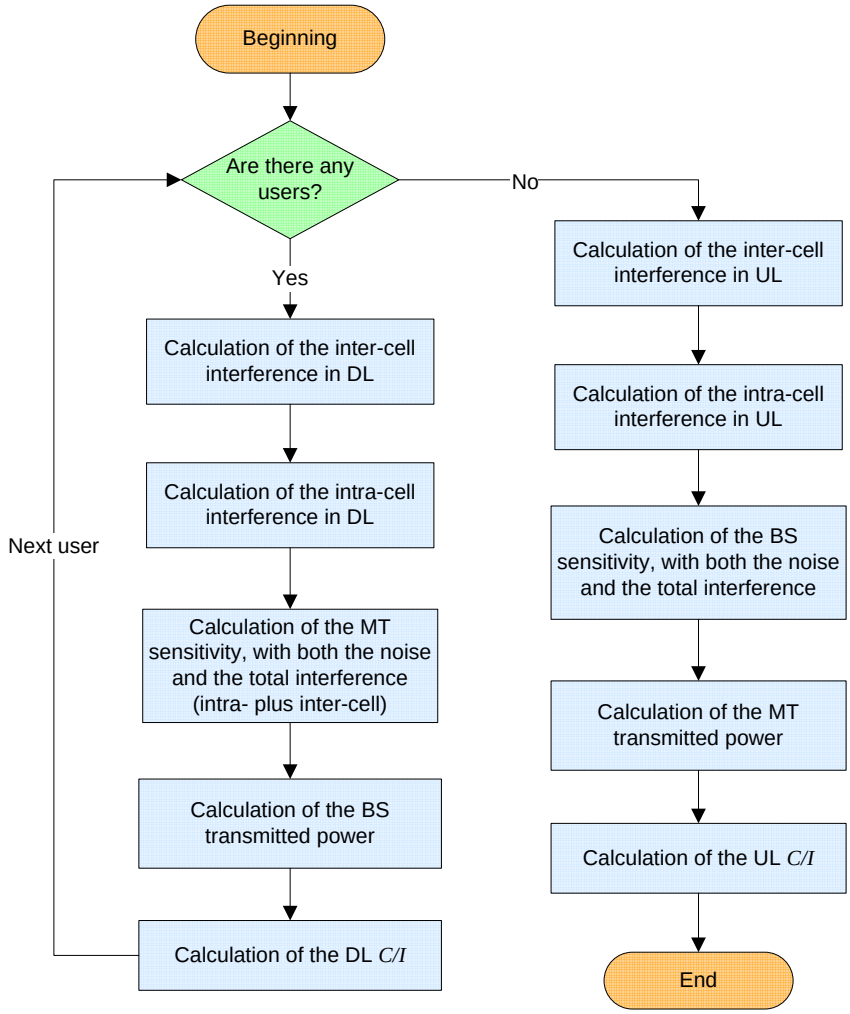

Figure 4.5. Interference module operation.

The interfering BSs can be positioned in front or behind the sector being studied. Note that in the environments being studied, each BS is composed of two sectors, since this is a normal approach in these cases. Figure 4.6 illustrates the relative positions of each interfering BS. The antenna in blue represents the sector being studied. Therefore, both sectors of the BS represented in green are positioned in front of the sector being studied, while those illustrated with red are behind. The yellow one corresponds to the other sector of the BS studied. If a bridge is being studied, an additional assumption can be taken. A BS located in the margin of the bridge, which is intended to cover a certain area outside the bridge, can cause interference to the sector in study. Therefore, the simulator

allows the positioning of interfering BSs in such places as shown in orange in Fig. 4.6. In that case the angle δ is needed to know the location of that BS, being an input parameter.

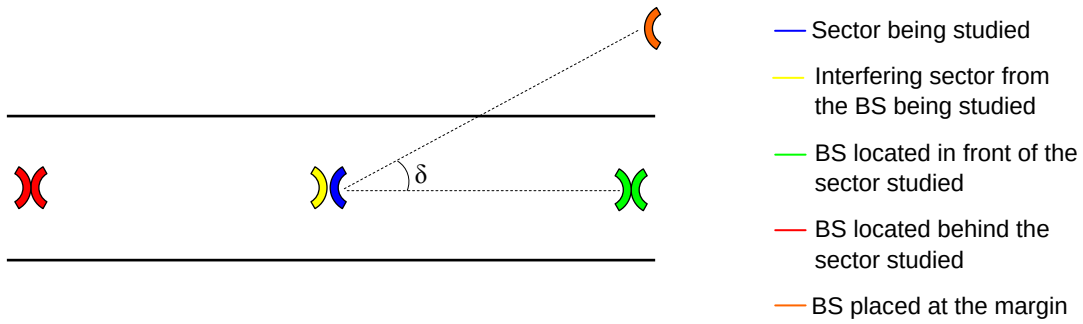

Figure 4.6. Representation of the positions of the interfering BS antennas.

The module begins with the estimation of the inter-cell interference in DL, for each user, with (3.19). For this purpose, the power transmitted by the interfering BSs is considered equal to the power transmitted by the BS being analysed, this being a good approximation, since the environmental characteristics are similar along the tunnel and the bridge. The path losses considered are those obtained in the previous block for the tunnel or the bridge, according to the environment being studied.

The intra-cell interference in DL is the next parameter analysed, using (3.17). This parameter is calculated for each user, considering that the remaining ones in the sector are interfering, since the interference suffered by each user is needed in the calculation of the sensitivity of the receivers, thus, to obtain the BS transmission power. Knowing the inter- and intra-cell interferences, the total interference for each user is obtained. Then, the sensitivity for each MT is calculated considering, in (A.6), the noise and the interference. The power transmitted required in the BS for each user is obtained with (A.1) as well as the total power transmitted by the BS. Finally, DL C/I is estimated. A relevant note is that the maximum BS transmission power is around 43 dBm, meaning that, if the power obtained is higher than this value, some users cannot be served.

In UL, the first step is also the calculation of the inter-cell interference, with (3.20). In this case, the number of users in each interfering cell as well as their position in the sector and their transmitted power are considered equal to those parameters in the sector being studied. Again, this is done to simplify the module operation and it is a good approximation, since, on average, the number of users in a sector, in tunnels and in bridges, is approximately the same. The BS received power from the interfering cells is estimated with (A.1).

The intra-cell interference in UL can be obtained with (3.18). The power received in the BS from each MT in the cell is at least equal to the sensitivity of the receiver plus a margin, since power control is taken into account. The sensitivity of the BS is obtained with (A.6) considering the noise and the total interference previously calculated. The power transmitted by the MT being studied is then calculated as well as C/I. In what concerns MTs, the typical value for the maximum transmission power is 21 dBm, meaning that a higher value for this parameter indicates that the MT is not able to

communicate with the BS.

This module ends with the presentation of the parameters calculated, as well as a graph with the variation of the MT received power with the distance. Additionally, an output file is created with the information concerning the inter-cell interference caused by each sector in UL and DL, the intra-cell interference for UL and DL, and the final values for both the BS and the MT transmitted powers.

4.3 Input and Output Files

In order to run the simulator, an input file, concerning the radiation pattern of the BS antenna, is needed in both the SIM_Tunnel and the SIM_Bridge modules. This file, here named “Antenna.TXT”, contains the information to create the radiation pattern of the antenna for the horizontal and vertical patterns. A function in the simulator reads this file and obtains the BS antenna gain for each direction.

The SIM_Tunnel module creates one output file, “Tunnel_parameters.xls”, which contains the input parameters inserted and the fading margins, the BS antenna gain, the path loss, the attenuation due to curves, the power received in the MT of the user being studied and in the BS for each distance, as well as the transmitted powers required in both the BS and the MT.

The SIM_Bridge module also creates one output file, “Bridge_paramters.xls”, containing the same information as that referred in the previous module except the attenuation caused by curves, since they are not considered in bridges.

The SIM_Interference module creates the “Results.xls” file, which contains the intra-cell interference values for UL and DL, the inter-cell interference caused by each BS in DL and the inter-cell interference caused by the MTs in UL. The total interference is also presented, as well as both the BS and the MT transmitted and received powers.

4.4 Simulator Assessment

In order to evaluate the simulator, it must be assessed. For that purpose, all the steps responsible for carrying out calculations were validated using several tools and approaches. The link budget and the propagation model calculations done by the simulator were confirmed and validated, step by step, using the Microsoft Excel software and a calculator. For both tunnels and bridges, several different approaches were carefully chosen and analysed to cover all the calculations done by the simulator so that it can be assured that it is working properly.

For the tunnel, for the first approach considered, the situations with and without a curve, with vehicles and without them, varying the number of users, the distances covered, the data rates of the users, the positions of the users and of the BS, and the fading margins, were tested using several different combinations. This way, all the steps were evaluated and confirmed with calculations. Moreover, for the second approach, which goal is to obtain the maximum distance covered by a BS, the same situations were analysed, but with one user, since this is the way this approach is used.

Regarding the bridge, similar to the evaluation done for the tunnel, several combinations were analysed. In this case, the situations with and without traffic, varying the distances covered, the positions of the users and of the BS, the types of service, and the fading margins, were studied. In what concerns the second approach described, the same procedure was taken, but with only one user being served.

For the interference analysis module, several cases were studied for both the tunnel and the bridge scenarios. The intra- and inter-cell interferences for UL and DL were simulated for all the situations previously referred, and the calculations were checked. The number of interfering BSs, as well as their positions and distances were varied. For all the cases analysed, all the calculations and results were confirmed, being the simulator validated.

Regarding the fading margins, simulations done in [Bati08] and in [Marq08] have shown that the Rayleigh and the Gauss distributions show coherence with the theoretical results, being the average mean error below 0.8 and 1.1%, respectively, for each distribution. As mentioned before, these distributions were adapted from [Bati08] and [Marq08],

Since random parameters are used in the simulator, there is the need to estimate the minimum number of simulations that must be performed to achieve statistical validity of the results. Therefore, an analysis was performed to obtain that number of simulations, concerning the simulation time – 100 simulations take approximately 1 hour – and the parameters variation with the increase of the number of simulations. This study was done for both the tunnel and the bridge; however only the first approach explained was considered, since for the second approach no random parameters are used.

In the case of tunnels, two situations were simulated in a tunnel of 8 m width and 6 m height, with 25 users randomly generated in a 500 m range, the user studied being at 20 m from the BS in the first case, and at 500 m in the second case. All users were considered with the voice service. These parameters were chosen to approximate the simulations to a real case. Moreover, the simulator principle is basically the same, meaning that the results, concerning the minimum number of simulations required to achieve statistical validity, can be generalised for other situations with different parameters.

In order to evaluate the performance of the simulator for the various numbers of simulations, the relative mean error is also analysed. Figure 4.7 presents the variation of the BS transmission power for different numbers of simulations, for both cases. The relative mean error of this parameter, comparing each case with the 100 simulations case, is presented in Fig. 4.8, being obtained as

$$\bar{e} = \left| \frac{z_r - z_i}{z_r} \right| ; \qquad (4.\ 1)$$

where:

- z_r : reference value;
- z_i : sample i .

It is possible to observe that the relative mean error is below 1% when the number of simulations is equal or higher than 50. Regarding the other parameters studied, the graphs concerning the relative mean error are not here presented since errors below 1% were obtained. Therefore, it can be concluded that 50 simulations is the most suitable number of simulations since the results are statistically valid and the simulation time is reduced to about half an hour.

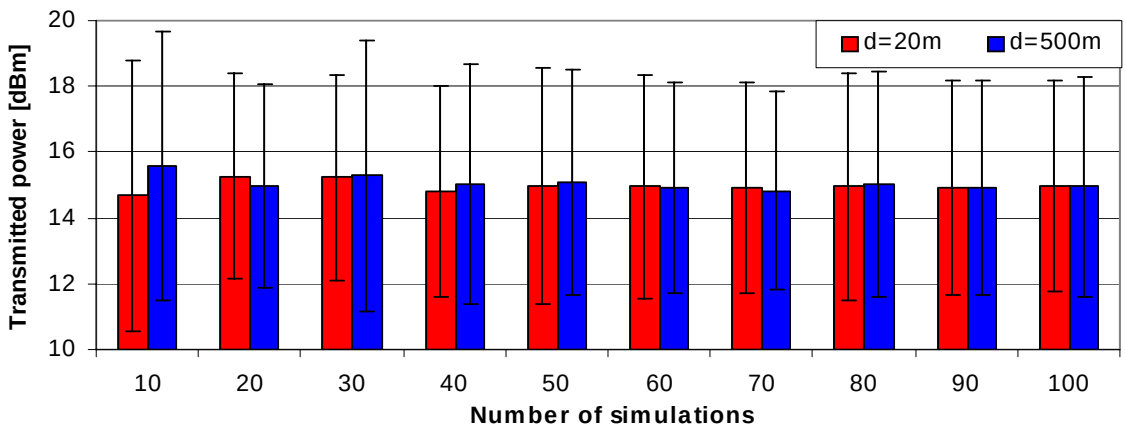

Figure 4.7. BS transmitted power in the tunnel, with the number of simulations.

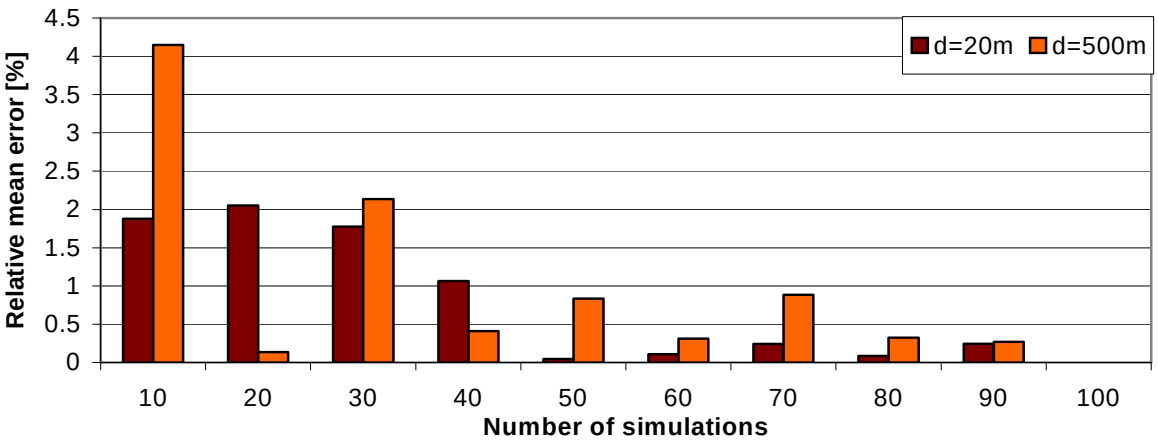

Figure 4.8. Relative mean error of the BS transmitted power, with the number of simulations, in the tunnel.

Concerning the bridge, the same analysis is considered. In this case, four different situations were studied all considering 20 users randomly distributed in a 500 m range. In the first case, no traffic was considered and the user being studied is at 20 m from the BS. In the second, the same situation is considered, but with the user at 500 m from the BS. In the third case, the user being studied is at 20 m

from the BS and traffic is considered. In the fourth, the user is 500 m far from the BS and again traffic is accounted for. Additionally, for all cases, 7º of down tilt was accounted in the BS antenna. These scenarios were considered, since they represent typical approaches in reality. It is important to point out the fact that the simulator principle is identical for other cases so the results, regarding the number of simulations, can be generalised for other cases.

The BS transmission powers for the cases with and without traffic are shown in Fig. 4.9 and in Fig. 4.10, respectively, the relative mean errors for both distances being presented in Fig. 4.11 and in Fig. 4.12. It is possible to conclude that 50 simulations seem to be the most suitable number of simulations to achieve statistically valid results, since the relative mean errors are below 1% and the simulation time is reduced. Similar to the evaluation done for the tunnel case, only the power transmitted by the BS is presented since for the other parameters this error is always below 1%.

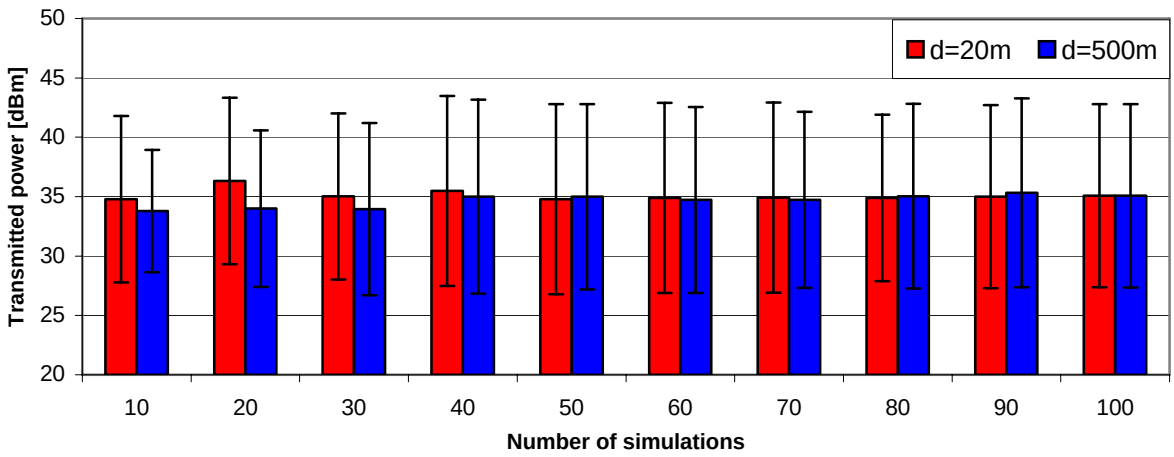

Figure 4.9. BS transmission power, with the number of simulations, in the bridge, with traffic.

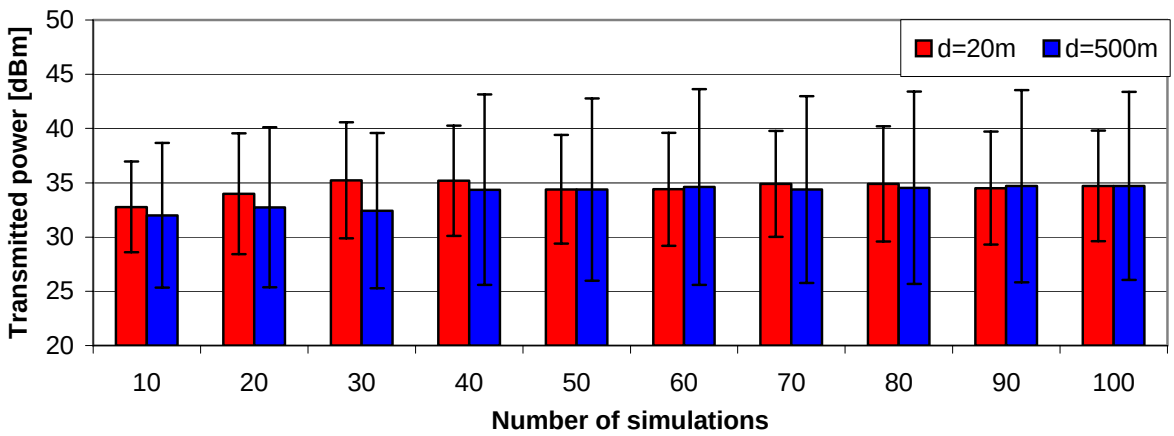

Figure 4.10. BS transmission power, with the number of simulations, in the bridge, without traffic.

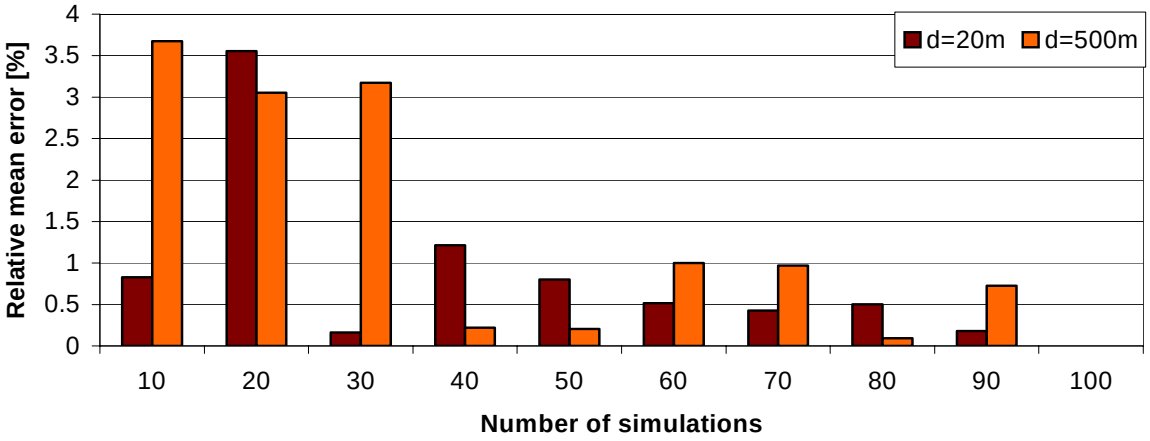

Figure 4.11. Relative mean error of the BS transmission power, with the number of simulations, with traffic.

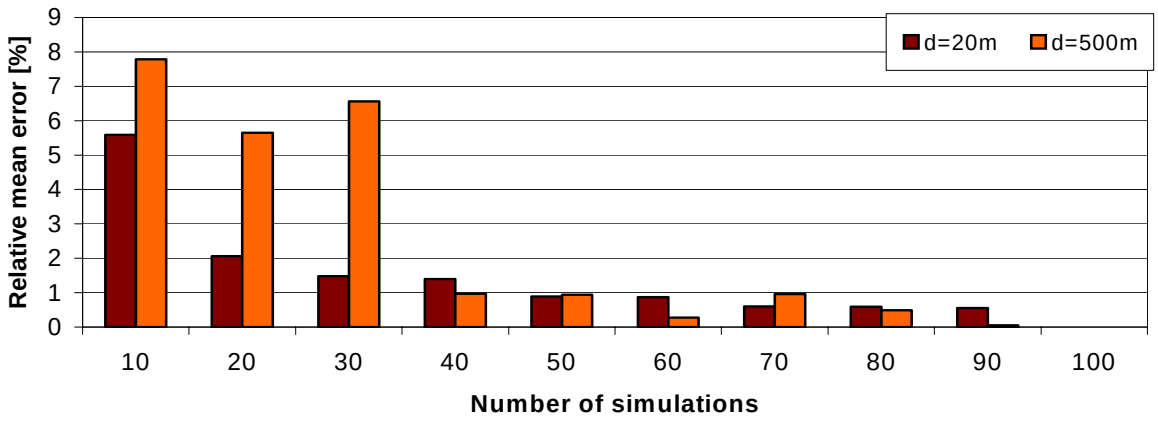

Figure 4.12. Relative mean error of the BS transmission power, with the number of simulations, without traffic.

Chapter 5

Results Analysis

This chapter contains the descriptions of the scenarios considered as well as the analysis of results. First, the default scenarios are presented, then the results concerning several parameter variations being studied. This analysis is performed for both the tunnel and the bridge. Additional studies were also performed for two particular scenarios. The chapter ends with the presentation and analysis of the results obtained in the measurements performed, a comparison with the theoretical results being done.

5.1 Scenarios Description

In order to evaluate the coverage, capacity and interference in the environments being studied, a default scenario was conceived for each case.

For the tunnel, the scenario detailed in Table 5.1 is used in the first approach detailed in Chapter 4. Thus, the objective is to obtain the power transmitted by the BS and by the MT, as well as C/I. The tunnel dimensions and the permittivity are typical values observed in railway tunnels. The number of users is also a reasonable value in the range of 500 m. The BS position in the tunnel is presented in Fig. 5.1, being at 4 m height and at 4 m way from horizontal walls. Several variations in the parameters were performed, presented in Section 5.2, in order to analyse their impact on the results.

Table 5.1. Default scenario for the tunnel.

Tunnel width [m]	8
Tunnel height [m]	6
Permittivity	5
Number of users	25
Sector range [m]	500
MT distances to the BS [m]	50, 100, 200, 300, 400, 500
BS position (*x*, *y*) [m]	(0,1)
MT position (*x*, *y*) [m]	(2,-1)
Other MTs positions	Random
Indoor penetration attenuation [dB]	9
K parameter of the Rice distribution [dB]	1.5
Gaussian standard deviation [dB]	4

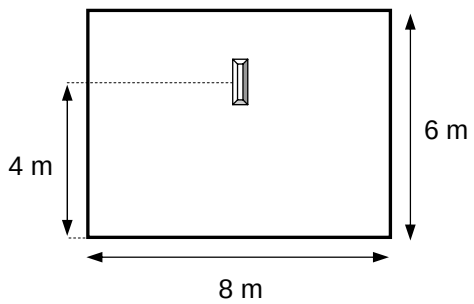

Figure 5.1. Representation of the BS position in the tunnel.

Regarding the bridge, the values presented in Table 5.2 were carefully chosen to represent a normal scenario in a bridge. In this case, a non traffic situation is considered, with 15 users in a 500 m range. The influence of the parameters on the final results is analysed in Section 5.3, where comparisons are made with the default scenario.

Table 5.2. Default scenario for the bridge.

Bridge width [m]	22
BS position (*x*) [m]	0
BS height [m]	5
MT position (*x*) [m]	6
Other MTs positions	Random
MTs height [m]	1
Distances of the MT to the BS [m]	50, 100, 200, 300, 400, 500
Number of users	15
Sector range [m]	500
Indoor penetration attenuation [dB]	6
K parameter of the Rice distribution [dB]	1.5
Gaussian standard deviation [dB]	5
BS antenna tilt [º]	7

In what concerns the BS antenna, the K742266 [Kath08] is one of the antennas used in the environments studied, thus this is the antenna considered, the radiation pattern being presented in Annex F. The frequencies, the noise figure, and the user and cable losses are also typical values used in UMTS, presented in Table 5.3. In the default scenario, all users are considered with the voice service; however, the variation of this parameter is studied for both scenarios. In all the BS transmission powers presented in the next sections, 25% additional signalling and control power is considered. All the analysis are performed considering a single carrier.

For the interference analysis, for both cases, four interfering BSs are considered, two being at 1 km from the BS, one in front and one behind it, considering the distribution shown in Fig. 4.6, and two at 2 km, one of them being in front and the other behind the sector.

Additionally to the default scenarios, some particular scenarios in the city of Lisbon are presented, for both tunnels and bridges. In what concerns to tunnels, the Lisbon Underground and the Rossio tunnel are analysed. The bridges considered are the 25 de Abril and the Vasco da Gama ones. These scenarios were chosen since they constitute the main tunnels and bridges in the city of Lisbon, thus,

providing good conditions and being important places to be analysed.

Table 5.3. Default parameters for the link budget.

Parameter	DL	UL
Frequency [MHz]	2110	1920
Noise Figure [dB]	8	3
Signalling and control power [%]	25	0
BS radiation pattern	K742266	
MT antenna gain [dBi]	0	
User losses [dB]	4	
Cable losses [dB]	4	
Service	Voice (12.2 kbps)	

The Lisbon Underground has a length of approximately 37.7 km, and the construction in concrete is dominant [Metr08]. A representation of the section of the Underground tunnels is presented in Fig. 5.2, the section area being of approximately 44 m^2. It should be noted that the section presented is not equal in the whole extension of the Underground, however, it represents the most common cases, and the differences, when they exist, are not significant [Fari99].

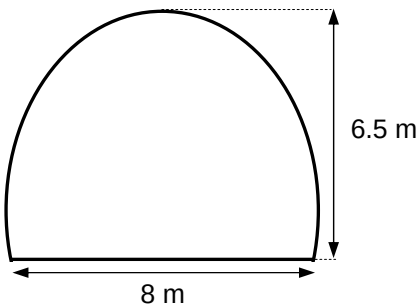

Figure 5.2. Representation of the Lisbon Underground's tunnels sections (based on [Fari99]).

The Rossio tunnel is a straight railway tunnel with a length of 2.6 km, the construction being also in concrete [Enge08]. Figure 5.3 shows an approximate representation of the tunnel section, which is circular, the height and the width of the tunnel being also presented. The section area is estimated to be of about 39 m^2.

In what concerns bridges, the main characteristics of both bridges are presented in Table 5.4. The 25 de Abril Bridge has a metallic structure and a significant number of steel wire strand cables, thus, an intense fading is expected due to the material characteristics. Since this is a relative short bridge, see Table 5.4, a considerable interference is expected, since the powers from the BSs located on the

margins of the river can be received along the bridge. In what concerns the Vasco da Gama Bridge, the construction is mainly in concrete, thus being different from the 25 de Abril one regarding the fading characteristics. Furthermore, this being a long bridge, the interference caused by the BSs located on the river margins is not so intense as that observed in the previous case, since the distances to those BSs are normally high.

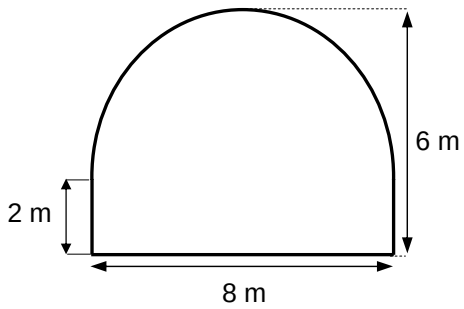

Figure 5.3. Representation of the Rossio tunnel section (based on [Enge08]).

Table 5.4. Characteristics of the 25 de Abril and Vasco da Gama Bridges [Fern99], [Luso08].

Bridge	Length [km]	Width [m]
25 de Abril	2.3	22
Vasco da Gama	17.2	30

5.2 Parameters Influence for the Tunnel Case

In this section, the results of the simulations performed for the tunnel are presented and analysed. First, the results obtained for the default scenario are shown. Afterwards, the results obtained with the variation of some parameters, regarding the tunnel dimensions and the number of users, among others, are presented and compared with the default scenario.

5.2.1 Default Scenario Analysis

In order to study the default scenario for the tunnel case, 50 simulations were performed. This number is, according to the study done in Section 4.4, the most suitable number of simulations to achieve statistically valid results.

For this analysis, and for all the studies performed in Section 5.2, the transmitted powers, for both DL and UL, were obtained with (A.1). The slow fading margin is around 6.6 dB while the fast fading margin is 10.5 dB.

The variation of the BS transmission power with the distance of the user to the BS is presented in Fig. 5.4. It is possible to observe that the transmitted power does not show significant variations when the user goes away from the BS. This was expected, since there are 25 users covered by the BS, randomly generated in a 500 m range. The power transmitted by the BS is distributed among all users, meaning that, if one user changes his position, the total power is not significantly affected. The value of 16.2 dBm obtained for the total power (including 25% of signalling and control) is acceptable since it is below the maximum transmission power allowed in a BS, which is about 43 dBm.

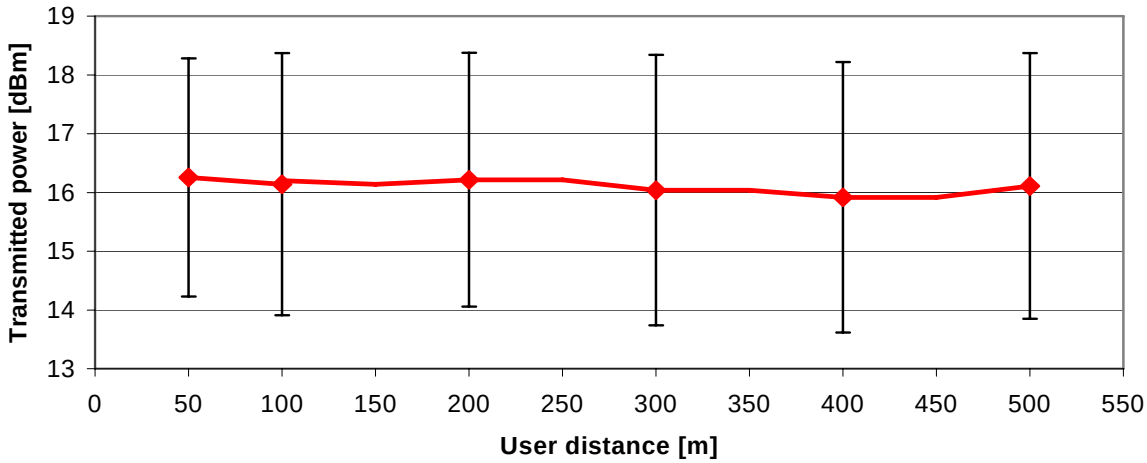

Figure 5.4. Power transmitted by the BS in the default scenario, with distance, in the tunnel.

Regarding the UL case, the variation of the MT transmission power with his distance to the BS is presented in Fig. 5.5. In this case, the power decreases from about 0.7 to -11 dBm when the distance increases from 50 to 500 m. It could be expected that the power transmitted by the MT would increase with his distance, but this is not what happens. This fact is related to the radiation pattern of the BS antenna, since when the MT is at 50 m from the BS, in the *x*=2 m position, the receiving antenna gain is about 8.6 dBi, increasing with distance to about 16.4 dBi at 500 m. Therefore, despite the increase in the path loss with distance, there is also an increase of the BS antenna gain, causing a decrease in the transmission power required in the MT when the user is far from the BS. Moreover, the path loss increase when the MT goes from 50 to 500 m from the BS, is of about 1 dB due to the small propagation attenuation with distance observed in a tunnel after the break point, which is located at around 87 m in this case. For all the cases, powers are below the maximum transmission power allowed to the MT which is around 21 dBm.

In what concerns the total noise power, the values were obtained with (A.7), being of about -124 dBm for DL and -129 dBm for the UL case. The interferences in UL and DL, for each distance considered, are presented in Annex G, Fig. G.1 and Fig. G.2, respectively, being possible to observe that, for DL, the interference is about 20 dB above noise while for UL the difference is of about 34 dB. Therefore, it is possible to conclude that noise is almost negligible in comparison with the interference when the receiver sensitivity is calculated with (A.6). In DL, the variation of the interference when the user changes his position is almost negligible. This is explained noting that neither the power transmitted to

the MT being studied nor the path loss between the BS and the MT experience significant variations, as already explained, therefore, according to (3.17) and (3.19), the interference remains almost unchangeable. It can be observed that the inter-cell interference is about 16 dB higher than the intra-cell one, since 4 interfering BSs are considered, each one with two sectors. Additionally, one sector from the BS studied is also causing interference, thus, a total of 9 sectors are interfering. Therefore, since the path loss decreases very slowly, after the break point, with distance, the powers transmitted by the interfering BSs are slightly attenuated, so their interference is higher than the intra-cell one. For the UL case, the same explanations are valid. In this case, the user distance is not relevant, since interference is caused by the other users. Interference is strongly dependent on the number of users, according to (3.18) and (3.20), being normally higher than in DL, since there are many MTs causing interference in the BS.

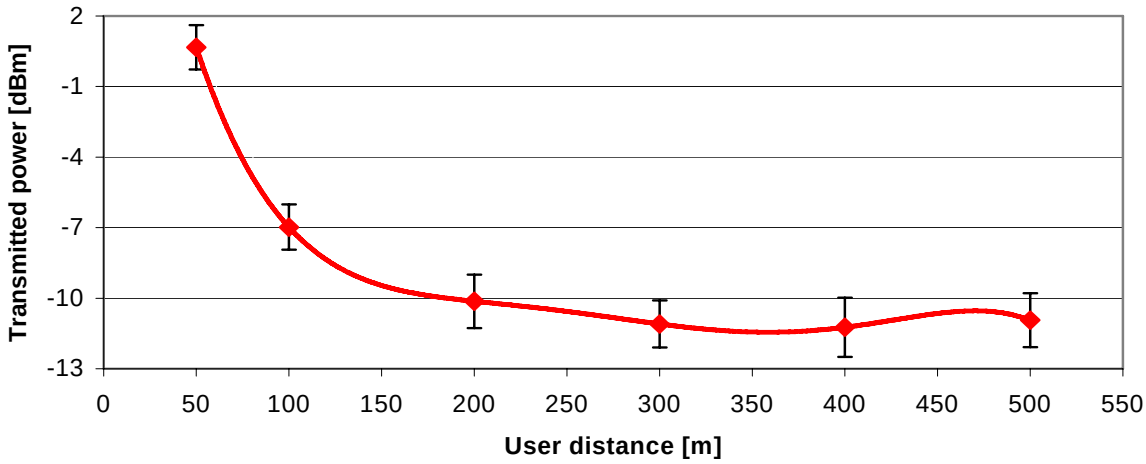

Figure 5.5. Power transmitted by the MT in the default scenario, with distance, in the tunnel.

C/I for both DL and UL is shown in Fig G.3. For the DL case, C/I is of about 13.6 dB, being around 10.5 dB for UL. It is possible to observe that the variation with the user's distance is almost null. This is explained by the behaviour of both the interference and the received power, where no significant variations are found when the distance of the user to the BS increases. In what concerns the received power, it is calculated considering the interference, therefore, it accompanies the variations experienced by interference, C/I being almost constant. For the same reasons, the standard deviation is almost negligible. In UL this ratio is lower than in DL, which is a normal situation since the SNR is lower in UL, causing a decrease in the received power, thus, in C/I. Another important note is that the ratio must be higher than 0 dB, as it is in this case, to allow the communication between the BS and the MT. Otherwise, the interference would be higher than the received power and the communication would not be possible.

5.2.2 Variation of the Tunnel Dimensions

With the purpose of analysing the variation of the BS and MT transmitted powers, as well as the variation in the interference and in C/I, when the tunnel dimensions are changed, a set of

simulations is performed, where only one parameter is changed in comparison to the default scenario, namely, the one concerning the tunnel dimension.

The first case studied is the increase of the tunnel width from 8 to 12 m. In this case, the main difference in terms of propagation is that the waveguide phenomenon appears for a distance higher than that observed in the default case. Specifically, the break point is located at around 92 m from the BS while it is at 87 m in the default scenario. This was expected since, when the width increases, the waveguide phenomenon is lower. In the limit, it is possible to imagine a tunnel with an infinite width, where no waveguide phenomenon is present being the path loss given by the free space propagation model, since the break point would also be located at an infinite distance from the BS. Therefore, as expected, the transmitted power required in the BS is higher, since there is an increase in the path loss for all the users located at more than 87 m from the BS, the increase in the power being of about 3 dB, as shown in Fig. 5.6.

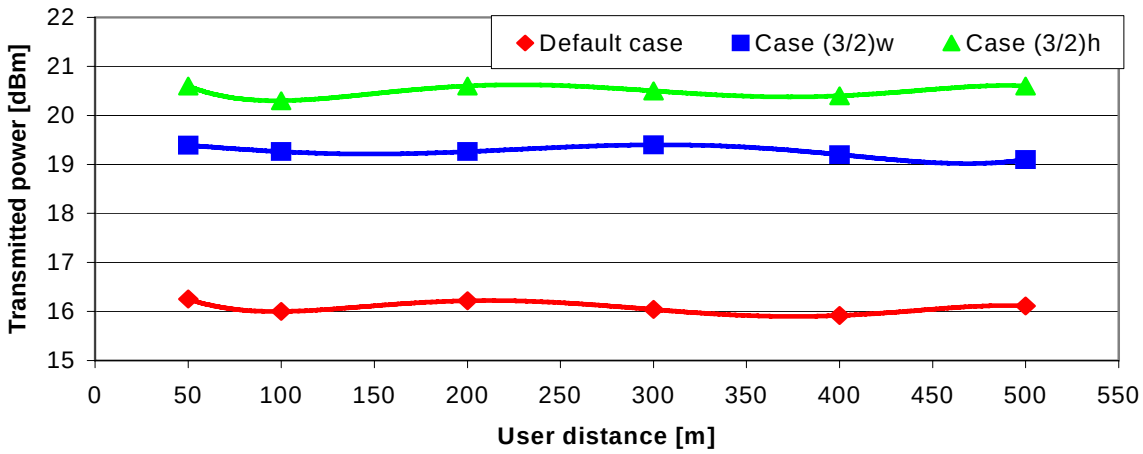

Figure 5.6. BS transmitted power, with distance, for different tunnel dimensions.

The power transmitted by the MT increases between 1 and 3 dB, as shown in Fig. 5.7, comparing with that observed in the default scenario, which is explained by the increase of the path loss between the MT and the BS.

The second case studied is the increase of the tunnel height from 6 to 9 m. In this case, as expected, the transmitted power required in the BS increases, as shown in Fig. 5.6, in comparison with the default case. The reason is similar to the previous case, being the break point at 111 m from the BS. The increase is in the order of 4.4 dB, thus, higher than in the previous case due to the increase in the break point location.

Concerning the MT transmitted power, there is also an increase, between 2 and 5 dB, comparing with the default case, as shown in Fig. 5.7. This behaviour is due to the significant increase in the break point, thus, in the path loss, which causes an increase of the transmitted power required in the MT. Moreover, there is also an increase in the UL interference, which contributes to the increase in the transmitted power.

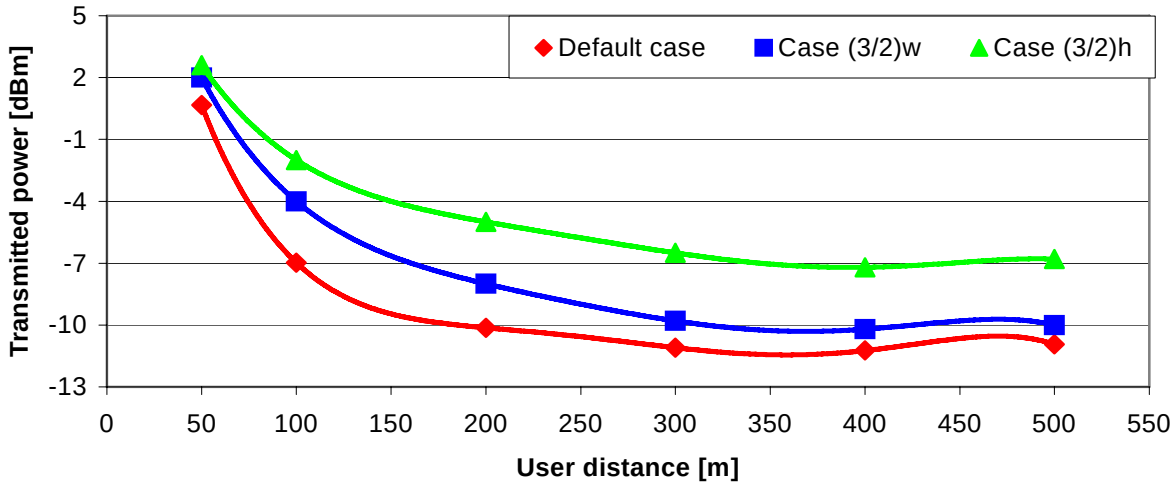

Figure 5.7. MT transmitted power, with distance, for different tunnel dimensions.

Concerning C/I, there are no variations, for the same reasons mentioned in the previous subsection.

5.2.3 Variation of the Number of Users

The variation of the number of users trying to communicate with the BS is important to analyse, since it causes variations in the transmitted power required in the BS and in the MT, as well as in the interference. Moreover, the capacity study is performed with this analysis. In that sense, four different numbers of users were considered in the sector being analysed, for each user distance referred to in the default scenario.

In Fig. 5.8, the variation of the BS transmission power with the number of users is represented. As expected, the power increases when more users are active. This increase varies from 12 to 17 dB according to the user distance, when 15 users are covered in spite of 5, while when 25 users are covered, the increase, comparing to the 15 users case, is of about 8 dB. With 35 users, the transmitted power increases about 5 dB comparing with the 25 users case. The higher increase from 5 to 15 users is explained by the higher increase in the interference in this range, due to triplication of the number of users. The variation with the user distance to the BS is almost negligible for more than 15 users. For 5 users this variation is more significant, since the position of one user is more important due to the lower number of users.

The standard deviations are not presented to allow a better observation of the graph; however, they are approximately the same as those presented in the default scenario. It is relevant to mention that the power transmitted is always below the maximum, 43 dBm, meaning that no coverage or capacity problems are expected. In Fig. 5.9, it is possible to observe the variation of the power with the number of users, for the user at 200 m, confirming the fact that higher variations are observed for lower number of users.

The variation of the MT transmitted power with the number of users is presented in Fig. 5.10. In this case, the increase of the power with the number of users is mainly due to the increase in the interference when a higher number of users is considered. Similar to the previous case, the transmitted power required in the MT is below the maximum, 21 dBm, thus no coverage problems are expected.

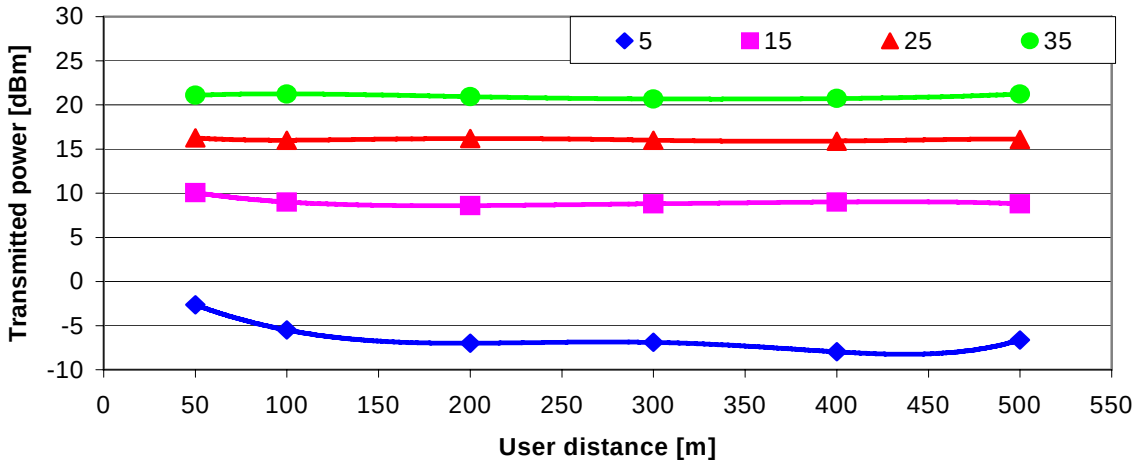

Figure 5.8. Power transmitted in DL, with distance, for different number of users, in the tunnel.

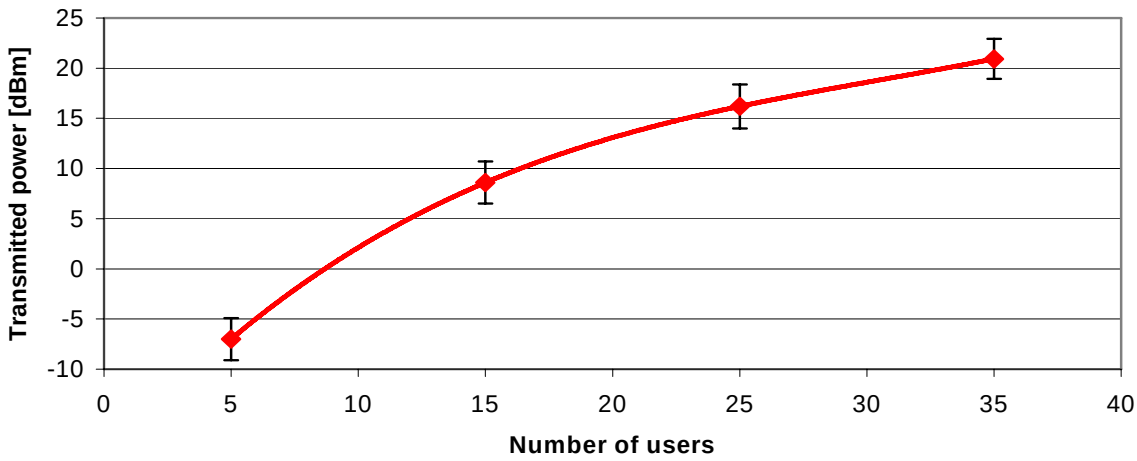

Figure 5.9. DL transmitted power with the number of users, in the tunnel.

The intra- and the inter-cell interferences variation with the number of users are presented in Fig. G.4 and Fig. G.5, respectively, for DL and in Fig. G.6 and Fig. G.7, respectively, for UL. As expected, the interference increases, for both cases, when the number of users increases. The behaviour of the DL and UL interferences is similar to that observed for the DL and UL transmitted power, respectively, since a variation in the interference causes a variation in the received power, thus, causing also a similar variation in the required transmission power.

Regarding C/I, no significant variations are observed with the number of users.

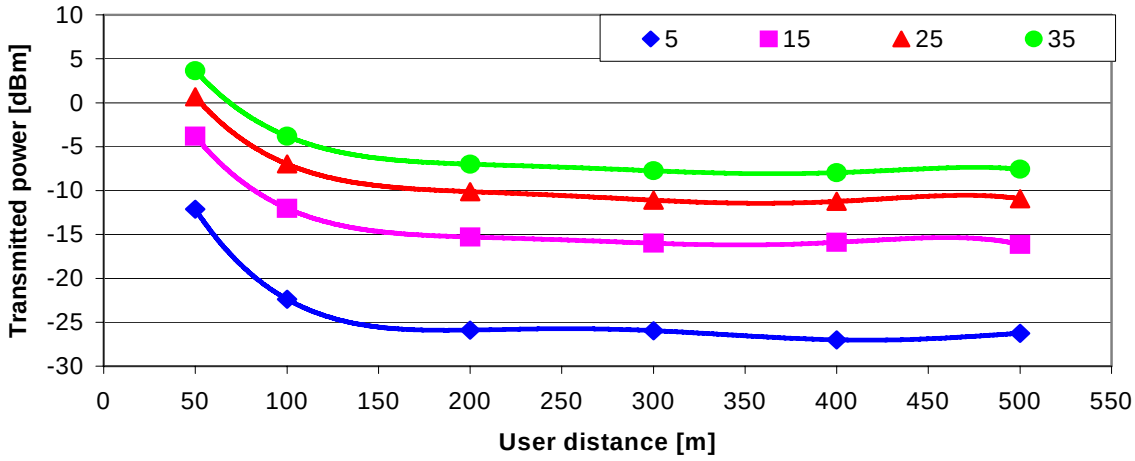

Figure 5.10. Power transmitted in UL, with distance, for different number of users, in the tunnel.

5.2.4 Variation of the BS Range

In the default scenario, the BS is covering the users located in a 500 m range. This is done since the simulator considers that the user is connected to only one BS. Therefore, the users in the BS range are covered only by that BS, the other BSs causing interference. It is interesting to analyse the variations in the transmitted power and in the interference when this range is changed. For this purpose, the ranges considered are 100, 300, 700 and 900 m, the comparison being done among all cases and the default scenario. In this case, since the range is not constant, only the case where the user studied is at 50 m is considered. The results and conclusions can be extended to the other cases, since the behaviour of the powers and of the interferences is already known. Moreover, according to the results already presented, this has proven to be the most demanding case in what concerns the required transmission powers.

The number of interfering BSs for each case is 4, however, the distance of the interfering BSs to the BS being studied varies for each case. In the first case, where the range of the BS is 100 m, two interfering BSs at 200 m and two at 400 m are considered. In the second case, two at 600 m and two at 1200 m are considered. For the 700 m range, two BSs are located at 1400 m and the other two at 2800 m. Finally, for the 900 m range, two interfering BSs are located at 1800 m and the other two are at 3600 m. This is done to allow a more efficient analysis of the influence of the BS range variation, in the sense that it approximates the planning to a real situation, where the BSs are normally equally spaced. This planning is done according to the number of users that it is wanted to cover in a certain region within a certain range. If the number of users is higher in a certain region, it is necessary to put the BSs closer to allow a good coverage and also the desired capacity of the system. Therefore, this study is important to help finding an optimum solution for the problem being studied.

The variation of the BS transmitted power for each case is presented in Fig. 5.11. The required transmitted power decreases when the BS range increase, mainly due to the behaviour of the BS

antenna radiation pattern, since higher gains are obtained for higher distances. Moreover, the interference decreases when the BS range increases, Fig. G.8, which is explained by the increase of the distance between the sector studied and the interfering BSs. The reduction in the power transmitted is in the order of 8 dB when the range goes from 100 m to 900 m.

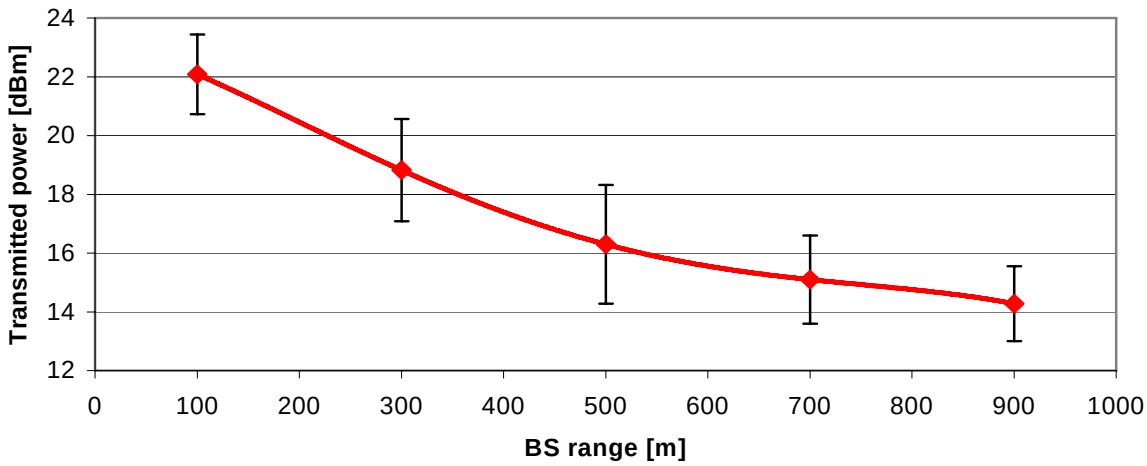

Figure 5.11. Power transmitted in DL with the BS range, in the tunnel.

In what concerns the MT transmission power, presented in Fig. 5.12, the same analysis can be done. The required transmission power in the MT decreases about 7 dB when the range of the BS increases from 100 m to 900 m. The main reason for that is again the increase of the BS antenna gain and the decrease of the interference, as shown in Fig. G.9. Similar to the previous case, the transmitted power is below the maximum allowed, meaning that no coverage problems are expected, for the user located at 50 m and also for the other distances, since the 50 m case is the most demanding situation regarding the transmitted power.

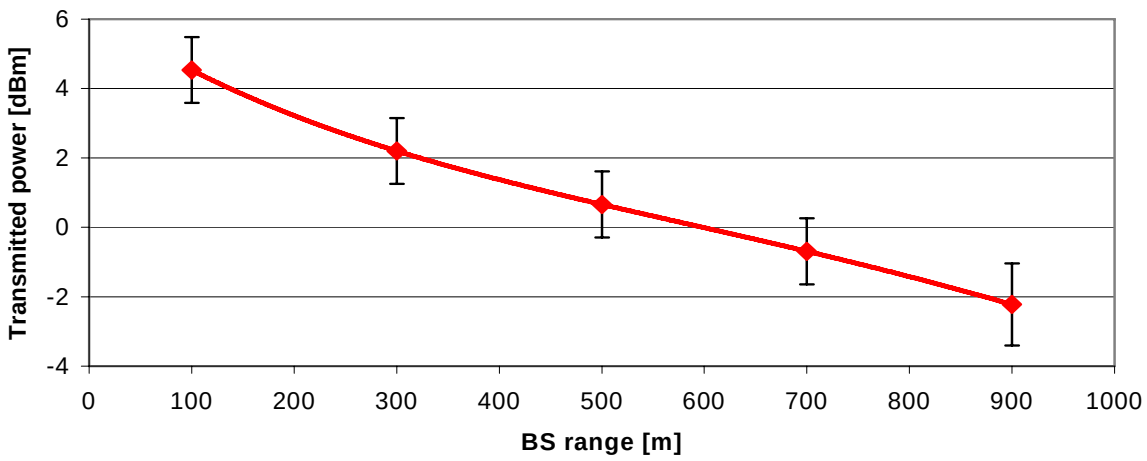

Figure 5.12. Power transmitted in UL with the BS range, in the tunnel.

C/I for both BS and MT do not show significant variations comparing with the default scenario.

5.2.5 Variation of the Services Used

The simulations performed so far consider that all the users are using the voice service, with 12.2 kbps data rate. However, since UMTS is being studied, it is important to analyse the influence of the variation of the services performed by the users.

For this purpose, several simulations are done, to analyse all combinations. For each case, the user service and the services performed by the other users are chosen. Similar to the previous case, only the case where the user is at 50 m from the BS is studied, since the results can be generalised for the other cases. In Fig. 5.13, it is possible to observe the variation of the BS transmitted power when the service of the studied user and of the other users is changed. For all the services, when the other users' services are fixed and the service of the user studied becomes more demanding, i.e., the data rate increases, the transmitted power increases, as expected, since more power is required in the BS to serve the user due to the higher sensitivity of the receiver. This increase is of about 15 dB comparing the more and the less demanding cases for the user studied.

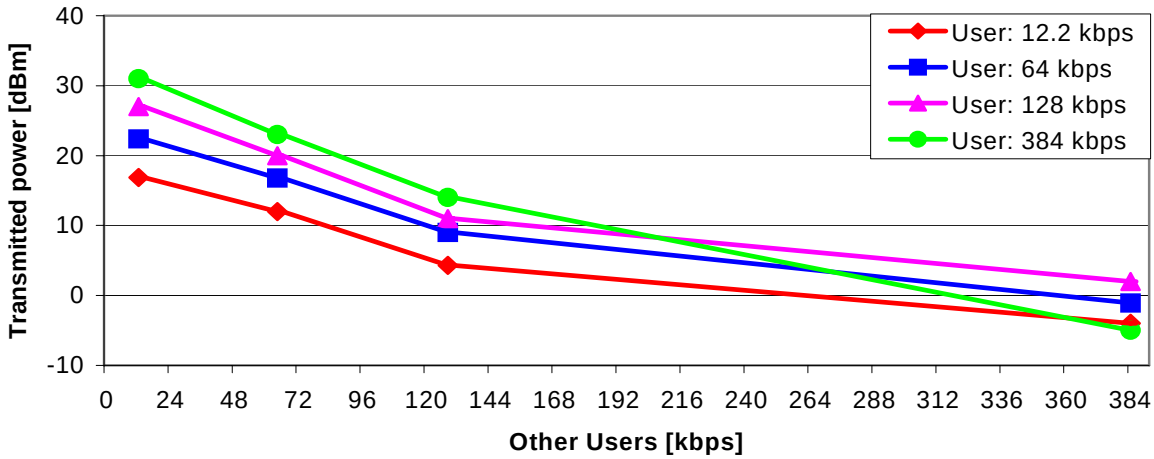

Figure 5.13. Power transmitted in DL with the services used, in the tunnel.

One interesting point is that, when the other users are performing a more demanding service, the power transmitted by the BS decreases. This is apparently incoherent with the explanation given in the previous paragraph. Actually, this is caused by the limitations in capacity present in UMTS, as mentioned in Chapter 2. When the users' data rates increase, a lower number of users can communicate with the BS due to that limitation, as shown in Table 5.5. Therefore, although the service is getting more demanding, the transmitted power decreases since the number of users served also decrease. To be more precise, when all the users are performing the voice service, 25 users are considered being all served by the BS. However, when all users are performing the most demanding data service, only 3 users are served by the BS; for the other cases the number of users is between these values. Therefore, even increasing the users' data rates, the transmitted power decreases due to this reduction in the number of users served. When all the users are considered with the 384 kbps service, a more significant decrease is observed in the power comparing with the other cases, since the number of users served is reduced to three, while when the user is performing other service being

the other users with the most demanding service, 4 users are served. Similar to the cases so far analysed, the transmitted power required in the BS is, for all the cases, below the maximum.

Table 5.5. Number of users for different services performed, in the tunnel.

Number of users		Other users [kbps]			
		12.2	64	128	384
User [kbps]	12.2	25	18	10	4
	64	25	18	10	4
	128	25	17	9	4
	384	25	13	7	3

In what concerns the MT transmitted power, the variation with the users' data rate is shown in Fig. 5.14. The analysis done for the BS power is also valid in this case. However, the difference is lower than that observed for the power transmitted by the BS, which is explained by the fact the MT does not consider directly the other users services when it communicates with the BS, so it is not so dependent on their data rates. A slight increase in the required transmission power is observed when the other users are performing the 64 kbps service. This can be explained by the small reduction in the number of users served, 18 users are served in spite of 25, in comparison with the case when they are performing the voice service. Therefore, since the UL interference increases when the users' data rate increase, the power required in UL also increases. However, when the user studied is considered with the 384 kbps data rate, that increase is not observed, since there is a reduction of 12 users in the capacity of the system. Therefore, a slight decrease is observed in the power required. Again, the powers are, for all the cases, below the maximum allowed.

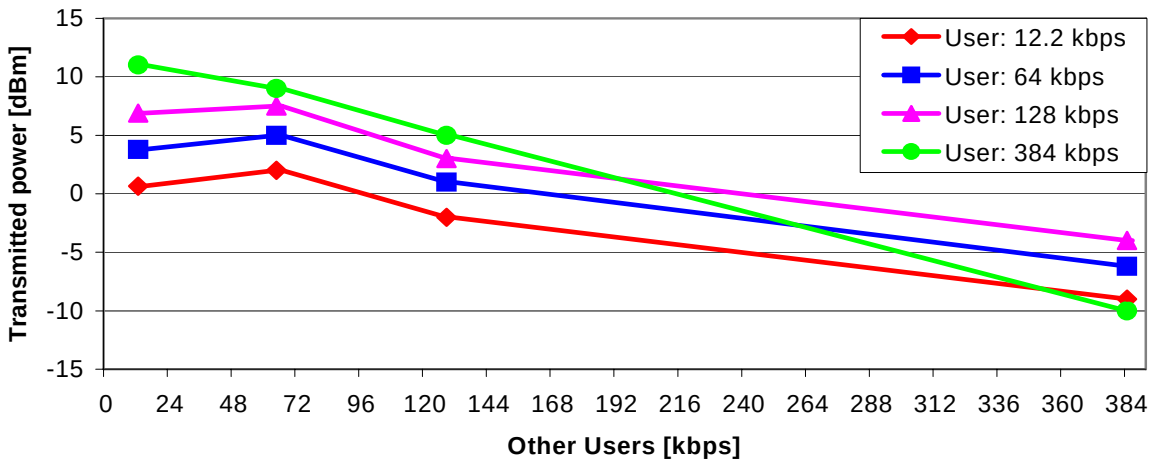

Figure 5.14. Power transmitted in UL with the services used, in the tunnel.

The variations in the interferences for DL and UL are presented, respectively, in Fig. G.10 and

Fig. G.11. The interference behaviour, for both cases, is similar to that observed for the transmitted powers, as expected, since they are related.

C/I variation is shown in Fig. G.12 and Fig. G.13, for DL and UL, respectively. As expected, C/I decreases when the service of the user becomes more demanding, the difference between the voice and the data services being in the order of 4 dB. This is explained essentially by the SNR values used, presented in Table A.2, which are lower for the data services, causing a decrease in the received power, thus in C/I .

5.2.6 Variation of the BS Antenna Radiation Pattern

So far, the BS antenna considered is the K742266, with the radiation pattern presented in Annex F. The influence of the BS antenna radiation pattern in the parameters studied is important to analyse, since it must be carefully chosen to have a more efficient system in terms of coverage and capacity. For that purpose, a study is done considering an omnidirectional antenna with 15.3 dBi gain.

Regarding the BS transmitted power, an increase of about 4 dB is observed when the omnidirectional antenna is considered. One of the reasons for this behaviour is the fact that the path loss is related with the antenna gain, (3.8), thus, a variation of the gain causes a variation in the transmitted power. Another reason is the increase of the interference, as shown in Fig. G.14 and Fig. G.15, respectively for the intra- and inter-cell interferences. Other important point is that the maximum antenna gain in the default case is about 1 dB higher than the omnidirectional antenna gain considered, thus, as expected, the power required is lower in the default scenario. However, for some users located close to the BS, the transmission power is higher in the default scenario, since the BS antenna gain is lower due to the high directive antenna used.

In what concerns to the MT transmitted power, the results are presented in Fig. 5.15. In this case, no significant variations in the power, with distance, are observed since, opposite to the default case, the antenna gain is constant, the small increase with distance being explained by a similar increase in the path loss. It should be noted that the power required in the MT is in most of the cases higher than that obtained in the default case, as expected, since an increase of about 3 dB is observed in the interference, Fig. G.16 and Fig. G.17, respectively for the intra- and inter-cell ones, and since the antenna gain is lower for most of the distances considered, except for the 50 m case, where the gain is lower in the default case. Therefore, the difference of powers for both cases is higher for higher distances, for distances above 300 m the difference being about 7 dB.

Concerning C/I , again, no variations are observed.

This study reveals that, as expected, the usage of directive antennas in this type of environment is more appropriate, a more efficient coverage and a higher capacity being obtained, since the transmission powers required are lower comparing to a less directive antenna.

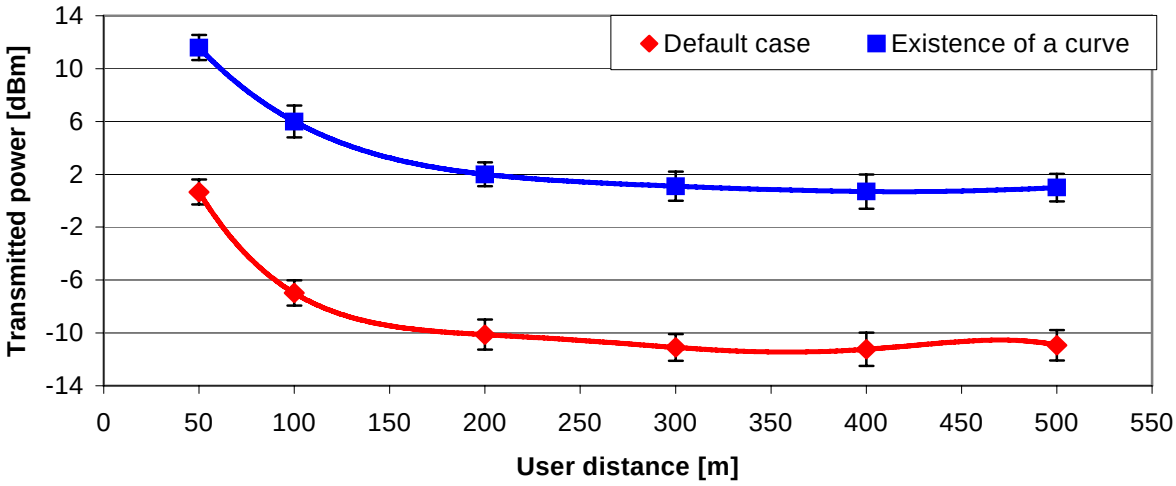

Figure 5.15. Power transmitted in UL, with distance, for different BS antenna radiation patterns.

5.2.7 Influence of a Curve in the Tunnel

Since the tool is able to predict the path loss when a curve is considered, it is interesting to analyse the variation of the results in comparison with the default scenario when there is a curve in the tunnel. For that purpose, a set of simulations is performed, considering $\rho=0.125\ \mathrm{m}$, with a curve of 1000 m radius and 100 m length, starting in the position where the BS is located. Therefore, the user located at 50 m from the BS is in the curve, the other users being located after the curve.

An increase of about 11 dB comparing with the default scenario is observed in the BS transmission power, caused by the increase in the path loss, in the interference, and in the fast fading margin, since the Rayleigh distribution is used when an NLoS situation is observed. The increase in the path loss, for the case studied, is, in the maximum, about 2 dB per user, depending on his position. Regarding the fast fading margin, an increase of about 4 dB is observed comparing with the default case. The DL interference is presented in Fig. G.18.

In what concerns the MT transmitted power, presented in Fig. 5.16, an increase between 11 and 13 dB is observed for all the considered distances. The reasons for this increase are the same presented for the DL case. When the user is at 50 m from the BS, the increase in the power transmitted is lower than that obtained for the other distances, since at this distance the attenuation caused by the curve is of about 1 dB, being lower than that observed for the other distances, where the extra attenuation is of about 2 dB. The UL interference is shown in Fig. G.19.

Regarding C/I, an increase of about 2.2 dB is observed in the DL case, while for UL the increase is of about 2.7 dB. These behaviours are explained by the consideration of the Rayleigh distribution, which causes an increase of the fast fading margin. Since this margin is used for the calculation of the received power, (A.10), C/I increases.

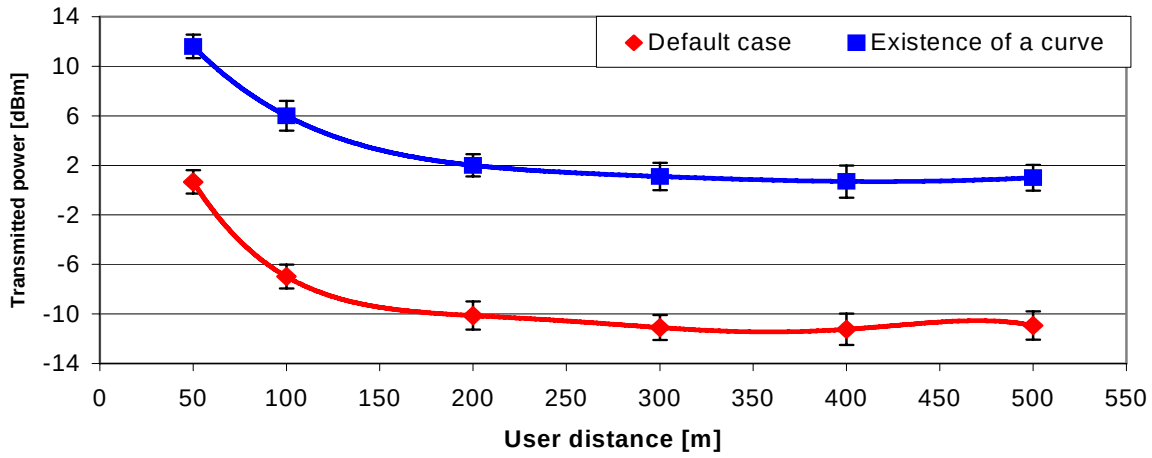

Figure 5.16. Power transmitted in UL, with distance, with and without a curve.

5.3 Parameters Influence for the Bridge Case

In this section, the simulations performed for the bridge are presented and analysed. First, the results obtained for the default scenario are shown. Afterwards, the results obtained with the variation of some parameters, namely the number of users, the services used and the BS range, among others, are presented and compared with the results obtained for the default scenario.

5.3.1 Default Scenario

Similar to the procedure done for the tunnel, the default scenario for the bridge is also analysed, where 50 simulations have been performed. Again, the transmitted powers are obtained with (A.1). The slow and fast fading margins have the same values presented for the tunnel, in Subsection 5.2.1.

The transmitted power required in the BS is presented in Fig. 5.17, for each distance between the BS and the MT. The power exhibits an almost constant behaviour for the different distances of the MT, which is expected, since the other 14 users in the sector are randomly generated; therefore, the position of a user, the one being studied, is not significant when 15 users are being covered. The values obtained for this parameter are around 31.1 dBm, thus, below the maximum transmitted power allowed in the BS, therefore, no coverage or capacity problems are expected.

It is interesting to point out the fact that the values obtained for the BS transmission power are about 15 dB above those obtained for the tunnel case. This is explained by the fact that, even considering a lower number of users in the bridge, the propagation models used for both cases are different. In the tunnel, as mentioned in Section 3.2, the waveguide effect is present, the propagation attenuation being lower in comparison with the bridge.

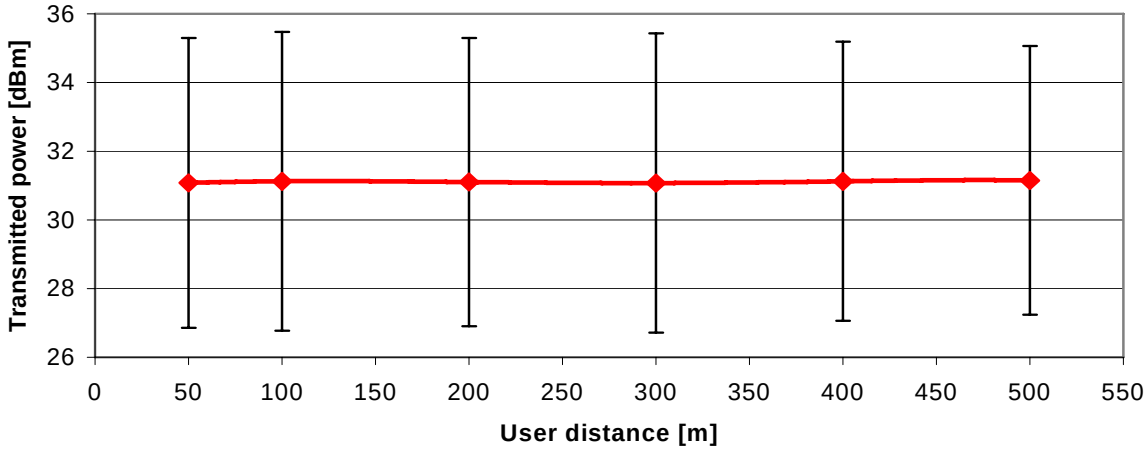

Figure 5.17. Power transmitted in DL, with distance, for the default scenario, in the bridge.

In what concerns the power transmitted by the MT, Fig. 5.18 shows the results obtained for each distance considered. When the user distance to the BS increases from 50 to 500 m, it is possible to observe an increase on the transmitted power from about -13 to 19.4 dBm. This increase is due to the increase in the path loss when the user goes far from the BS and also to the decrease observed in the BS antenna gain. This decrease is explained by the 7º of down tilt considered in the BS antenna. With this value for the antenna tilt, the maximum antenna gain is obtained when the user is at around 40 m from the BS. Therefore, when the distance increases, the gain tends to decrease, from about 14 dBi at 50 m to -7 dBi at 500 m, which implies that the transmitted power needs to increase to compensate the behaviour of the radiation pattern. The transmitted power is again below the maximum allowed, however, looking at the standard deviation when the MT is at 500 m, it is possible to conclude that some coverage problems may exist, since the transmission power needed in the MT is, in some cases, above the maximum allowed, i.e., 21 dBm. In a real situation, some procedures could be taken, such as a decrease in the antenna tilt or a decrease of the BS coverage area.

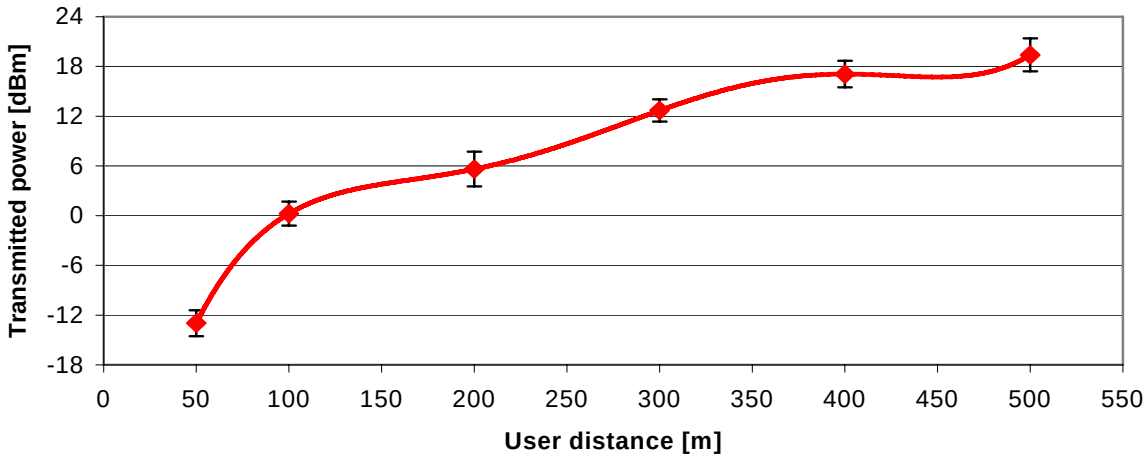

Figure 5.18. Power transmitted in UL, with distance, for the default scenario, in the bridge.

The standard deviations in this case are lower than those observed for the BS transmitted power,

since in the former the position of the other MTs is not as relevant as in the latter. For the BS, the power transmitted experiences higher variations when the MTs change their positions, since the path loss and the BS antenna gain are affected. However, for the MT, the situation is different, since it only needs to transmit the power to the BS, which is fixed.

Similar to the tunnel case, the DL and UL noise powers, obtained with (A.7), are of about -124 and -129 dBm, respectively. The interferences for DL and UL are presented in Annex H, Fig. H.1 and Fig. H.2, respectively. For the DL case, it is possible to observe that the total interference decreases when the user goes far from the BS. This is explained by the fact that, when the MT is close to the BS, a higher intra-cell interference is observed, due to the power that the BS transmits to the other MTs in the same sector, which is causing interference in the MT studied. Regarding the inter-cell interference, when the MT is at 50 m from the BS, it is of about -114 dBm. This interference tends to decrease with distance since the BS is considered with two sectors, one being studied and the other causing interference, as shown in Fig. 4.6. Therefore, when the distance to the BS increases, the inter-cell interference caused by that sector also decreases due to the increase of the path loss. A slight increase is observed from 400 m, which is caused by the BSs of the adjacent cells. It is possible to mention, from Fig. H.1, that the inter-cell interference contribution to the total interference is almost negligible since the intra-cell interference is, for all cases, at least 20 dB higher. This is explained by the orthogonality factor and by the high path loss between the interfering BSs and the MT studied, but the main reason is that the tilt of the BS antenna is considered in the simulations. This parameter causes a significant decrease in the inter-cell interference, since the BS antenna gain for far distances is very low. In fact, this is one of the objectives underlying the use of down tilt in the BS antennas.

For the UL case, it is possible to observe, in Fig. H.2, that the total interference is almost the same for the distances considered. This is explained by the fact that in UL the interference is caused by the MTs, and, since they are randomly generated in the sectors, the interference is, on average, the same, being independent of the position of the MT studied.

C/I for both DL and UL are presented in Fig. H.3. For DL, C/I is around 14.5 dB for all the cases, while for UL it is of about 11.4 dB. The standard deviations are negligible for both cases, for the same reasons mentioned in the previous section.

5.3.2 Variation of the Number of Users

The number of users, similar to the tunnel case, is one of the parameters that need to be analysed in order to quantify the variations in coverage, capacity and interference. For this purpose, different number of users is considered, with the other parameters remaining unchangeable comparing with the default case.

The power transmitted by the BS, for each number of users and for the different distances, is presented in Fig. 5.19. In order to allow a better analysis concerning the influence of the variation of

the number of users, Fig. 5.20 presents the variation of the power with distance, for the 200 m case, the conclusions being valid for other distances, since, as verified for the default scenario, the power transmitted in DL is almost independent of the user distance. As expected, the power required in the BS increases when more users are trying to communicate. When only 5 users are considered, the required transmitted power is about 20 dB lower than that obtained for the default case, while when 25 users are considered the power required is of about 43 dBm, thus the maximum allowed in the BS. Therefore, it is possible to conclude that, for the parameters considered, the capacity of the system is in the order of 25 users. The power required to serve 35 users is also presented, being about 6 dB above the maximum. The standard deviations are not presented in Fig. 5.19, however, the values are similar to those presented for the default scenario and they must be taken into account. Therefore, even with 25 users, some coverage and capacity problems are expected since the powers required are above the maximum, in some cases.

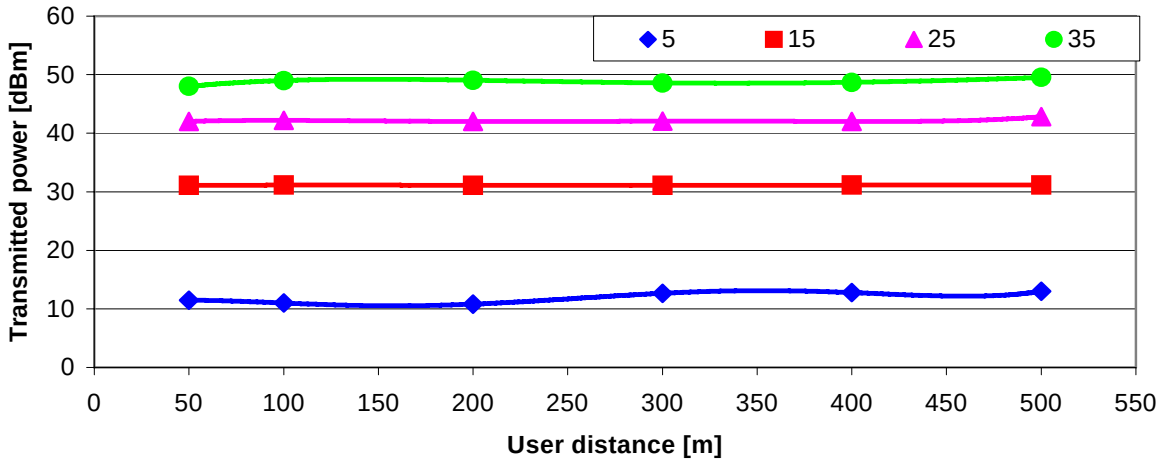

Figure 5.19. Power transmitted in DL, with distance, for different number of users, in the bridge.

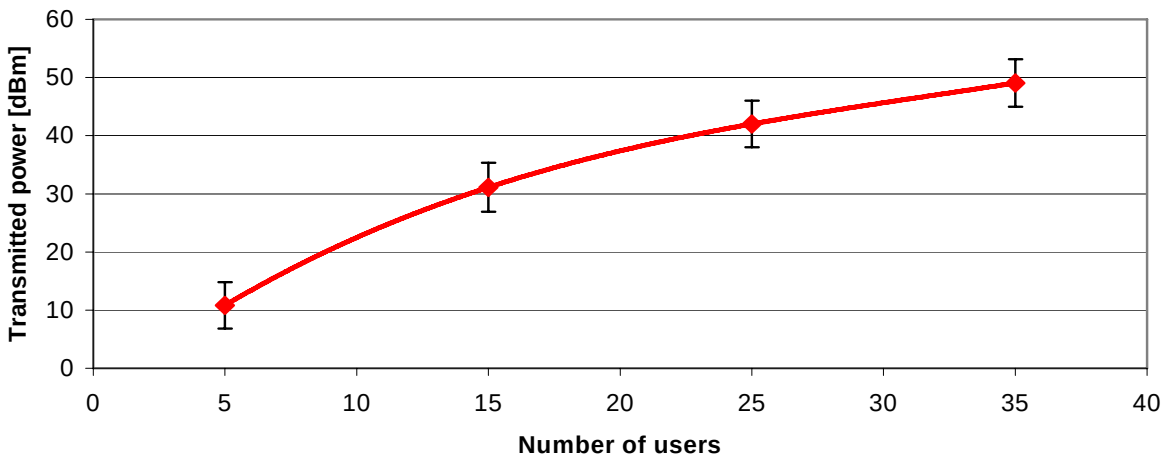

Figure 5.20. DL transmitted power with the number of users, in the bridge.

In what concerns the power transmitted by the MT, the results obtained are presented in Fig. 5.21. As verified for the default scenario, when the user goes far from the BS, the power required is higher. It is

also possible to observe an increase in the power when the number of users increases. When 5 users are considered, the power is about 5 dB lower than the default case. On the other hand, when the number of users is 25 the power increases about 6 dB comparing to the default case. The increase is in the order of 15 dB when 35 users are considered. This behaviour of the power transmitted in UL is caused by the increase of the interference when the number of users increases. Since the interference is higher, the sensitivity of the receiver also increases due to the relation between these two parameters.

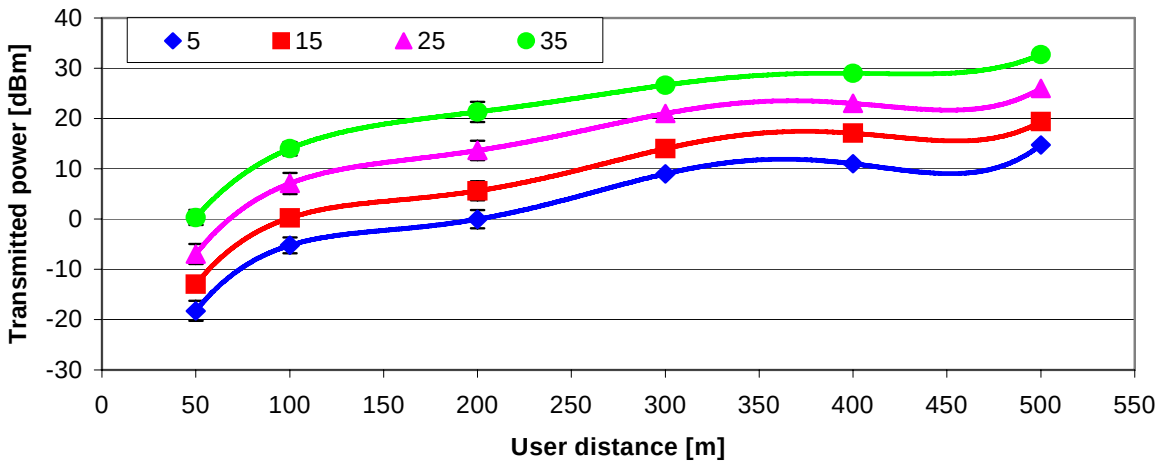

Figure 5.21. Power transmitted in UL, with distance, for different number of users, in the bridge.

Analysing the values obtained, it is possible to observe that, for 25 users, when the MT is at least at 300 m from the BS, the power required is above 21 dBm, which is the maximum allowed. When 35 users are considered, the same situation is observed, although in this case it happens for distances above 200 m. It is possible to conclude that, when the number of users is above 25, the planning should be done taking these results in consideration. For instance, one solution to the problem could be the reduction of the BS range. In that case, the BSs would be close to each other, meaning that the MT would be at a shorter distance from the BS, being possible the coverage. However, with this approach, the interference would also increase leading to an increase of the transmitted power, which could be again above the maximum allowed. The conclusion is that the planning must be carefully done taking in consideration coverage, capacity and interference aspects to design and optimise the network according to the desired requirements.

Regarding the intra- and inter-cell interferences, the variations with the number of users are presented in Fig. H.4 and Fig. H.5, respectively, for DL and in Fig. H.6 and Fig. H.7, respectively, for UL. It is relevant to mention that the inter-cell interference is almost negligible for both cases, essentially due to the BS antenna tilt. For DL, the interference decreases about 9 dB comparing to the default scenario, when 5 users are considered. When the number of users increases to 25 and 35, the interference increases about 3 and 5 dB, respectively, in comparison with the case with 15 users. In what concerns UL interference, comparing with the default case, it is possible to observe a decrease of about 8 dB when 5 users are considered, and an increase of about 3 and 5 dB, respectively, when 25 and 35

users are chosen. This behaviour of the interference is expected, since an increase in the number of users leads to a higher interference. Therefore, the importance of this study is the quantification of the differences observed in the interference when a different number of users are considered.

In what concerns C/I, the results are not presented since the values obtained are almost the same as those presented for the default scenario.

5.3.3 Variation of the BS Range

As mentioned in Subsection 5.2.4, the influence of the variation of the BS range is interesting to study. Therefore, the same approach used for the tunnel is considered, with the interfering BSs at the same distances, only being analysed the case with the user at 50 m from the BS.

The power transmitted in DL for the different ranges is presented in Fig. 5.22. It is possible to observe an increase in the power when the BS range increases, since, when there are users covered at higher distances, there is a significant increase in the path loss due to the propagation models used.

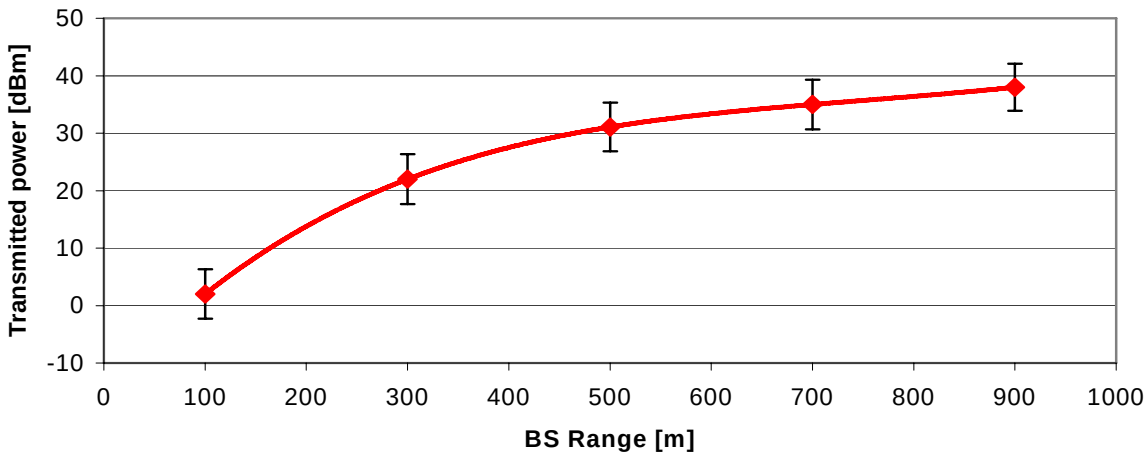

Figure 5.22. Power transmitted in DL with the BS range, in the bridge.

When the range is 100 m, the transmitted power is about 29 dB below that required in the default scenario, due to the lower path losses. Moreover, since the tilt is considered, the BS antenna gain is higher for the distances considered in that range. For the 300 m range, the difference is that the path loss increases and the antenna gain suffers a decrease, both caused by the higher distances between the BS and MTs; in this case the average power is about 9 dB below that obtained in the default scenario. For the 700 m range, the power required is about 5 dB higher comparing with the default case, due essentially to the increase in the path loss. Furthermore, since the break point is located at around 442 m, there are some users located between that distance and the maximum range and, noting that the average power decay is higher for the flat earth model, the path loss suffers an increase after the break point, contributing to the increase in the power required in the BS. For the 900 m range, the situation is similar.

The interference in DL is also a reason behind the observed behaviour of the DL transmitted power, being presented in Fig. H.8. In fact, the interference increases about 30 dB between the extreme cases considered, since, as the range increases, more power is required in the BS, thus causing more interference in the MT.

In what concerns the power transmitted in UL, it is possible to observe in Fig. 5.23 a decrease of about 11 dB between the 100 and the 500 m ranges. This behaviour was expected since, in UL, the interference, shown in Fig. H.9, decreases with the increase of the BS range. The explanation for this fact is that, when the range increases, the distance to the interfering MTs also increases, which, together to the tilt considered in the BS antenna, causes the decrease in the interference.

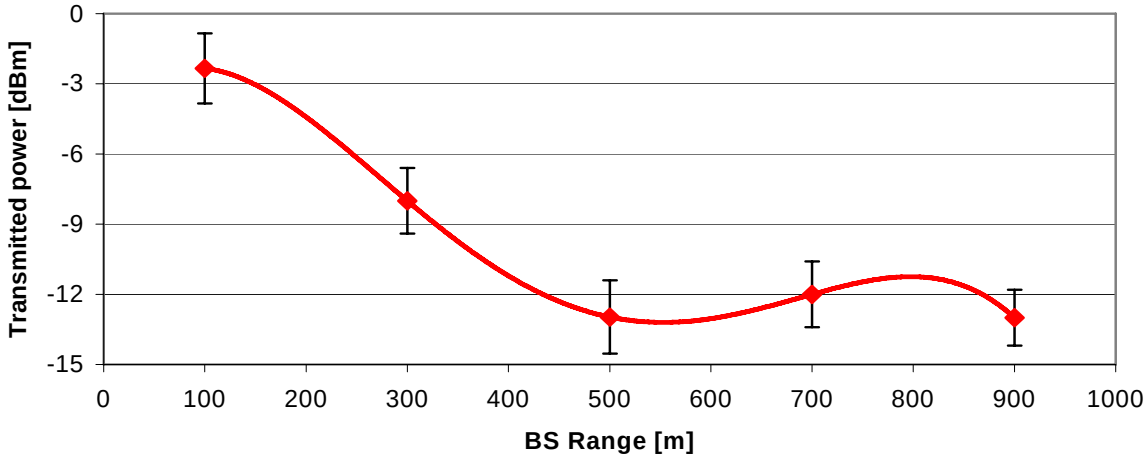

Figure 5.23. Power transmitted in UL with the BS range, in the bridge.

Until the 300 m range, the intra-cell interference is negligible, since it is more than 10 dB below the inter-cell. This is explained by the fact that, since users are placed at short distances from the BS, the transmitted powers are not too high to cause more considerable intra-cell interference. Moreover, since the users in the interfering cells are at shorter distances comparing with the other cases, the inter-cell interference is more significant. With the increase in ranges, the intra-cell interference tends to increase while the inter-cell one decreases, since the path losses increase with distance and the interfering users are at higher distances. For distances above 500 m, the intra-cell interference is the most significant in the total one. For the 700 m range a slight increase is observed in the interference and in the power transmitted by the MT. This increase is explained by the results obtained for the intra- and the inter-cell interferences. As explained, while the former increases with the distance, the latter tends to decrease. For the 700 m case, the sum of these two components is higher than in the 500 m and 900 m cases, causing the mentioned increase. Additionally, the BS antenna gain, when the MT is at 700 m, is lower than that observed in the 500 m and in the 900 m ranges. This is caused by the radiation pattern of the BS antenna considered.

C/I values are not presented, since the differences comparing with the default case are negligible.

5.3.4 Variation of the Services Used

Similar to the evaluation done for the tunnel, the influence of the data rates on coverage, capacity and interference is analysed for the bridge. The same approach is considered here, the user studied being at 50 m from the BS and all combinations being analysed.

Regarding the BS transmission power, the variation with the different services is presented in Fig 5.24. When the data rate of the user is 12.2 kbps and the other users are considered with 64 kbps, a slight increase is observed in the required power, comparing with the default case, which is caused by the more demanding services used, by the increase in the DL interference, Fig. H.10, and by the fact that the same number of users, i.e., 15, is considered. For the other services considered for the user studied the situation is similar, noting the fact that a slight decrease in the power is observed when the user is considered with 384 kbps. This is explained by the decrease of the number of users, from 15 to 13. Table 5.6 presents the number of users for the different data rates. In fact, the limitations in capacity influence this analysis, since significant variations in the power are observed when the number of users is changed.

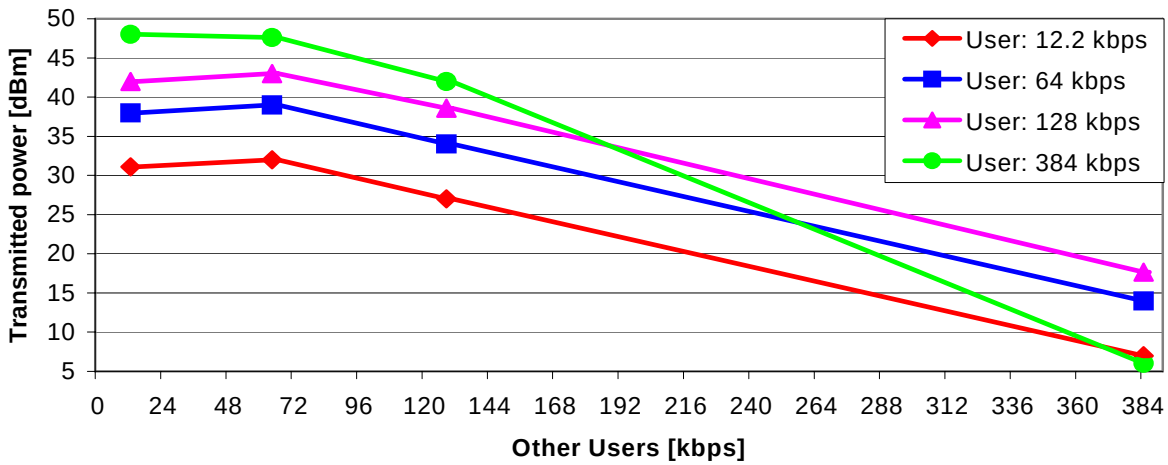

Figure 5.24. Power transmitted in DL with the services used, in the bridge.

Table 5.6. Number of users for different services performed, in the bridge.

Number of users		Other users [kbps]			
		12.2	64	128	384
User [kbps]	12.2	15	15	10	4
	64	15	15	10	4
	128	15	15	9	4
	384	15	13	7	3

When the other users are considered with 128 kbps, a decrease of about 4 dB is observed comparing with the reference case, explained by the fact that, even having higher data rates, due to the limitations in capacity, only 10 users are served, causing a decrease in the interference and in the power required in the BS. If the user studied is considered with the voice service and the other users with 384 kbps, a decrease of about 24 dB is observed comparing with the default case. The explanation is again the fact that the number of users is reduced, in this case being only 4 users served. The higher decrease observed when the user is considered with the most demanding service and the other users change their data rates from 128 to 384 kbps is explained by the same reason mentioned for the tunnel case, i.e., the reduction of the number of users served from 4 to 3. It should be noted that in two cases the power obtained is above the maximum, about 5 dB, namely when the other users are performing the voice service or the 64 kbps service and the user is considered with 384 kbps.

In what concerns the MT transmitted power, the variation with the users' data rates is presented in Fig. 5.25. For the user's distance considered, the power is, for all the cases, below the maximum allowed. However, for higher distances, the power required in UL can be above that limit being impossible to communicate with the BS. In fact, as analysed for the default scenario, the power in UL increases with the increase of the user distance. Therefore, this study must be carefully done according to the requirements, in order to obtain a good coverage. The variation of the interference in UL is presented in Fig. H.11.

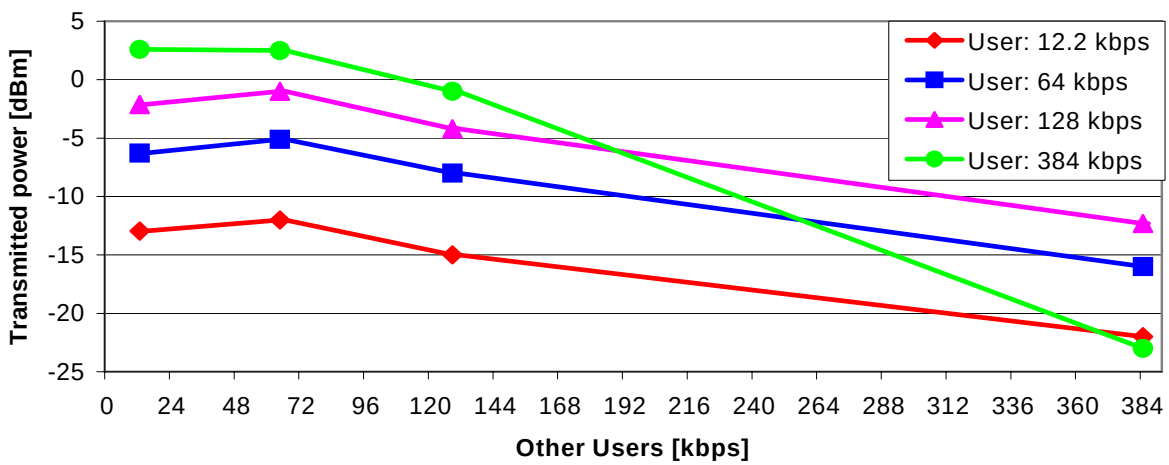

Figure 5.25. Power transmitted in UL with the services used, in the bridge.

Concerning C/I, the variations are presented in Fig. H.12 and Fig. H.13, respectively for DL and UL. It is possible to observe that, for both cases, this relation is about 3.8 dB higher when the user is considered with the voice service, comparing with the data services. This is explained by the fact that the SNR is lower for the data services, thus the received power being lower.

5.3.5 Variation of the *K* Parameter of the Rice Distribution

In the default scenario, the *K* parameter considered for the Rice fading distribution is 1.5 dB. However, since there are changes in the environment, namely, in this case, the variation of the number of cars in the bridge, it is important to analyse the variation in the results when other values for *K* are considered. In that sense, a set of simulations is performed to study this variation, considering 0, 4, 9, and 19 dB for this parameter. It should be noted that the specific case of *K*=0 dB corresponds to the Rayleigh distribution.

The variation of the BS transmission power with the *K* parameter, for the user at 200 m, is presented in Fig. 5.26. This variation is only presented for one distance, since, as already mentioned, the power does not show significant variations with distance. As expected, the transmission power decreases when the *K* parameter increases, since it corresponds to a clearer LoS condition due to the lower movements observed in the environment. This decrease is in the order of 22 dB, between the extreme cases considered, i.e., among *K*=0 dB and *K*=19 dB. It is possible to observe, in Fig. 5.26, that the power required in the BS is below the maximum allowed, for all the cases.

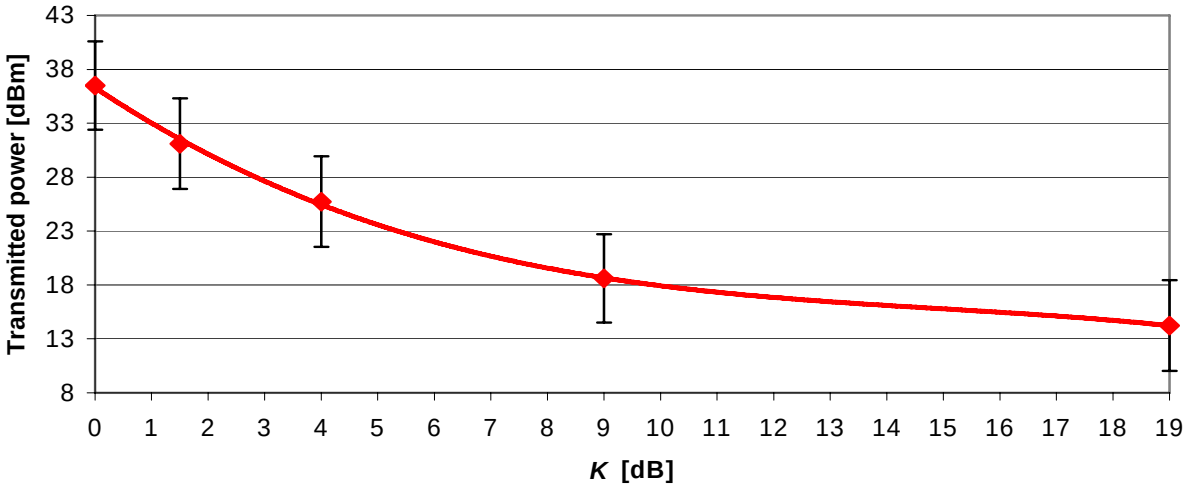

Figure 5.26. Power transmitted in DL with the *K* parameter.

The results obtained concerning the power transmitted by the MT are presented in Fig. 5.27. In this case, an increase in the power required is also observed when the *K* parameter decreases, the differences between the *K*=0 dB and *K*=19 dB cases being of about 22 dB. The explanations for this fact are the same mentioned for the BS transmission power. It should be noted that, for the *K*=0 dB case, the user cannot communicate with the BS if located at more than 300 m, since the transmitted power for those distances is above the maximum allowed.

Regarding DL and UL interferences, the variations with the *K* parameter are presented in Fig. H.14 and Fig. H.15, respectively. Both intra- and inter-cell interferences increase with the decrease of the *K* parameter for both DL and UL, due to the higher changes in the environment, as explained in the previous paragraphs.

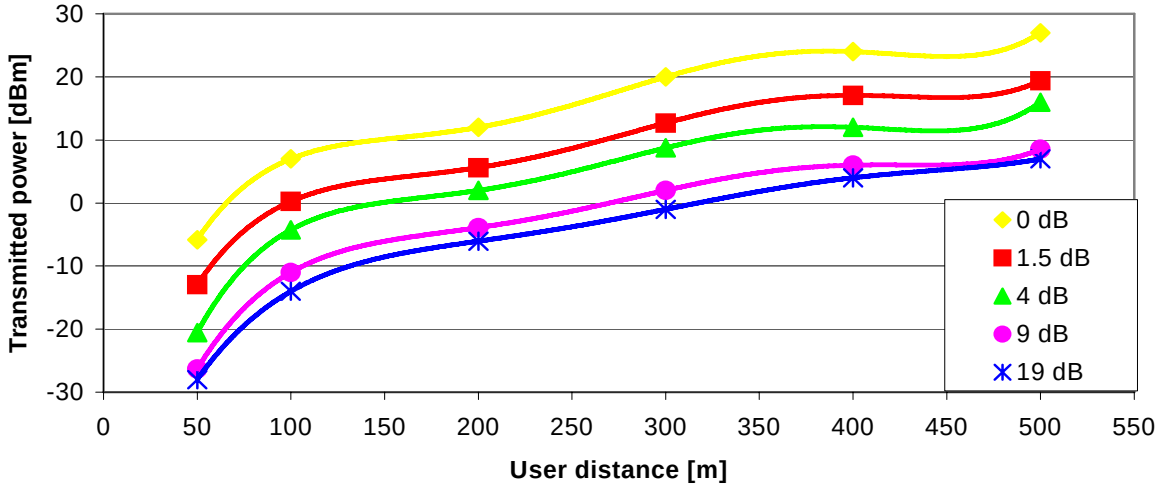

Figure 5.27. Power transmitted in UL, with distance, for different *K* parameters.

In what concerns C/I, an increase of about 5 dB is observed when the *K* parameter decreases from 19 to 0 dB, for both DL and UL, presented in Fig. H.16 and Fig. H.17, respectively. This is explained by the fact that, in the calculation of the received power, detailed in Annex A, a parameter proportional to the fading margin is considered, thus, when the *K* parameter decreases, the fading margin increases, increasing also the received power. Therefore, although being observed an increase in the interference, a higher increase in the power received is obtained, leading to an increase in C/I.

5.3.6 Influence of Traffic

Since the tool is able to consider a traffic situation, it is interesting to compare the cases with and without traffic, as considered in the default scenario. For this purpose, all the parameters considered in the default case are maintained, only being changed the environment for a traffic situation.

The power transmitted by the BS increases about 0.5 dB comparing with the default scenario. This small increase is explained by the fact that, when traffic is not considered, the free space propagation model is used until the break point, which is located at about 442 m from the BS, the flat earth propagation model being then used. In the traffic situation, only the free space propagation model is used. Since the BS range is 500 m, the cases with and without traffic are very similar due to the location of the break point, which is close to 500 m.

In what concerns the power transmitted in UL, the same situation mentioned for DL is observed. One of the reasons for this is the tilt considered in the BS antenna causing the inter-cell interference to be almost negligible in comparison with the intra-cell one. If the tilt was not considered, the inter-cell interference in the traffic case would be more significant than in the case without traffic, since the path loss for the free space propagation model is lower comparing with that obtained with the flat earth model at high distances as those where the interfering MTs are located. Therefore, the transmitted power would also increase due to the increase in the interference. Other reasons, already mentioned,

are the range considered for the BS antenna and the position of the break point.

From the analysis done, it is possible to conclude that both DL and UL interferences remain similar to those obtained for the default scenario, as shown in Fig. H.18 and Fig. H.19 respectively. In fact, an increase between 1 and 3 dB is observed in the inter-cell interference in DL for the distances considered, however, since the inter-cell interference is almost negligible when compared with the intra-cell one, this increase is not significant to the total interference in DL. For UL, the situation is similar.

In what concerns C/I, the values obtained are approximately the same as those obtained for the default scenario. The reasons for this behaviour have already been explained in the previous Section.

5.4 Rossio Tunnel Analysis

The results obtained for the analysis of coverage, capacity and interference for the particular case of the Rossio Tunnel are presented here. The main characteristics of this tunnel have been presented in Section 5.1. In this analysis, 20 users are considered with the sector covering a 1 km distance. The BS is considered in the position (*x*,*y*)=(0,2) and the MT studied is placed at (*x*,*y*)=(2,0), to approximate a real case where the MTs are inside trains. The considered BS antenna is the same as presented in Section 5.1, as well as the fading parameters and the indoor penetration attenuation. Regarding the interfering BSs, two are considered, both at 2 km, one being in front and the other behind the BS analysed. Several distances of the studied user to the BS are considered, in order to evaluate the variations in the parameters being analysed. The transmitted powers for both DL and UL are obtained with (A.1).

As expected, the power transmitted by the BS does not show significant variations when the user changes his distance, since 20 users are considered meaning that a change in the distance of one user does not cause an appreciable modification in the total power transmitted by the BS. It can also be noted that the required power, which is around 17 dBm, is below the maximum allowed, thus no coverage problems are expected for the conditions considered.

Regarding the power transmitted by the MT, the variation with distance is presented in Fig. 5.28. It is possible to observe a decrease of about 2.3 dB when the distance increases from 125 to 375 m. This behaviour is due to the radiation pattern of the BS antenna, since the gain at 375 m is higher than the one at 125 m. At 500 m an increase of about 0.6 dB is observed, caused essentially by the increase of the path loss. From 500 to 750 m no significant variations in the power exist. In fact a slight increase was expected since the path loss increases, however, again, the explanation to the insignificant variation in the power is the radiation pattern of the BS antenna. At 875 m the power required is about 0.8 dB higher due essentially to the increase in the path loss. When the user is at 1000 m from the BS,

an increase of about 0.2 dB in the power is observed for the same reason.

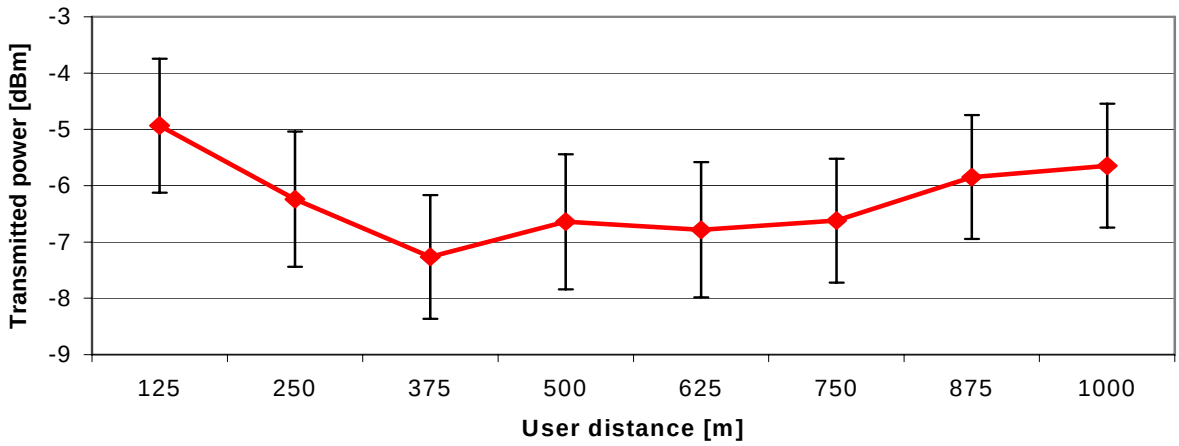

Figure 5.28. Power transmitted in UL for the Rossio Tunnel, with distance.

The interferences for DL and UL are presented, respectively, in Fig. I.1 and Fig. I.2, C/I being presented in Fig. I.3. The analysis for these parameters is similar to the one done for the default scenario presented in Subsection 5.2.1.

5.5 Vasco da Gama Bridge Analysis

The results obtained regarding the analysis done for the Vasco da Gama Bridge are presented in this section. It should be noted that the coverage of UMTS in this bridge is obtained from the BSs located close to the river margins, whose objective is not to cover the bridge. Therefore, as can be understood, the communications in the bridge, for UMTS, can be more carefully designed in order to obtain a better coverage. The idea behind this study is to provide some important results using the simulator developed, that can be taken into account when the planning and optimisation of the system, in this particular scenario, is done.

In this study, the parameters are chosen to approximate simulations to the real case. In this sense, the BS is considered at 5 m height and positioned at *x*=0 m, while the user is considered at four different distances, being located at *x*=6 m. The considered BS range is 800 m and the number of users in that range is 16. The chosen number of users is explained by the fact that the bridge has two roads, one in each way. On average, if 8 users are considered in each way in that range, the spacing between the users is 100 m, which is a reasonable value for the case studied. Additionally, since there is an increase in the range comparing with the default case analysed in Subsection 5.3.1, the down tilt of the BS antenna is reduced to 4º. Additionally, four interfering BSs, two in front and two behind the BS, are considered, two being at 1600 m and two at 3200 m. Similar to the previous case, the transmitted powers for both DL and UL are obtained with (A.1).

As expected, no significant variations are observed in the BS transmission power, when the user position is changed. The value obtained for this parameter is of about 30.5 dBm, thus, being below the maximum allowed.

The power transmitted in UL is presented in Fig. 5.29. It is possible to observe an increase in the required power when the user goes away from the BS. From 200 to 800 m the increase is of about 26 dB, caused by the increase in the path loss and also by the decrease of the BS antenna gain at higher distances, due to the tilt. It is relevant to mention that, when the MT is at 800 m from the BS, the average transmission power required is 20 dBm, thus, below the maximum. However, taking the standard deviation into account, it is possible to conclude that, for some cases, the MT cannot communicate with the BS, since the power required is above 21 dBm.

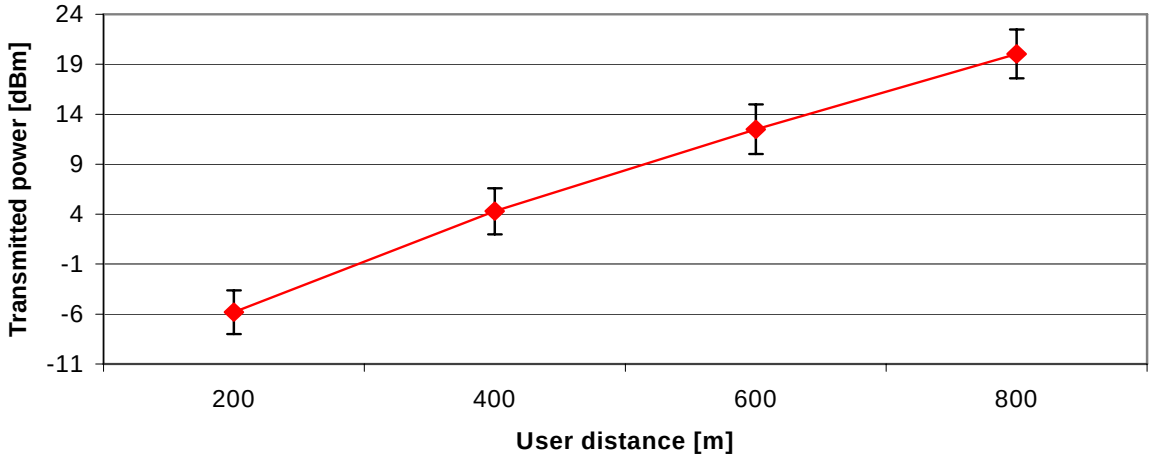

Figure 5.29. Power transmitted in UL for the Vasco da Gama Bridge, with distance.

The interferences obtained for both DL and UL are presented in Fig. J.1 and Fig. J.2, respectively. The total interference also decreases due to the behaviour of the intra-cell interference, since the inter-cell one is almost negligible. In what concerns UL, the inter-cell interference is about 3 dB higher than the intra-cell one. This behaviour is essentially caused by the decrease in the down tilt comparing with the default case analysed in Subsection 5.3.1, thus, increasing the power received in the BS from the interfering MTs.

Regarding C/I, the values obtained for DL are between 14.4 and 16.5 dB, while for UL they are around 11.5 dB, as shown in Fig. J.3. For DL, the increase observed with the distance is caused by the considerable decrease of DL interference, causing the noise power to be more significant in the calculation of the receiver sensitivity with (A.6)

5.6 Measurements vs. Simulations

5.6.1 Measurements Configuration

In order to evaluate the simulator, some measurements were done for both studied environments. In the tunnel, measurements were taken in two tracks of the Lisbon Underground, including 18 stations. Regarding the bridge, the 25 de Abril Bridge was the one chosen to do the measurements, since it has UMTS coverage and is one of the main bridges in the city of Lisbon.

The equipment used in the measurements was an MT with UMTS (Nokia N80), a laptop and a USB cable to connect the MT to the laptop, Fig. 5.30. Additionally, for the measurements in the bridge, a car was used as well as a GPS device. The software used was the NEMO Outdoor V.4.24 [ANIT08], which is a very useful tool to visualise and store the data obtained in measurements. In this study, the voice service and the Vodafone network were used.

Figure 5.30. Equipment used in the measurements (extracted from [Marq08]).

For both cases the parameters obtained are the MT transmitted and received powers. C/I values were also an objective of this analysis, however, due to some problems in the software, it was not possible to obtain in the measurements.

In the Underground, measurements were performed between the Baixa-Chiado and the Campo Grande stations, and between the Campo Grande and the Marquês de Pombal ones. The first stretch includes a total of 11 stations, while the second is composed by 7. In this study, the analysis of the measurements is done for shorter tracks, since the simulator considers that one BS is being studied, thus, the tracks that are covered by only one BS were chosen. Additionally, interfering BSs were considered for each case. The tracks between Intendente and Alameda, Campo Pequeno and Saldanha, and Picoas and Marquês de Pombal were considered in this study, Fig. K.1.

Regarding the 25 de Abril Bridge, when the car was entering the bridge, a voice call was made, which was disconnected after crossing the bridge. In this case, since a GPS was used together with the other equipment, the NEMO software has registered the measurements and the coordinates where they were taken, enabling a more precise identification of the location in the bridge of each result. Both ways, northbound and southbound, were analysed, with the existence of traffic. Another aspect taken

into account was the position of the car in the bridge, since this parameter is used in the simulations. Additionally, the speed of the car was almost constant, being of about 40 km/h, in order to reduce the speed influence in the results, enabling a better analysis. In fact, since the simulator uses a snapshot approach, the speed of the MT is not considered, thus, if it was not constant, the results would be affected by those variations that are not accounted in the simulations. The track considered in the results analysis is presented in Fig. L.1.

5.6.2 Lisbon Underground

Among the tracks studied in the Underground, it is observed that no handovers are performed, thus, a comparison with the simulations can be done. Regarding the position of the MT in the carriage, it is the same for all cases, being of about x=1 m and y=0 m. In what concerns the BS position, it was considered at x=3.5 m and y=1 m, however, this is an assumption, since no information was obtained for these values. The number of users in the ranges mentioned had to be estimated. Noting the observations done on the surrounding environment during the measurements, and the distances considered, 15 users were chosen for all cases.

Since no precise information was obtained regarding the number of BSs and their positions in the Underground, two interfering BSs are considered for all tracks, both at 2.5 km from the studied BS, one being in front and other behind the BS. In the track between Picoas and Marquês de Pombal, only one interfering BS is considered in the simulations, since the Marquês de Pombal station is the last of this line. Actually, the assumption concerning the interfering BSs is taken regarding the results obtained, since the locations of the handovers performed are given by the software. This parameter is, in fact, important since it allows the estimation of the positions of the BSs. The fading parameters and the indoor penetration have the same values as those considered in Subsection 5.2.1. In what concerns the BS antenna, the same used in Section 5.2 is considered. However, according to the information obtained, other types of antennas are used with the main characteristics presented in Table F.1. Since all antennas have high directivities and noting that the K742266 antenna can be a good approximation according to the parameters presented in Annex F, this was the antenna used.

Since simulations results are valid for tunnels, the power behaviour in the stations is not discussed here, although being presented in the figures. However, in what concerns the stations, it is relevant to point out the differences in terms of the analysis that could be done. In the tunnel, when the train is moving, powers are affected by many factors, such as the variation of the path loss, due to the increase or decrease of the distance between BS and MT, the variations in the interference, caused by the variation of both the user distance to the BS and the number of active users, and the variations of the fading associated to the movement of the MT; in the stations, however, the path loss is not changing, since the train is stopped, the variation of the interference is observed, since the number of active users is changing, and what concerns fading, the changes are due to the movements of people.

The first case studied is the track between Intendente and Alameda. Actually, the analysis starts a few

metres before the Intendente station and finishes a few metres before the Alameda one. This is done, since in this period the coverage is achieved with only one BS, handovers being performed outside this track. The length of the track considered is about 1.5 km, Fig. K.1. The power transmitted by the MT obtained in measurements and in simulations is presented in Fig. 5.31. It should be noted that, since the speed of the train is not known, the distances presented can be different than the real distances between the BS and the MT. Therefore, the variation of the transmitted power with time is also presented, Fig. M.1, since, in this case, the speed of the train is not relevant, moreover, the times of both arrival and departure for each station were noted, thus, more accurate results are obtained. The variation in time is presented for all the cases analysed in Annex M, being valid the analysis done for the variation with the distance, since results are similar.

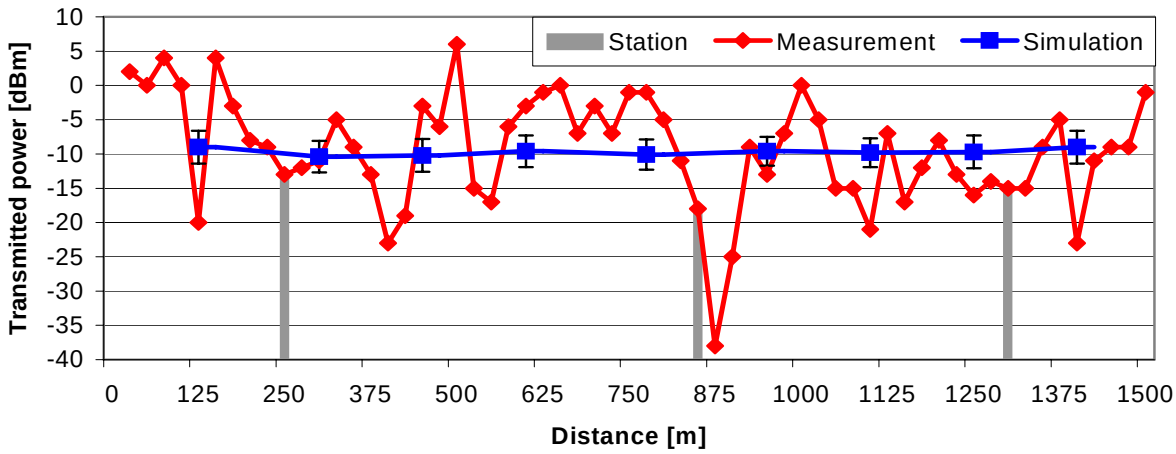

Figure 5.31. Power transmitted by the MT between Intendente and Alameda, with distance.

The general behaviour of the transmitted power is predicted by the model, the average difference between measurements and simulations being about 6.5 dB, and the standard deviation around 5 dB, thus, significant differences in some cases being observed. The rapid fluctuations of the power observed in the measurements are essentially due to the changes in the environment, such as people moving in the train, and due to the variations on the speed of the train. It is possible to note that no significant variations are observed in the power predicted by the simulations, since the path loss increases very slightly with the distance in a tunnel; furthermore, the BS antenna gain increases slightly when the distance increases, thus, the variations being negligible. The simulations were performed for distances separated each other of 150 m. The stations presented are Intendente, Anjos and Arroios.

The received power obtained in the measurements and in the simulations, for the track considered, is presented in Fig. 5.32. It is possible to observe that in most of the cases the values obtained in the simulations are below the values measured. One of the reasons for this behaviour can be the fact that many assumptions are taken in this study, as the BSs positions, the number of users served and the fading parameters. Moreover, it is observed that the differences between both approaches increase when the MT is close to the stations. In fact, the simulator is used to predict coverage, capacity and interference in tunnels, and not close to the stations, where the propagation characteristics are

different. In this case, the average difference between measurements and simulations is about 10.7 dB, the standard deviation being 7 dB. The variation of the power in time is presented in Fig. M.2.

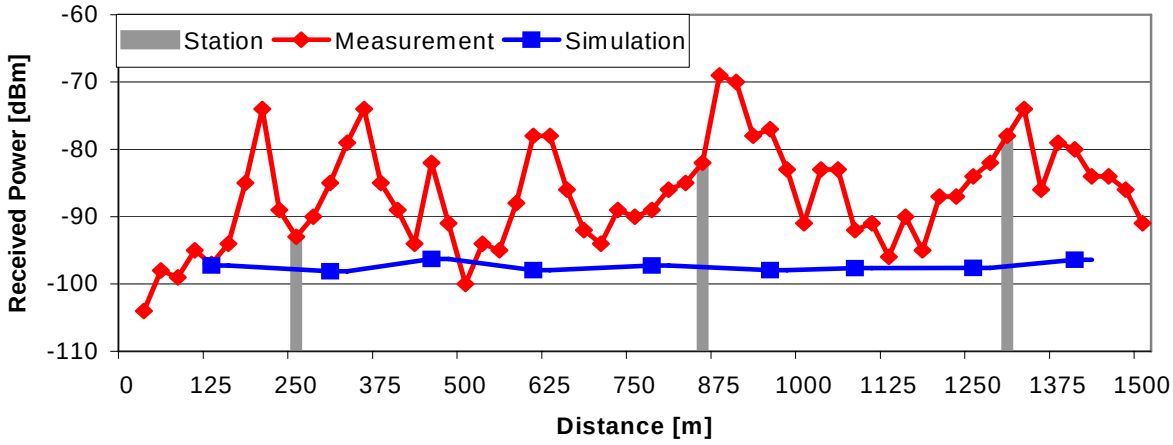

Figure 5.32. Power received by the MT between Intendente the Alameda, with distance.

It is interesting to compare the behaviours of the transmitted and received powers. In some cases, it is possible to observe that, for a certain distance, when one of them increases, the other tends to decrease. This can be explained by the changes in the environment, namely the movements of people in the train, causing obstructions in the signal and variations in the fading, forcing an increase in one of them, and a decrease in the other.

For the second track, the measurement started a few metres before Campo Pequeno, finishing after Saldanha, the analysis being done for the region between both stations. The total length is of about 1.2 km, as shown in Fig. K.1. Figure 5.33 presents the power transmitted by the MT obtained in the measurements and predicted by the simulations. In the simulations, a step of 150 m was considered for the user position. Similar to the fist track considered, the prediction generally follows the measurements, the average difference between both approaches being around 7.6 dB and the standard deviation about 7.4 dB, thus, significant variations being observed, as in the previous case. Again, some fluctuations are observed in the power, caused by the reasons already mentioned. The variation of this parameter in time is presented in Fig. M.3.

The power received by the MT, for both measurements and simulations, is presented in Fig. 5.34. Again, a good agreement between both cases is observed, in general, the average difference being around 8 dB and the standard deviation around 7 dB. In some particular points, the differences are significant, being caused by the reasons already mentioned. The variation of the power in time is presented in Fig. M.4.

Regarding the third track, between Picoas and Marquês de Pombal, the MT transmitted powers obtained in the measurements and predicted by the simulations are presented in Fig. 5.35. Only the region between these stations is analysed, since no stations are in between these two, the total length being of about 700 m, Fig. K.1. Since this track is shorter than the previous ones, the distances

considered in the simulations are separated by 100 m. In general, the behaviour of the transmitted power is predicted by the simulations, the average difference between measurements and simulations being around 5.4 dB, while the standard deviation is 4.4 dB. The fluctuations observed are caused by the previously mentioned factors, not predicted by the model. The variation in time is presented in Fig. M.5.

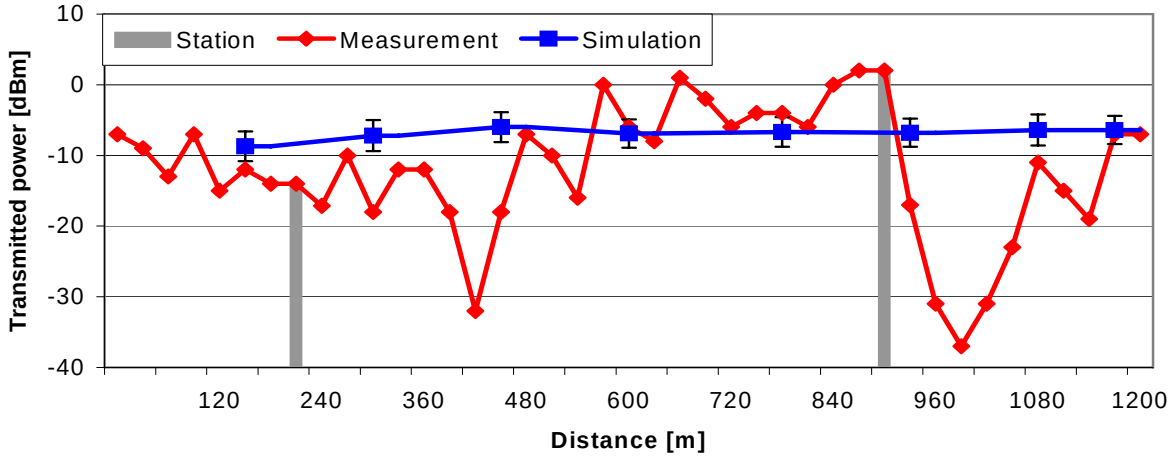

Figure 5.33. Power transmitted by the MT between Campo Pequeno and Saldanha, with distance.

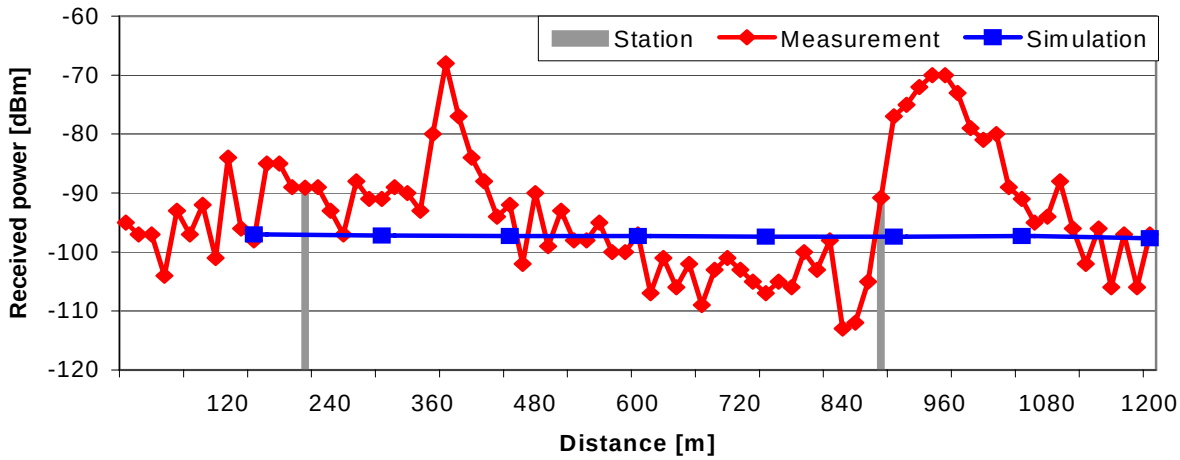

Figure 5.34. Power received by the MT between Campo Pequeno and Saldanha, with distance.

The received power obtained for this track, for both measurements and simulations, is presented in Fig. 5.36. A reasonable agreement is obtained between measurements and simulations, the average difference between both approaches being around 5.9 dB, and the standard deviation about 4.7 dB. At about 300 m, a rapid increase is observed in the received power, which can be explained by the presence of a small crack to the street in this region, causing the fluctuation observed. As already mentioned, the changes in the environment can cause significant variations in the power. The variation of this parameter in time is presented in Fig. M.6.

In some of the tracks, the situation of two trains passing inside the tunnel simultaneously was observed, however, no particular variation was detected neither in the transmitted nor in the received

powers. In fact, since both powers show significant variations along the tunnel, no conclusion can be taken regarding the influence of the obstruction caused by the other train.

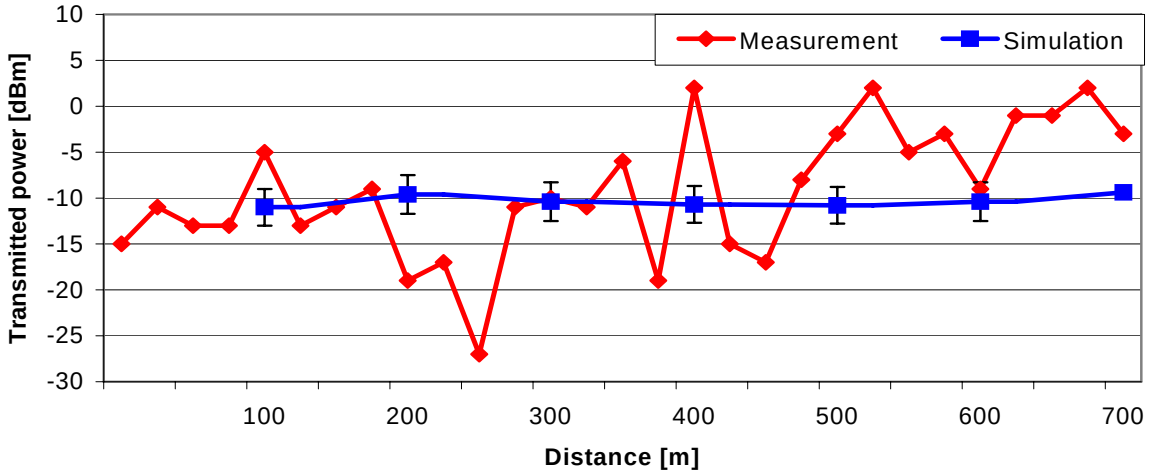

Figure 5.35. Power transmitted by the MT between Picoas and Marquês de Pombal, with distance.

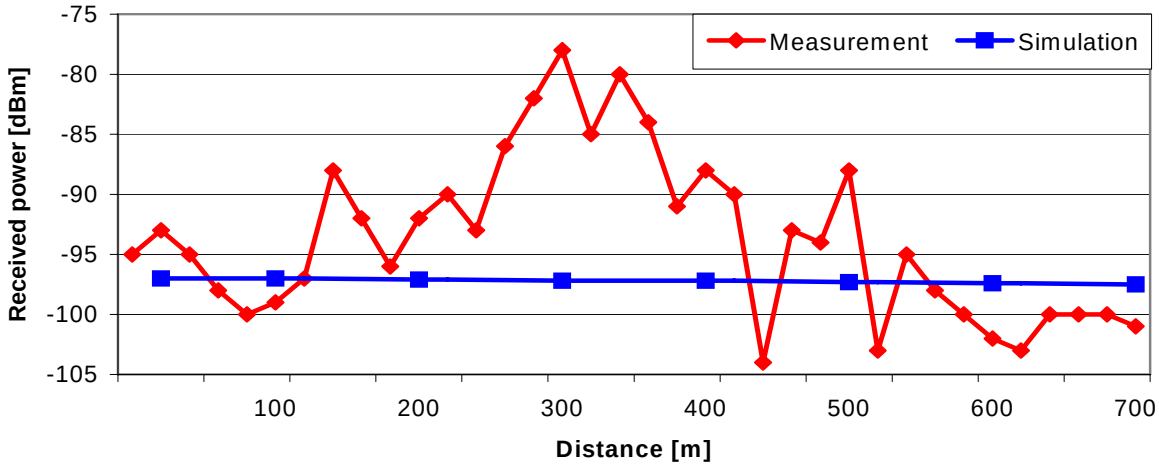

Figure 5.36. Power received by the MT between Picoas and Marquês de Pombal, with distance.

5.6.3 25 de Abril Bridge

This subsection presents the results obtained in the measurements and the comparison with the simulations for the 25 de Abril Bridge. The results were analysed in order to perform simulations in similar conditions as those observed during the measurements. To be more specific, one of the important aspects is the existence of handovers, since in the simulator one BS is studied in a certain range. If there is a high number of handovers, the ranges are too short and the simulations are not too precise. This was observed when the south bound way was analysed, since many BSs in the river margins are also used to cover the bridge, none of them providing a clearly better signal than the others. In the other way, the situation is not the same. This happens due to the presence of a BS in the south entry of the bridge, that covers about 900 m of the bridge in that way, the remaining route

being covered by those BSs mentioned. Therefore, this is the BS considered in this analysis, the track being presented in Fig. L.1.

The BS is located at 8 m height, at approximately *x*=0 m, and has a down tilt of 2º. One assumption that had to be taken is the number of users considered, since it is not possible to know this parameter. A 900 m range being studied, and since a traffic situation is observed, 10 users is a reasonable number to be considered. The MT was positioned at 1 m height and at about *x*=5 m, the fading parameters being equal to those used in Subsection 5.3.1. Regarding interfering BSs, some were detected in the measurements, in the simulations being considered 4 interfering BSs. From this 4, two are considered in front of the BS at a 3 km distance, which is the approximate distance between the BS studied and the interfering BSs located on the other side of the river, while the other two are considered behind the BS at 1 km. All these parameters and assumptions are important since they are used in the simulations.

The simulations are performed for several distances: for 40 m and for 100 to 900 m with a step of 100 m. The results concerning the MT transmission power for the measurements and for the simulations are presented in Fig. 5.37. It is possible to observe a very good agreement between the measurements and simulations, the average difference between both approaches being around 4 dB, the standard deviation being 2.9 dB. The variations of the transmitted power in measurements are essentially caused by the changes in the environment, such as passing cars or trucks close to the MT and by the variation of the number of active users; however, the behaviour of the curves and the values obtained for both cases are very similar. The increase of power with distance is essentially caused by the increase in path loss.

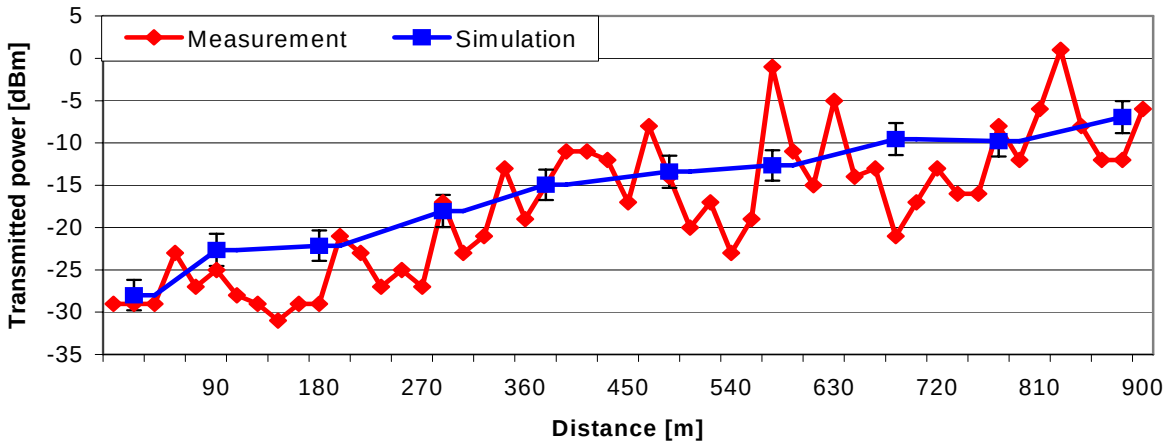

Figure 5.37. Power transmitted by the MT in the 25 de Abril Bridge, with distance.

In what concerns the MT received power, the results for both cases are presented in Fig. 5.38. In this case, the differences between measurements and simulations are more significant, varying between 7 and 20 dB. The average difference is about 14 dB, while the standard deviation is 4.4 dB. However, a good agreement in the behaviour of both curves is observed, especially for distances above 200 m.

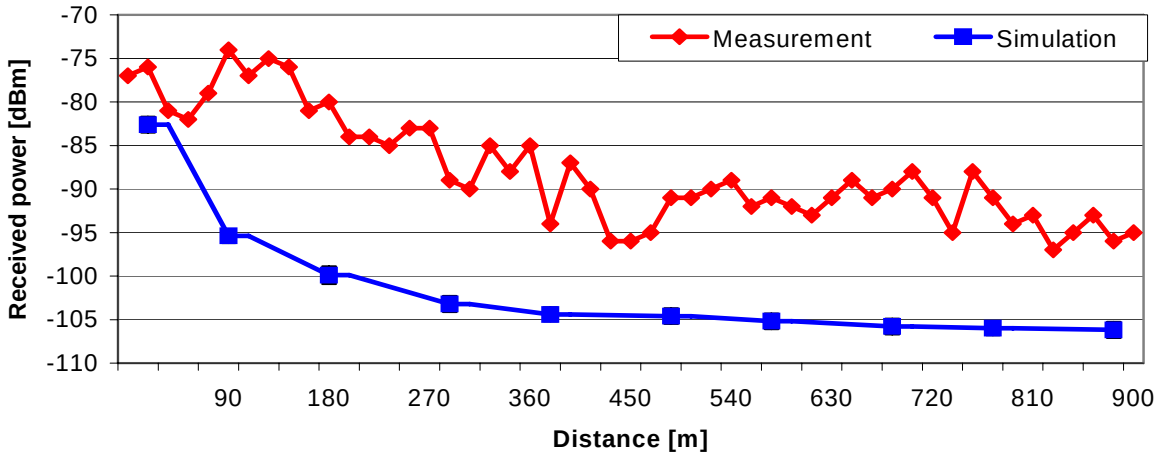

Figure 5.38. Power received by the MT in the 25 de Abril Bridge, with distance.

The differences can be explained by some of the assumptions taken in the simulations. One of them is, as mentioned, the distances considered for the interfering BSs. This is an important aspect in the sense that it influences the interference which is used for the calculation of the receiver sensitivity with (A.6). Furthermore, in the simulations, the characteristics of the interfering BSs, namely their height and their tilt, is considered equal to that defined for the BS studied, this approximation being possibly one of the reasons for the differences observed between the measurements and the simulations. Another assumption taken in this analysis is the number of users considered. In fact, a variation in this number also causes a variation in the interference, thus, in the received power. Moreover, the fading parameters considered can also be different than those present during the measurements. In fact, the results obtained in the Subsection 5.3.5 show that the *K* parameter, used to describe the fast fading, can cause significant changes in the results obtained.

Considering all the mentioned factors, it should be noted that, when the planning or the optimisation of the coverage and capacity is being analysed in the bridge, it is important to perform a careful design and characterisation of the environment in order to obtain more reliable results in the simulations.

Chapter 6

Conclusions

In this chapter the main conclusions of this thesis are pointed out, as well as some suggestions for future work.

The main objectives of this thesis were to study the propagation, coverage, capacity and interference in linear environments, namely in tunnels and bridges, in UMTS, thus the study of a useful practical application. These goals were achieved through the development and implementation of a simulator in C++, which accounts for many parameters that can influence this analysis in such environments, providing the application wished. First, the models accounting for the propagation in tunnels and bridges were implemented, where the environment, link budget and fading characteristics are considered. These models allow the calculation of the required transmitted powers for both UL and DL for a certain distance or, alternatively, the calculation of the maximum distance at which BS and MT can communicate. All the results obtained in these models are used in the next step, where the interference is considered and the results concerning the transmitted powers, DL and UL interferences and C/I are obtained. With this tool, several results were analysed considering the variations of the environment characteristics, number of users, users' data rates, BS range, among others. Additionally, four scenarios in the city of Lisbon were studied, measurements being performed and comparisons with the theoretical results for two of them, namely for the Lisbon Underground and for the 25 de Abril Bridge being done.

In the tunnel, the propagation model used is presented in [Zhan03]. The module developed considers the tunnel sectional dimensions, number of users, position of users and of BS in the tunnel, frequencies used in DL and UL, BS antenna radiation pattern, MT antenna gain, indoor attenuation, and both slow and fast fading margins. Additionally, the extra attenuation caused by a curve in the tunnel is predicted, in this case, being the permittivity of the walls needed. For the bridge, the free space and flat earth propagation models are considered. The parameters required are the same considered for the tunnel case, although the bridge width is considered in spite of the tunnel characteristics and the curve is not considered in this case. To obtain the final results regarding coverage, capacity and interference, the interference is calculated in the third and final module, using the models described in Section 3.4 and the results previously obtained in the tunnel or bridge modules. The orthogonality factor and the number and distances of the interfering BSs are the required parameters. The model ends with the calculation, for both DL and UL, of the transmitted power, the intra- and inter-cell interferences and C/I. All these modules were implemented in the simulator, thus enabling a complete analysis of the parameters being studied for both the tunnel and the bridge environments.

Concerning the tunnel, it is observed that the path loss is lower in comparison with other environments due to the waveguide phenomenon, confirming the theoretical expectations. For the default scenario, the transmitted power required in the BS is 16.2 dBm. For the power transmitted by the MT, the results vary between -11 and 0.7 dBm, according to the user's distance to the BS. C/I for DL is in the order of 13.6 dB, being of about 10.5 dB for UL. From the results obtained, it is possible to conclude that no coverage or capacity problems are expected for the default scenario, since the powers obtained are below the maximums allowed, 43 and 21 dBm respectively for the BS and for the MT, thus, all 25 users considered in the 500 m range are served.

The increase in the tunnel dimensions leads to an increase in both DL and UL transmitted powers, since the location of the break point is highly related with these parameters. In fact, the larger the tunnel dimension is, the further the location of the break point is from the transmitting antenna, due to the reduction of the waveguide phenomenon. When an increase from 8 to 12 m is considered in the tunnel width, the BS power required suffers an increase of about 3 dB, while the power transmitted by the MT is between 1 and 3 dB higher than in the default scenario. When the height of the tunnel is changed from 6 to 9 m, a similar behaviour is observed in the powers, the DL transmitted power being about 4.4 dB higher and the UL one between 2 and 5 dB higher.

In order to study capacity, three alternative cases were considered regarding the number of users trying to connect with the BS, namely the situations with 5, 15 and 35 users. For the first case, a reduction of about 23 dB is observed in the BS transmission power, comparing with the default scenario. This is a significant decrease, caused by the reduction of DL interference. Regarding the MT transmission power, it is between 12 and 16 dB lower in comparison with the default case. The opposite situation happens when 35 users are considered. In this case, an increase of about 5 dB is observed in the BS transmission power, while the increase in the UL transmission power is of about 3 dB. However, even in the 35 users' case, the powers are below the maximum allowed.

A study is also performed to evaluate the influence of the variation of the BS range. For that purpose, ranges from 100 to 900 m, spaced by 200 m, were analysed. The BS transmission power decreases about 8 dB when the range increases from 100 to 900 m. This was not expected, but it can be explained by the behaviour of the radiation pattern, and by the fact that, when the range increases, the distance to the interfering BSs also increase leading to a decrease in the DL interference, thus, in the reduction of the power required. In UL the situation is similar, a decrease in the transmission power of about 7 dB being observed between the extreme cases considered. This study is important when the planning or optimisation of a network is being performed, since the distances between the BSs must be carefully chosen to improve the coverage and the capacity of the system.

The influence of the variation of the data rates is also studied, since a 3rd generation system is being analysed. In this case, significant variations in the transmitted powers and in capacity are observed. Due to the limitations in capacity, when all users are performing the most demanding service, i.e., the service with 384 kbps, only three users are served. The maximum value for the BS transmission power is obtained for the case where the user studied is performing the most demanding service, while the other users are considered with the voice service, being of about 31 dBm. The lower value for this parameter, about -4 dBm, is obtained when the user is performing the voice service, the remaining users being considered with the most demanding service. In what concerns the power transmitted by the MT, the same extreme cases are observed, powers being of about 11 and -10 dBm, respectively. In this case, C/I values are about 4 dB lower than the default case when the user is performing a data service. It can be concluded that no coverage problems are expected for the parameters considered, since the powers obtained are below the maximums allowed. However, if other parameters, such as the number of users, are changed, this study must be taken into account.

The variation of the BS antenna radiation pattern is also analysed, since this is an important parameter in system planning and optimisation. In fact, the radiation pattern influences strongly the results obtained concerning coverage and capacity. A directive antenna is more efficient than an omnidirectional one, in tunnels, since the required power in both BS and MT is lower, thus, increasing coverage and capacity. The difference between both approaches, for the MT transmission power, increases with distance, as expected, due to the differences in the directivity.

The influence of a curve in the tunnel is also studied. When a curve is considered, an increase of about 11 dB is observed in the BS transmission power. This behaviour is caused by the additional path loss and by the usage of the Rayleigh distribution to account for fast fading. In UL, the increase of power is between 11 and 13 dB. In what concerns C/I, an increase of about 2.2 and 2.7 dB is observed, respectively, for both DL and UL, since the fading margins are changed, this parameter being accounted in the calculation of the received power.

Concerning the bridge, for the default scenario, the power transmitted by the BS is of about 31 dBm. For the MT transmission power, an increase from -13 to 19.4 dBm is observed when the MT moves away from 50 to 500 m from the BS. This behaviour is explained by the increase in the path loss with the distance and by the down tilt considered in the BS antenna. In what concerns C/I, the values obtained are of about 14.5 and 11.4 dB for DL and UL respectively.

To evaluate capacity in the bridge, the study of the variation of the number of users is performed. A decrease of about 20 dB, in comparison with the default scenario, is observed in the BS transmission power when 5 users are considered. When 25 users are considered, the power is close to the maximum, being of about 43 dBm. Therefore, this is approximately the maximum number of users that can be served by the system, considering the DL situation. When the number of users is 35, the power is about 18 dB higher than that observed in the default case, being of about 49 dBm. This value is about 6 dB above the maximum power allowed in the BS. This behaviour is caused by the high path losses obtained for users as well as by the down tilt considered. In fact, this tilt is important to reduce the inter-cell interference; however, if a value below 7º is considered for this parameter, the results will be different, since the BS antenna gain for the users located at higher distances from the BS will increase. Therefore, this is an important parameter when the planning of a network is being studied, since the more appropriate value must be found to obtain the desired results when the balance between interference, coverage and capacity is done.

Concerning the MT transmission power, a decrease of about 5 dB is observed when 5 users are considered in spite of 15. When 35 users are considered, the user can only communicate with the BS at distances below 200 m, since at higher distances the transmission power is above the maximum allowed. However, since the DL and UL cases must be analysed together, this case is not relevant, since it has been verified that 35 users cannot communicate simultaneously with the BS. Considering the 25 users case, it is possible to conclude that when the user is at more than 300 m from the BS, communication with the BS is not possible, the required power being above 21 dBm. Therefore, the

conclusion that can be obtained is that, with 15 users, no coverage problems are expected and, as the number of users increase, the analysis must be carefully done, in order to estimate capacity.

The influence of the variation of the BS range is also studied for the bridge. In this case, an increase of about 36 dB is observed in the DL transmission power when the range of the BS increases from 100 to 900 m. This increase is, again, caused by the increase in the path loss and by the decrease in the BS antenna gain at higher distances due to the down tilt considered. However, for all the cases studied, no coverage problems are observed, since powers are below 43 dBm. Concerning the UL transmission power, it is possible to conclude that, when BSs are closer, power decreases for ranges up to 500 m, due to the decrease of the UL interference. Again, this behaviour is highly dependent on the down tilt considered. As in DL, no coverage problems are expected for any of the ranges considered.

Similar to the study performed to the tunnel, the influence of the services' types is also analysed for the bridge. In this case, the BS transmission power obtained is above the maximum for the cases where the user is performing the most demanding data service, while the other users are performing voice or 64 kbps. In fact, in these cases the power required is about 48 dBm. Regarding the MT transmission power, values below the maximum are observed for all cases.

To simulate the variation of the number of cars in the bridge, the *K* parameter of the Rice distribution is varied. The BS transmission power decreases 22 dB when the *K* parameter increases from 0 to 19 dB, which corresponds to a case with a very low number of movements in the environment. Regarding the MT transmission power, a similar decrease is observed. In this case, the MT cannot communicate with the BS for distances above 300 m, if *K*=0 dB, since at this distance the power is about 20 dBm, thus, closer to the maximum. Therefore, it can be concluded that, when the planning is being performed for the bridge, this parameter must be carefully chosen according to the environmental characteristics observed.

The influence of the existence of traffic in the bridge is also studied in this work. The BS transmission power increases about 0.5 dB when traffic is considered, in comparison with the default case. The increase is not significant, since the break point is close to the BS range, thus, the flat earth model is used in a short distance. For the same reason, the changes in the UL transmission power are negligible. However, if a higher range is considered or if the BS or the MT heights are changed, a more significant change can be observed in powers.

A study concerning the planning of coverage in the Rossio Tunnel is also performed. With the results obtained, and with the assumptions taken, it can be concluded that a good coverage can be obtained since the BS transmission power is about 17 dBm, thus below the maximum, the same analysis being valid for the MT transmission power, since it is between -7.3 and -4.9 dBm. This study can be used when the planning of UMTS is done in this tunnel.

For the Vasco da Gama Bridge, the same study is performed. Regarding the transmission power, the

values obtained are about 30.5 dBm, thus, below the maximum. In what concerns the MT transmission power, the values obtained are between -6 and 20 dBm. The maximum value is obtained for the maximum distance, due to the high path loss experienced by the MT. No coverage problems are expected in this case, however, at 800 m, taking the standard deviation into account, the transmission power can be above 21 dBm. This study is important since, with the assumptions taken, it can be concluded that a planning of the system can be done in this bridge with the BSs spaced of about 800 m and considering 4º of down tilt for the BS antennas.

The measurements performed in the Lisbon Underground show that, in general, a good agreement is obtained with the results predicted by the model, for the MT transmitted and received powers, the variations being explained by some of the assumptions taken in the simulations. Therefore, it is possible to conclude that the model was validated for the tunnel case.

Regarding the measurements performed in the 25 de Abril Bridge, a very good agreement is achieved in what concerns the MT transmission power. In what concerns the power received, the average difference between measurements and simulations is around 14 dB. This behaviour can be explained by the fact that some assumptions are taken in the simulations which, probably, need to be more carefully considered, such as the number of users, and the number and position of interfering BSs. In fact, the simulator considers that interfering BSs are similar to the BS studied, namely in what concerns to down tilt and height, thus, this being one of the reasons for the differences observed. However, bearing this in mind, it is possible to conclude that the model was also validated for the bridge case.

Noting that this model was started in this thesis, some suggestions for possible future work and upgrades in the model are presented here. First, a more intensive comparison could be done between measurements and simulations, namely performing measurements in different conditions and environments, such as with a different number of users, in railway and road tunnels, in different types of tunnels and bridges in what concerns to their materials, etc., collecting the maximum information possible regarding the surrounding environment. With this study, possible improvements, if needed, could be done in the models, for both the tunnel and the bridge. Other interesting idea is to include a module in the simulator to perform a temporal analysis together with the snapshot approach implemented, since in the environments studied the consideration of the vehicles or trains speed would supply a more powerful tool. The study of the influence on both coverage and capacity, of the introduction of MIMO techniques, could also be interesting for future researches. Finally, the upgrade of the models to new systems, such as HSPA, UMTS/LTE and WiMAX is both interesting and important, since it would create a more powerful tool.

Annex A - Link Budget

The link budget expressions and characteristics for UMTS R99 are presented here.

The path loss is given by [Corr07]

$$L_{p[\mathrm{dB}]} = P_{t[\mathrm{dBm}]} + G_{t[\mathrm{dBi}]} - P_{r[\mathrm{dBm}]} + G_{r[\mathrm{dBi}]}\,; \tag{A. 1}$$

where:

- P_t : power fed to the transmitting antenna;
- G_t : gain of the transmitting antenna;
- P_r : power available at the receiving antenna;
- G_r : gain of the receiving antenna.

The usual values of the transmitter output power, for both BS and MT, are presented in Table A.1. In this work, however, the maximum values used for both the BS and the MT transmission powers were suggested by Celfinet, being of 43 and 21 dBm, respectively.

Table A. 1. Typical values of the transmitter output power in UMTS (adapted from [Corr07]).

	BS			MT
Type of cell	Macro	Micro	Pico	
P_{Tx} [dBm]	[40, 43]	[30, 33]	[20, 23]	[10, 33]

The power balances are different in DL and UL, being the Equivalent Isotropic Radiated Power (EIRP) for each case expressed as [Corr07]

$$EIRP^{DL}_{[\mathrm{dBm}]} = P_{Tx[\mathrm{dBm}]} - L_{c[\mathrm{dB}]} + G_{t[\mathrm{dBi}]}\,; \tag{A. 2}$$

$$EIRP^{UL}_{[\mathrm{dBm}]} = P_{Tx[\mathrm{dBm}]} - L_{u[\mathrm{dB}]} + G_{t[\mathrm{dBi}]}\,; \tag{A. 3}$$

where:

- P_{Tx} : transmitter output power;
- L_c : losses in cable between transmitter and antenna;
- L_u : losses due to user, normally between [3,10] dB for voice service and between [0,3] dB for data service.

The received power depends on the link and on the system, being also different for DL and UL,

expressed for each case, respectively, by [Corr07]

$$P_{Rx[\mathrm{dBm}]}^{DL} = P_{r[\mathrm{dBm}]} - L_{u[\mathrm{dB}]}\,; \tag{A. 4}$$

$$P_{Rx[\mathrm{dBm}]}^{UL} = P_{r[\mathrm{dBm}]} - L_{c[\mathrm{dB}]}\,. \tag{A. 5}$$

In UMTS the receiver sensitivity can be obtained as [Corr07]

$$P_{Rx\min[\mathrm{dBm}]} = \left(N + I\right)_{[\mathrm{dBm}]} + E_b / N_{0\,[\mathrm{dB}]}\,; \tag{A. 6}$$

where:

- E_b / N_0 : signal-to-noise ratio (SNR);
- I : total interference;
- N : total noise power, given by

$$N_{[\mathrm{dBm}]} = -174 + 10\log\left(\Delta f_{[\mathrm{Hz}]}\right) + F_{[\mathrm{dB}]} + M_{I[\mathrm{dB}]} - G_{P[\mathrm{dB}]}\,; \tag{A. 7}$$

where:

- Δf :signal bandwidth, taken as the chip rate, $\Delta f = R_c = 3.84\mathrm{Mc/s}$;
- F : noise figure;
- M_I : interference margin.
- G_p : processing gain, given by

$$G_{P[\mathrm{dB}]} = 10\log_{10}\left(\frac{R_c}{R_b}\right); \tag{A. 8}$$

where:

- R_c : chip rate;
- R_b : bit rate.

The interference margin is obtained as [Corr07]

$$M_I = -10\log\left(1 - \eta\right); \tag{A. 9}$$

where η is the load factor.

As mentioned, the receiver sensitivity is given by (A.6). However, the power at the receiver is calculated with an additional margin, ΔP , due to fading, as

$$P_{r[\mathrm{dBm}]} = P_{Rx\min[\mathrm{dBm}]} + \Delta P_{[\mathrm{dB}]}\,; \tag{A. 10}$$

where:

$$\Delta P_{[\mathrm{dB}]} = M_{SF[\mathrm{dB}]} + M_{FF[\mathrm{dB}]} - 6\,; \qquad \text{(A. 11)}$$

where:

- M_{SF} : slow fading margin;
- M_{FF} : fast fading margin;

The typical values for R_b are presented in Table A.2, for voice and for data services, as well as the SNR values.

Table A. 2. Typical values for R_b and for the SNR (sources: [Corr07] and Celfinet).

Service	R_b [kbps]	SNR [dB]	
		DL	UL
Voice	12.2	9	6
Data	64	5.5	2.5
	128	5.2	2.2
	384	4.8	1.8

Some margins are taken into account to consider additional losses due to radio propagation and others [Corr07]:

$$M_{p[\mathrm{dB}]} = M_{SF[\mathrm{dB}]} + M_{FF[\mathrm{dB}]} + L_{pind[\mathrm{dB}]} - G_{SH[\mathrm{dB}]} \qquad \text{(A. 12)}$$

where:

- L_{pind} : indoor penetration;
- G_{SH} : soft handover gain.

The total path loss is given by [Corr07]

$$L_{ptotal[\mathrm{dB}]} = L_{p[\mathrm{dB}]} + M_{p[\mathrm{dB}]} \qquad \text{(A. 13)}$$

The number of codes required and the SF values for each data rate are shown in Table A.3.

Table A. 3. Number of codes and spreading factor for each service (extracted from [Corr07]).

Service [kbps]	SF	#codes (256)
12.2	128	2
64	32	8
128	16	16
384	4	64

Annex B – Fresnel Formulas for the Reflection Coefficients

This annex provides the reflection coefficients for the vertical and horizontal polarisations, being given, respectively, by [BrCA07]

$$\Gamma_v = \left| \frac{\varepsilon_r \sin(\varphi_1) - \sqrt{\sin^2(\varphi_1) + \varepsilon_r - 1}}{\varepsilon_r \sin(\varphi_1) + \sqrt{\sin^2(\varphi_1) + \varepsilon_r - 1}} \right| ; \tag{B. 1}$$

$$\Gamma_h = \left| \frac{\sin(\varphi_1) - \sqrt{\sin^2(\varphi_1) + \varepsilon_r - 1}}{\sin(\varphi_1) + \sqrt{\sin^2(\varphi_1) + \varepsilon_r - 1}} \right| ; \tag{B. 2}$$

where:

- ε_r : permittivity;
- φ_1 : grasing angle of incidence.

In modern concrete tunnels, the conductivity is low; therefore, the effect on the reflection coefficient is negligible, so the permittivity can be considered as real. The typical value of the permittivity for concrete is 5 [BrCA07].

Annex C – Propagation Loss Caused by Curves in a Tunnel

In this annex, a method to calculate the propagation losses in curves, in a tunnel, is presented.

The model presented is based on [BrCA07] and [NiSB98]. This method considers that the power after a certain number of reflections in the tunnel walls, in curves, for each ray of initial power P_0, can be computed as

$$\frac{P_{ref}}{P_0} = \left|\Gamma_1\right|^{2N_1} \left|\Gamma_2\right|^{2N_2} ; \qquad \text{(C. 1)}$$

where:

- N_1: number of reflections in the vertical walls;
- N_2: number of reflections in the horizontal walls;
- Γ_1: reflection coefficient of the vertical walls;
- Γ_2: reflection coefficient of the horizontal walls.

Normally, tunnels only have curves on the horizontal axis, thus there is an increase of the reflections in the vertical walls. Therefore, this extra attenuation is estimated calculating the number of times that the ray is reflected and the loss due to each reflection. A curved section is defined as shown in Fig. C.1, where R_{curv} is the radius of the curve, x_{curv} denotes the greatest distance between the wall and the incident ray, y_{curv} represents the dimension of the ray between two consecutive reflections in the wall, and φ_1 is the grasing angle of incidence with the vertical walls.

The y_{curv} parameter is given by

$$y_{curv} = \sqrt{R_{curv}^2 - \left(R_{curv} - x_{curv}\right)^2} ; \qquad \text{(C. 2)}$$

When the length $2y_{curv}$ increases, the number of reflections, per metre, in the vertical walls decreases, meaning that they are inversely proportional to the distance $2y_{curv}$, and can be written as

$$N_{1c} \propto \frac{1}{2y_{curv}} = \frac{1}{2\sqrt{R_{curv}^2 - \left(R_{curv} - x_{curv}\right)^2}} . \qquad \text{(C. 3)}$$

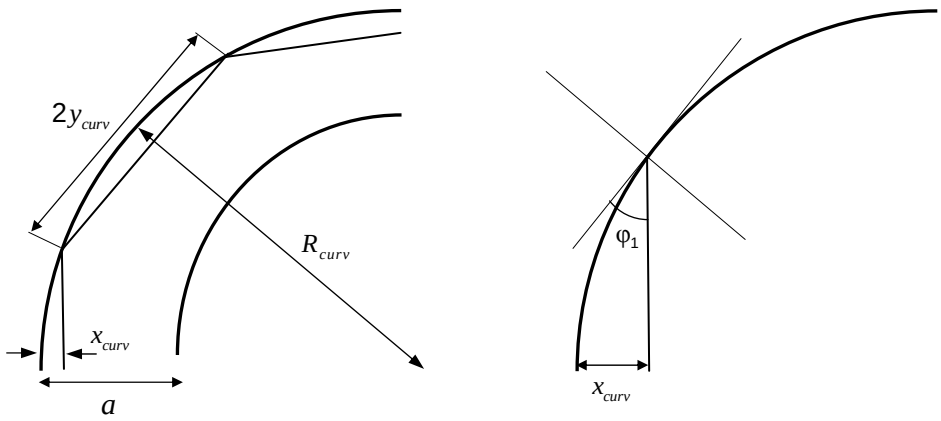

(a) Reflected rays in a curve (b) Representation of the grasing angle

Figure C.1. Geometry used to calculate the attenuation of curves (based on [BrCA07] and [NiSB98]).

The grasing angle of incidence φ_1 is obtained by

$$\varphi_1 = \tan^{-1}\left(\frac{\sqrt{R_{curv}^2 - \left(R_{curv} - x_{curv}\right)^2}}{R_{curv} - x_{curv}}\right). \tag{C. 4}$$

For simplification, the x_{curv}, in the simulator, is considered a constant value, equal to one fourth of the tunnel width.

Annex D – User's Manual

This annex presents the simulator's user manual.

When the application is started, the first window that appears allows choosing between the study of the tunnel or the bridge environment. When the tunnel option is selected, the window associated to the Tunnel Propagation Analysis Module is presented, shown in Fig. D.1. In this window, the user must choose the section type of the tunnel, the parameter to study, the existence or not of a curve in a tunnel as well as the file containing the radiation pattern of the BS antenna considered. Pressing the 'BS Antenna Radiation Pattern' button, a window, presented in Fig. D.2, appears where the file can be selected with a double click. Other input parameters, presented in Fig. D.1 and listed in Subsection 4.2.1, are needed. Several default values are already defined in the simulator, which can be selected by pressing the 'Default' button. Inserted all the input parameters, the 'Run' button must be pressed for the calculation of the output parameters of this module. Additionally, after being presented the results in the window, it is possible to observe a representation of the scenario chosen, where the BS and all the users position is shown, pressing the 'Graph' button. The variation of the path loss and of the power received by the MT is also presented in this window, as shown in Fig. D.3. When the 'Run' button is pressed, an output file named 'Tunnel_parameters.xls', is created in the same folder where the file of the BS antenna radiation pattern is located, including some of the main input and output parameters calculated.

The next window, shown in Fig. D.4, appears when the 'Interference' button is pressed. This window corresponds to the Interference Analysis module, where the final results of the simulator are obtained. Here, the orthogonality factor and the number of interfering BSs are the input parameters needed. Regarding the interfering BSs, it should be chosen the distance of each BS considered to the BS being studied, as well as their relative positions, i.e., for each BS it must be indicated if it is in front, behind or in a side position comparing with the studied BS, as explained in Subsection 4.2.2. Similar to the previous module, default values are also available which can be obtained by pressing the 'Default' button. If some modification needs to be done in the Tunnel Propagation Analysis Module, the 'Back' button can be pressed to return to that window. After the input of the requested parameters, the results are obtained by pressing the 'Run' button. The main results can be visualised in this window, while more detailed results are stored in a file named 'Results.xls' in the same folder previously mentioned. The new curve of the power received, obtained after considering the interference, can be seen pressing the 'Graph' button.

If the Bridge environment is chosen, the window shown in Fig. D.5 appears. This window corresponds to the Bridge Propagation Analysis Module and has the same objective that the window explained for the tunnel case, but regarding the bridge. Here, the parameters listed in Subsection 4.2.1 must be given, being also chosen the BS antenna radiation pattern similarly as in the tunnel case. The 'Default' option is also available in this case. When the 'Run' button is pressed, the results of the calculations

performed are presented, namely regarding the transmitted powers, the path loss and the break point. An output file, named 'Bridge_parameters.xls' is created and stored as in the tunnel case. Pressing the 'Graph' button, it is possible to visualise the distribution and the location of the users and of the BS in the bridge, as well as the variation of the path loss and of the received power with the distance, as shown in Fig. D.3. Pressing the 'Interference' button, the window relative to the Interference Analysis module is presented, being the behaviour similar to the explained previously.

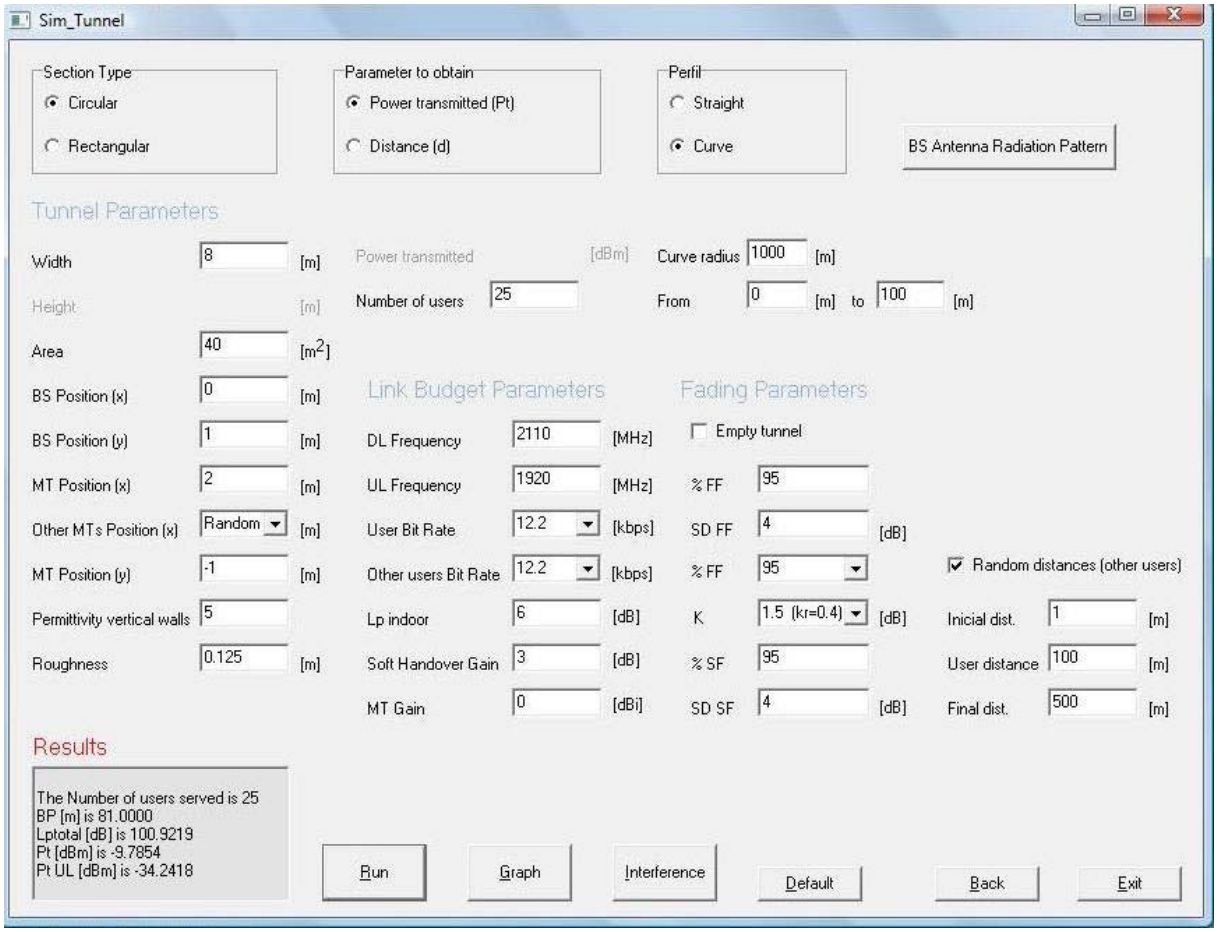

Figure D.1. Tunnel Propagation Analysis module window.

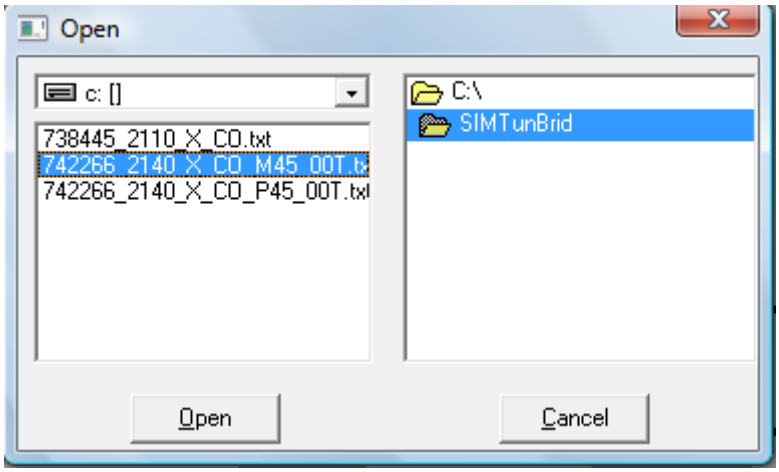

Figure D.2. Window where the radiation pattern of the BS antenna is selected.

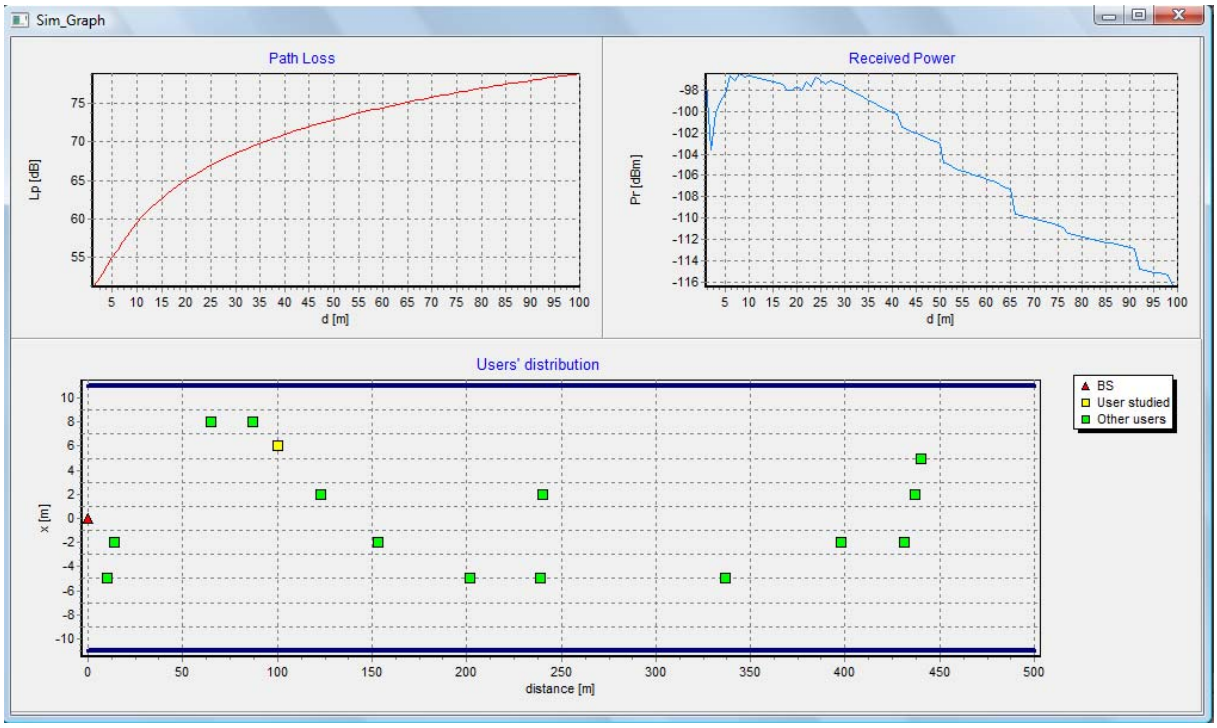

Figure D.3. Window representing the location of the users and the variation of the path loss and of the received power with the distance.

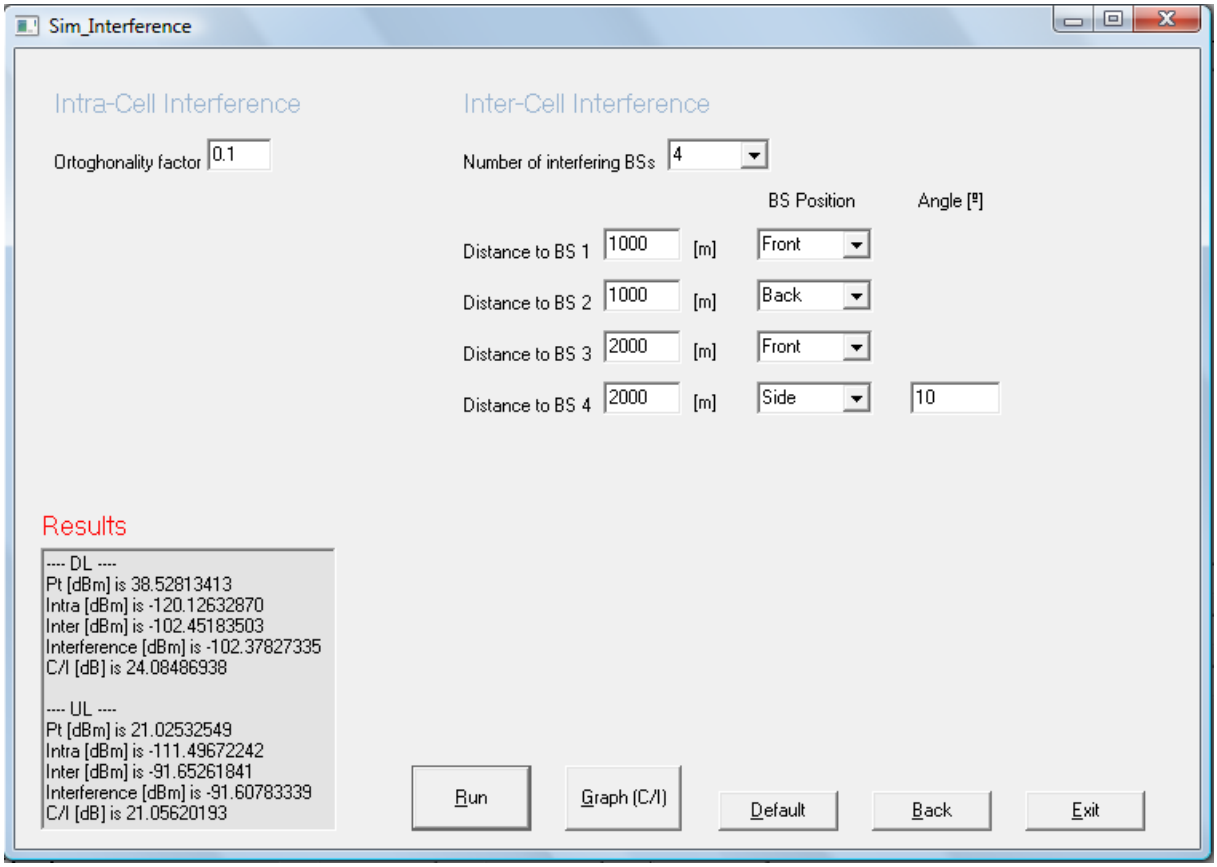

Figure D.4. Interference Analysis module window.

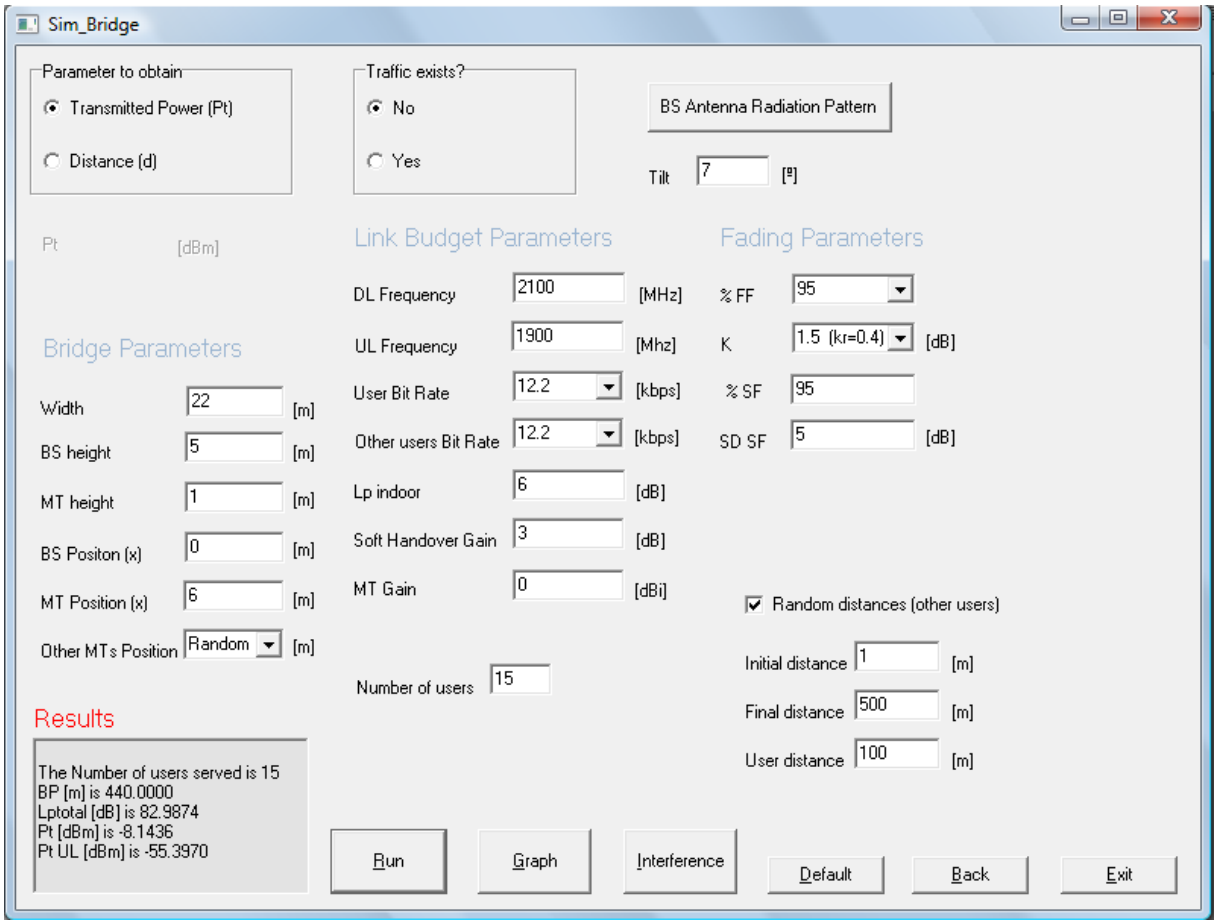

Figure D.5. Bridge Propagation Analysis module window.

In any of the main windows, it is possible to exit the simulator by pressing the ‘Exit’ button.

Annex E – Values Considered for the *K* Parameter of the Rice Distribution

The *K* parameter of the Rice distribution is the ratio of the power received via the LoS path to the power obtained from the NLoS paths. The *K* parameters used in this thesis and implemented in the simulator were obtained from an extrapolation done from the figure of the Rice Cumulative Distribution Function (CDF) presented in [Corr07]. This figure shows the curves of the CDF for different values of the k_r parameter, which is related with the *K* parameter as follows

$$K = \frac{1}{k_r} - 1. \qquad \text{(E. 1)}$$

In the extrapolation, the most used probabilities P_{FF} were considered as well as different curves, in order to consider different values for the *K* parameter. In Table E.1, the values for the *K* parameter and the fast fading margins obtained are presented for the probabilities considered.

Table E.1. Fast fading margins (M_{FF}) considered in the simulator for the Rice distribution.

M_{FF} [dB]		P_{FF} [%]				
		50	80	90	95	99
K [dB]	0	20	13	10	7	2
	1.5	18	10.5	8	5	1.6
	4	12	7	5	3.5	1.2
	5.67	9.5	5	4	3	0.8
	9	7	4	3	2.2	0.4
	19	4.4	2.5	2	1.5	0

Annex F – Radiation Pattern of the BS Antenna

This annex provides the radiation pattern, presented in Fig. F.1 for both the horizontal and vertical patterns, of the BS antenna considered – K742266 [Kath08] –, used in all the scenarios analysed for both the tunnel and the bridge cases. This antenna was suggested by Celfinet since it is commonly used in the environments studied, the information required to obtain the radiation pattern being also supplied by the company.

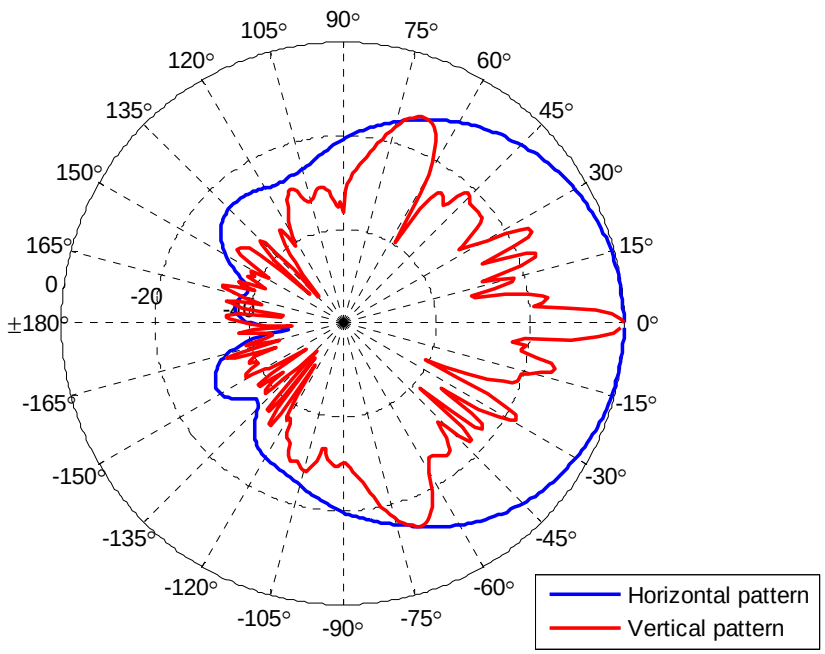

Figure F.1. BS antenna radiation pattern in the horizontal and vertical patterns.

This antenna is cross polarised with a maximum gain of about 16.4 dBi. For the frequencies considered, the half power beam width in the horizontal pattern is of about 62º, while in the vertical pattern it is 4.7º; therefore, it is a highly directive antenna. The usage of antennas with these characteristics is normal in the environments being studied, since they are linear.

According to the information obtained, in the Lisbon Underground other antennas are used, with smaller dimensions, these being also antennas with high directivities. Table F.1 summarises the main characteristics of the K742266 and of the other antennas normally used.

Table F.1. Main characteristics of some antennas used in linear environments [Andr08], [Kath08].

Antenna	Gain [dBi]	Half power beam width of the horizontal pattern [º]	Half power beam width of the vertical pattern [º]
K742266	16.4	62	4.7
K742192	11.5	50	45
K800 10251	19.8	33	8.5
DB992HG28N-B	16	30	30

Annex G – Additional Results for the Parameters Variation in the Tunnel

In this annex, the additional results obtained in the study of the parameters variation for the tunnel case are presented.

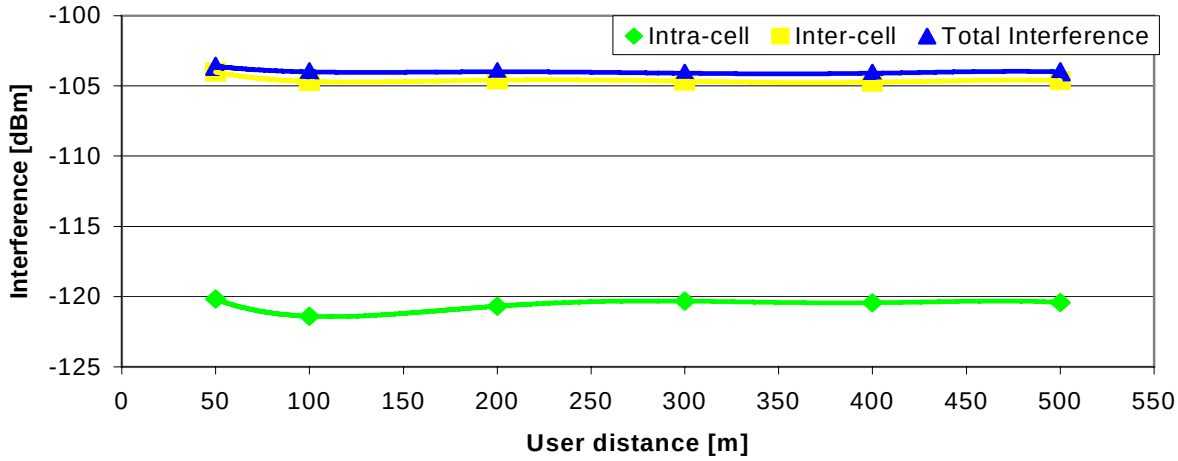

Figure G.1. DL interference for the default scenario, with distance, in the tunnel.

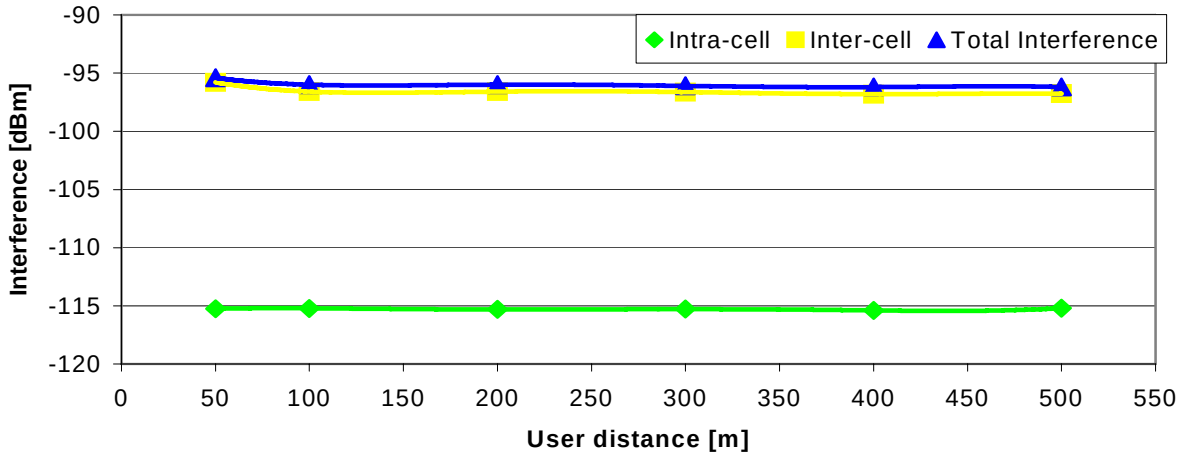

Figure G.2. UL interference for the default scenario, with distance, in the tunnel.

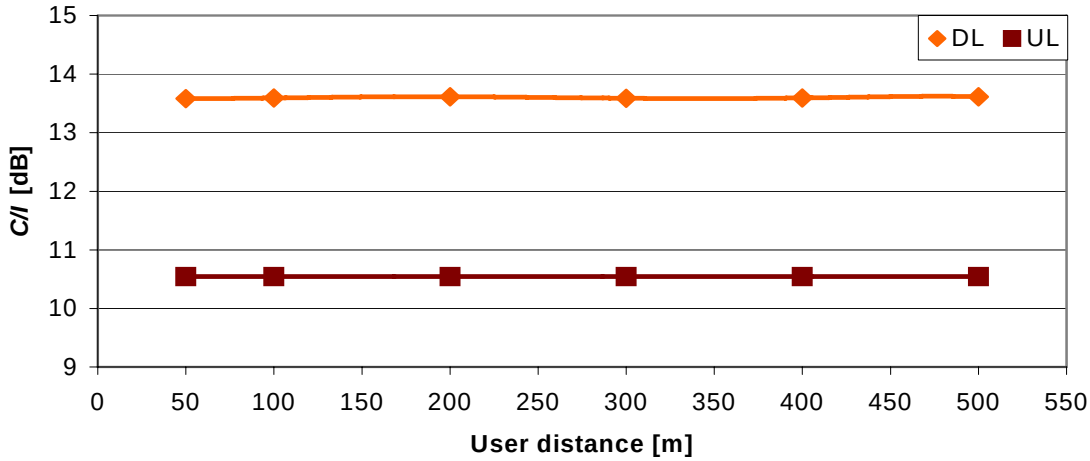

Figure G.3. C/I for the default scenario, with distance, in the tunnel.

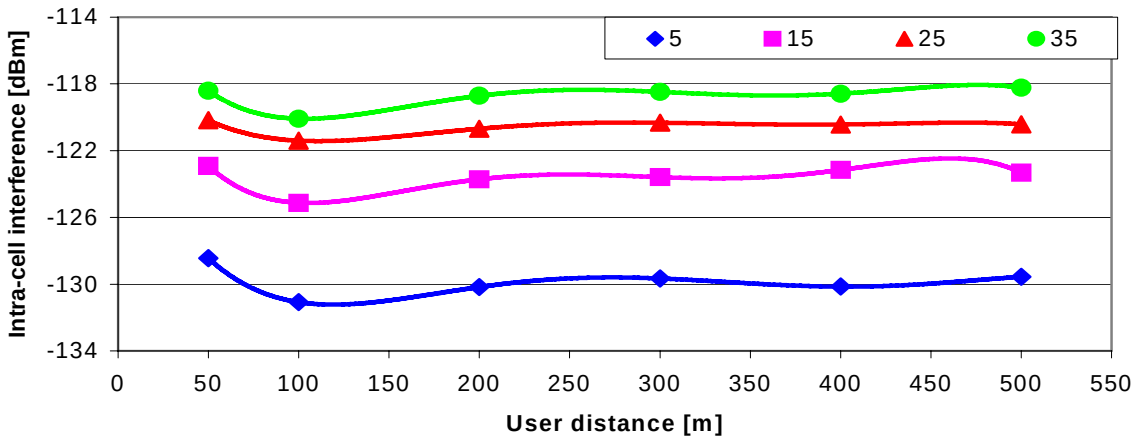

Figure G.4. DL intra-cell interferences, with distance, for different number of users, in the tunnel.

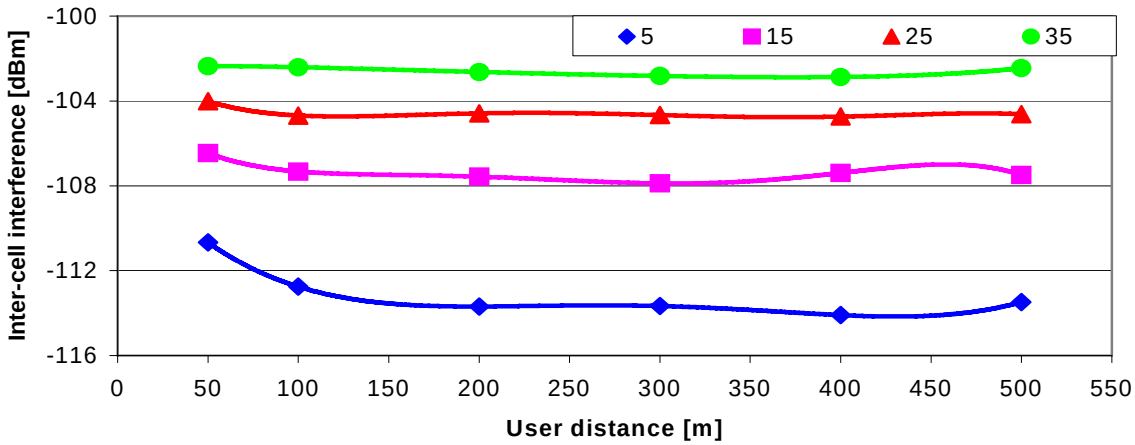

Figure G.5. DL inter-cell interferences, with distance, for different number of users, in the tunnel.

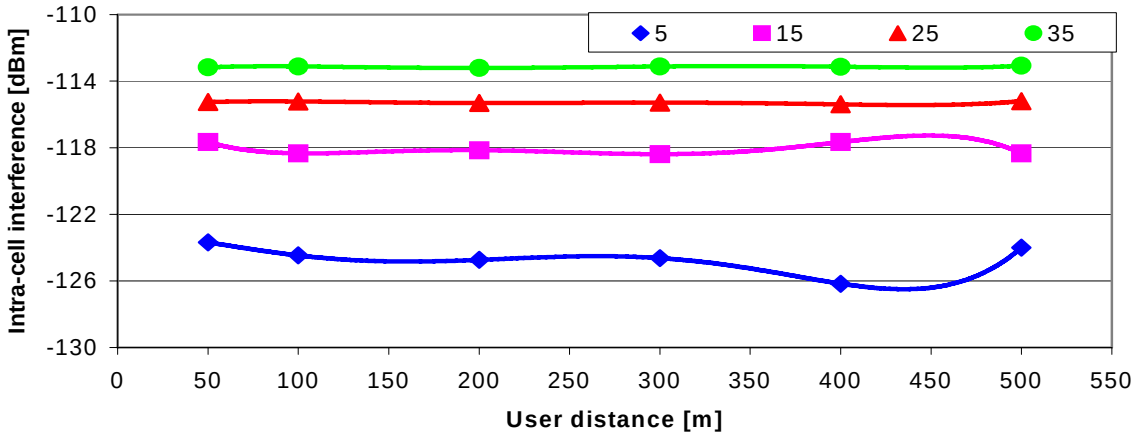

Figure G.6. UL intra-cell interferences, with distance, for different number of users, in the tunnel.

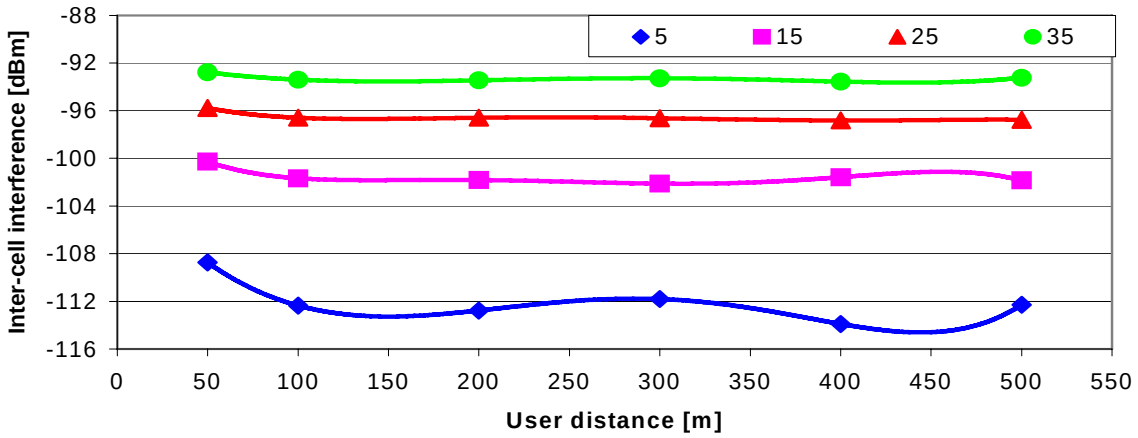

Figure G.7. UL inter-cell interferences, with distance, for different number of users, in the tunnel.

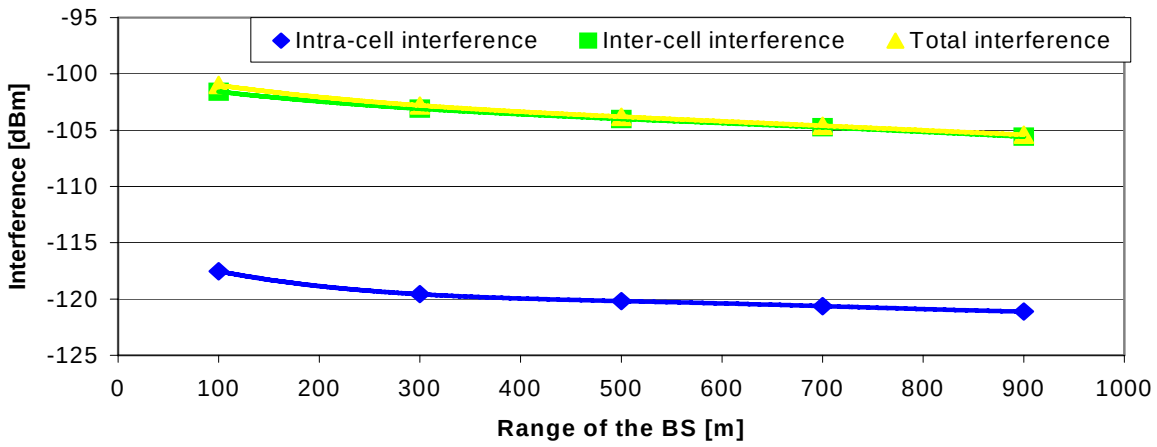

Figure G.8. DL interferences with BS range, in the tunnel.

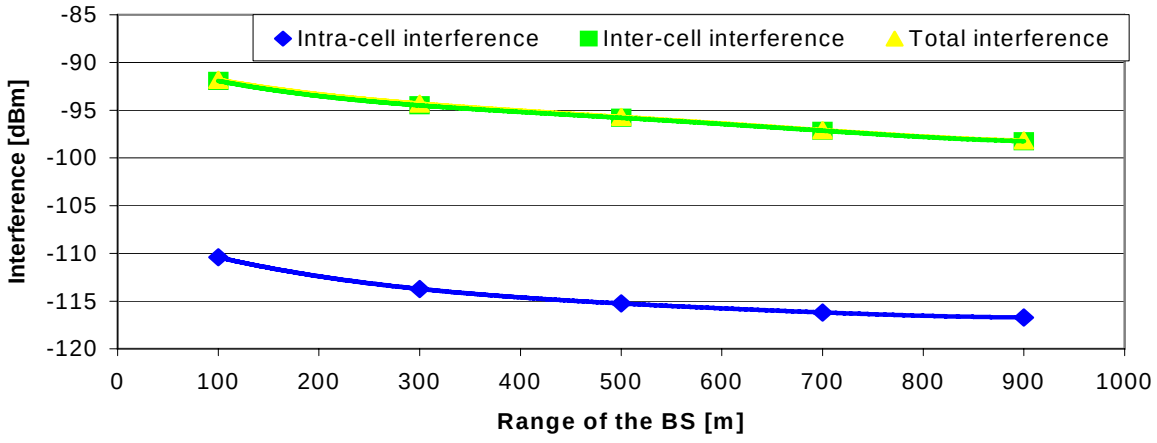

Figure G.9. UL interferences with BS range, in the tunnel.

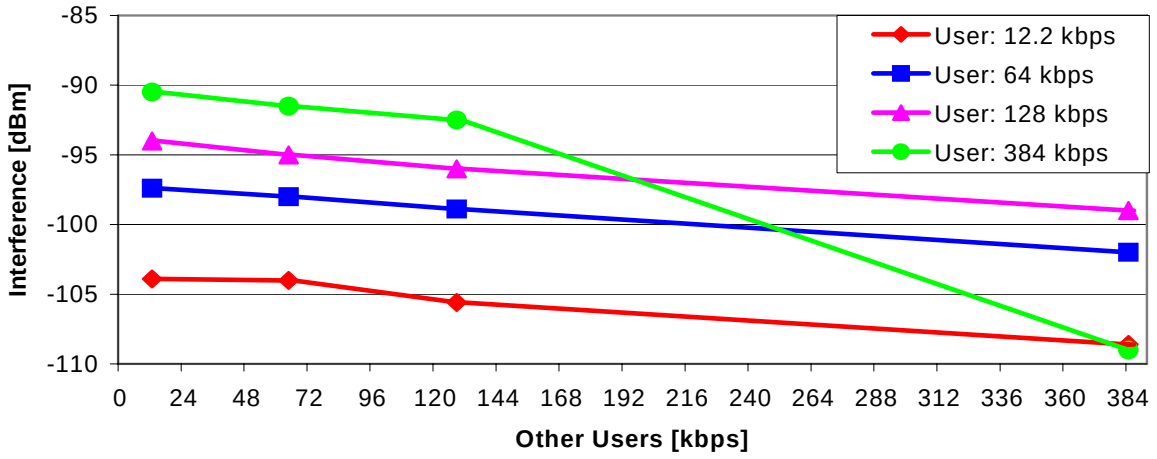

Figure G.10. Total DL interferences with different services, in the tunnel.

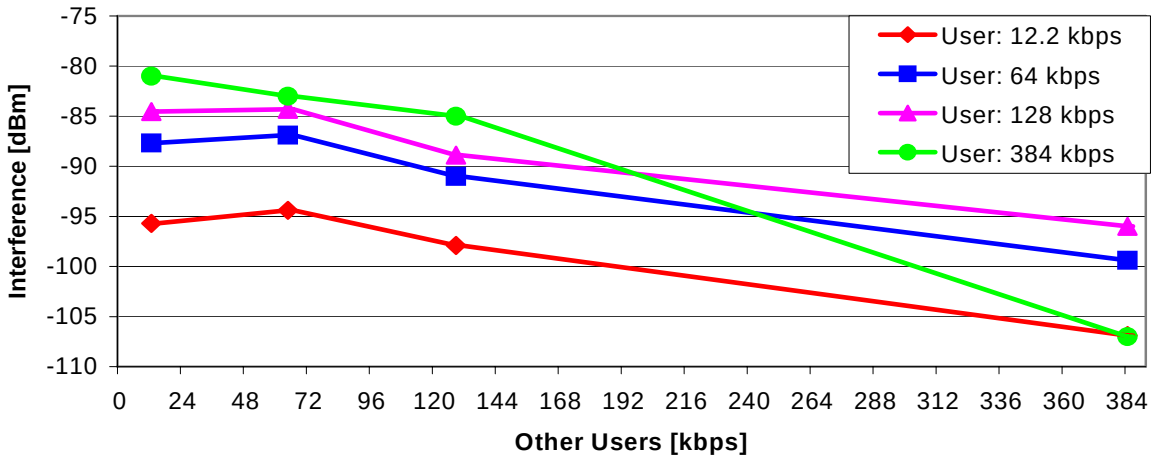

Figure G.11. Total UL interferences with different services, in the tunnel.

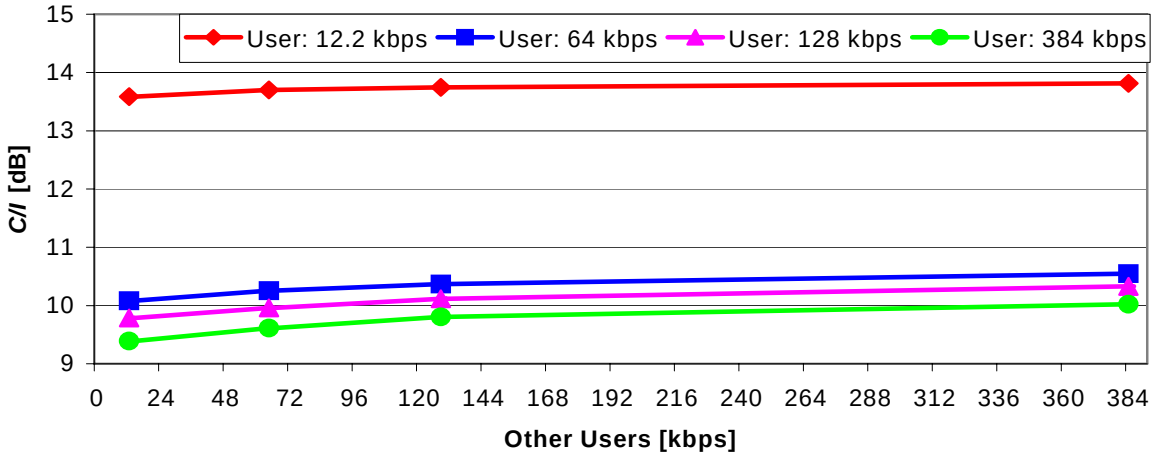

Figure G.12. DL C/I with different services, in the tunnel.

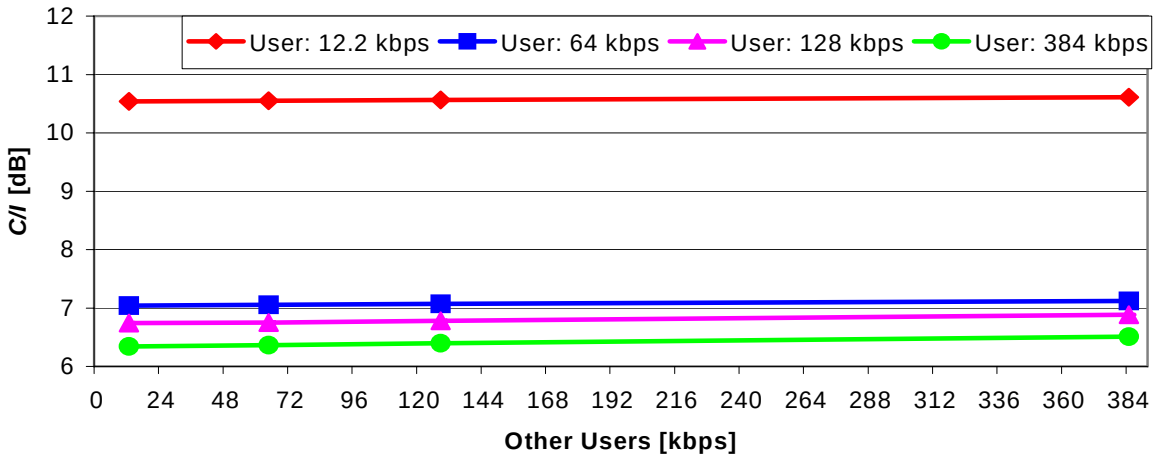

Figure G.13. UL C/I for different services, in the tunnel.

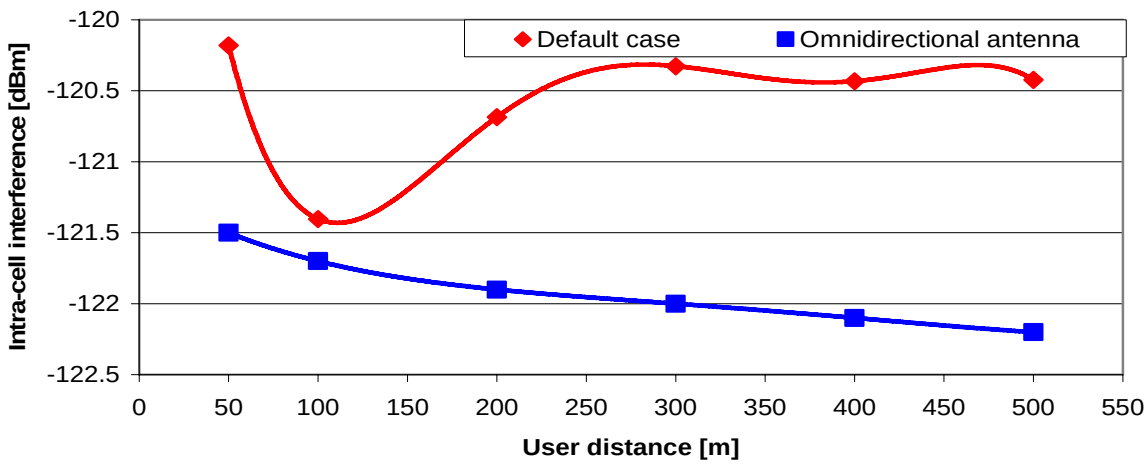

Figure G.14. DL intra-cell interference, with distance, for different BS antenna radiation patterns.

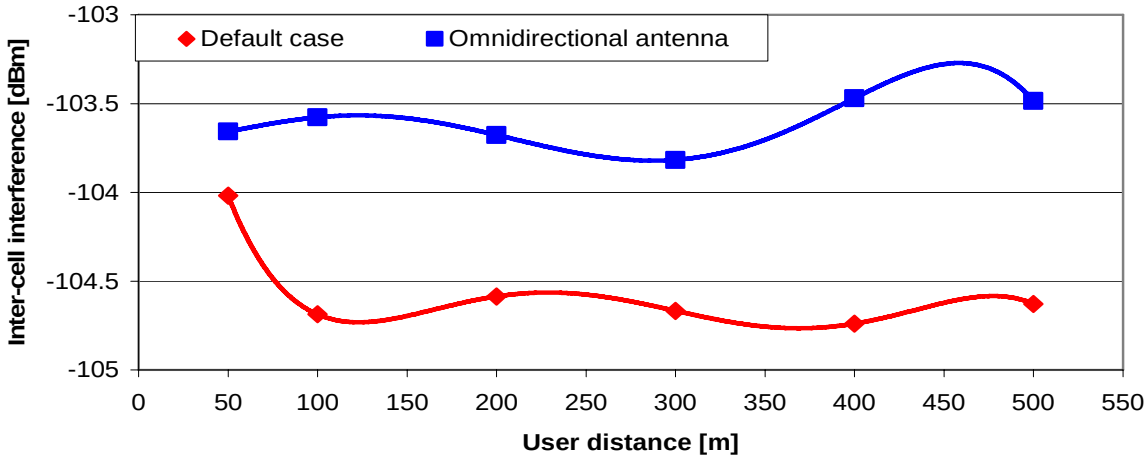

Figure G.15. DL inter-cell interference, with distance, for different BS antenna radiation patterns.

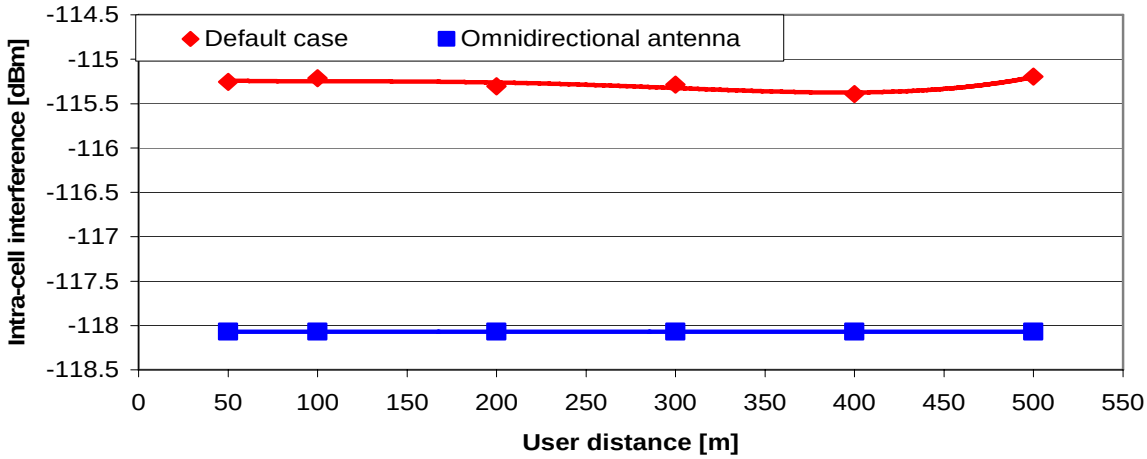

Figure G.16. UL intra-cell interference, with distance, for different BS antenna radiation patterns.

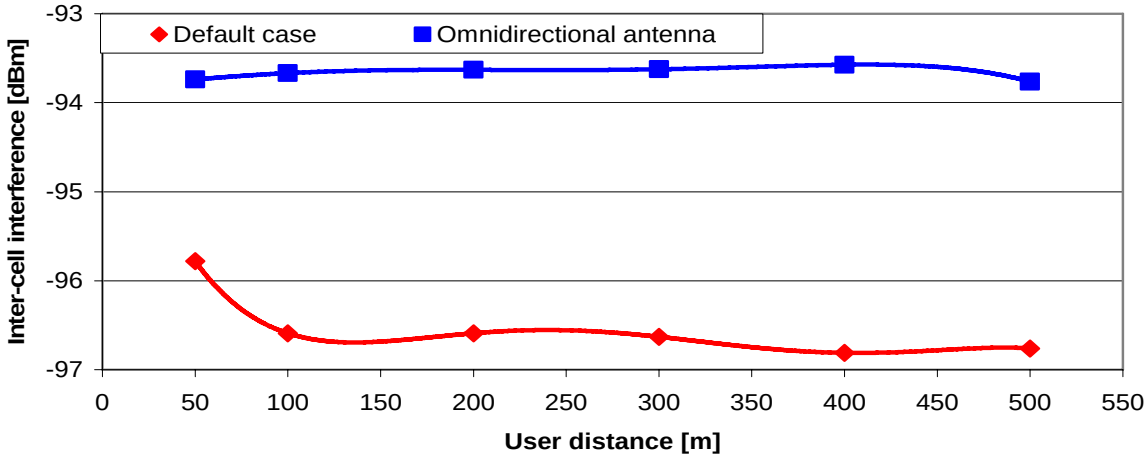

Figure G.17. UL inter-cell interference, with distance, for different BS antenna radiation patterns.

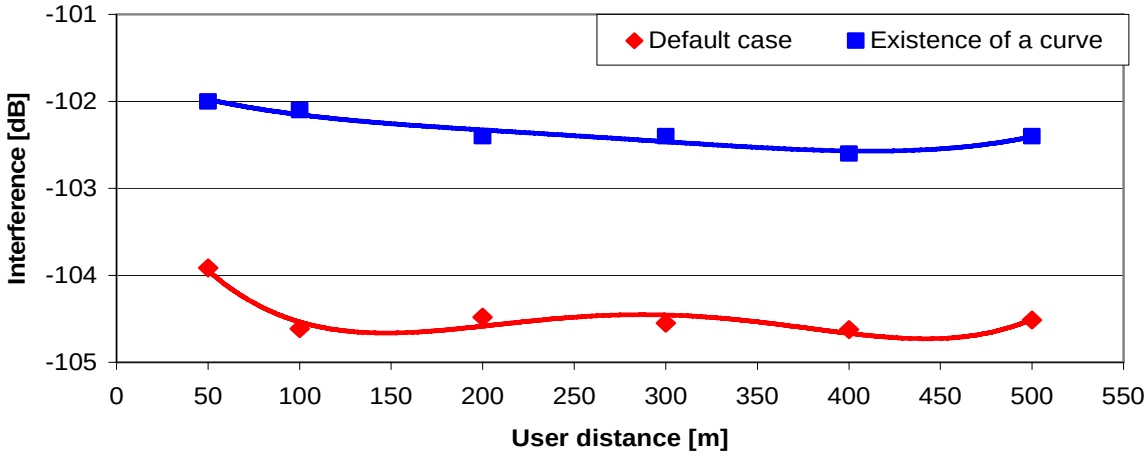

Figure G.18. DL interference, with distance, with and without a curve.

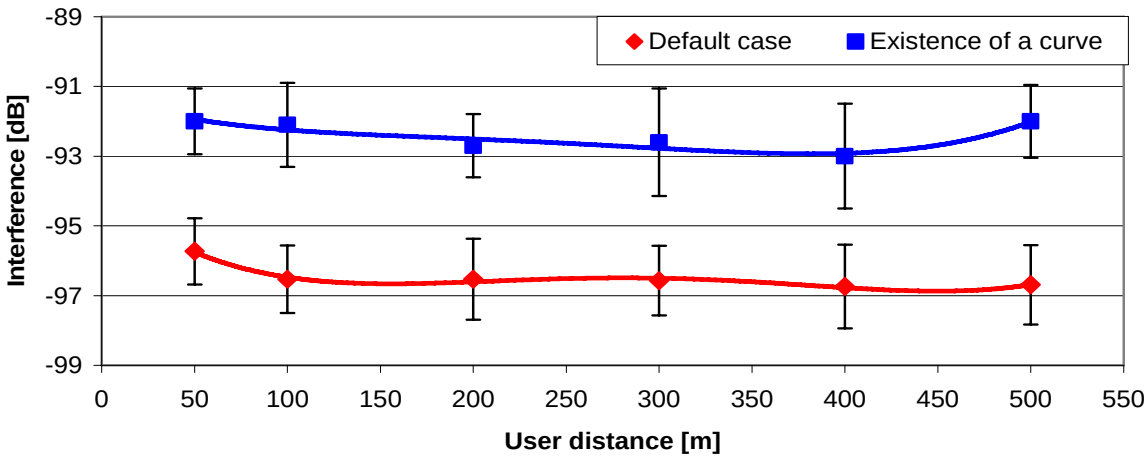

Figure G.19. UL interference, with distance, with and without a curve.

Annex H – Additional Results for the Parameters Variation in the Bridge

In this annex, the additional results obtained in the study of the parameters variation for the bridge case are presented.

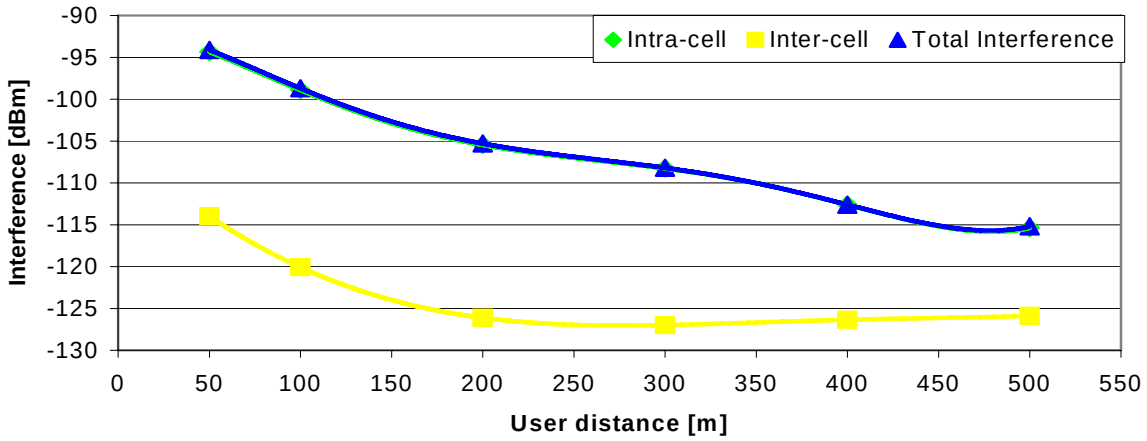

Figure H.1. DL interference, with distance, for the default scenario, in the bridge.

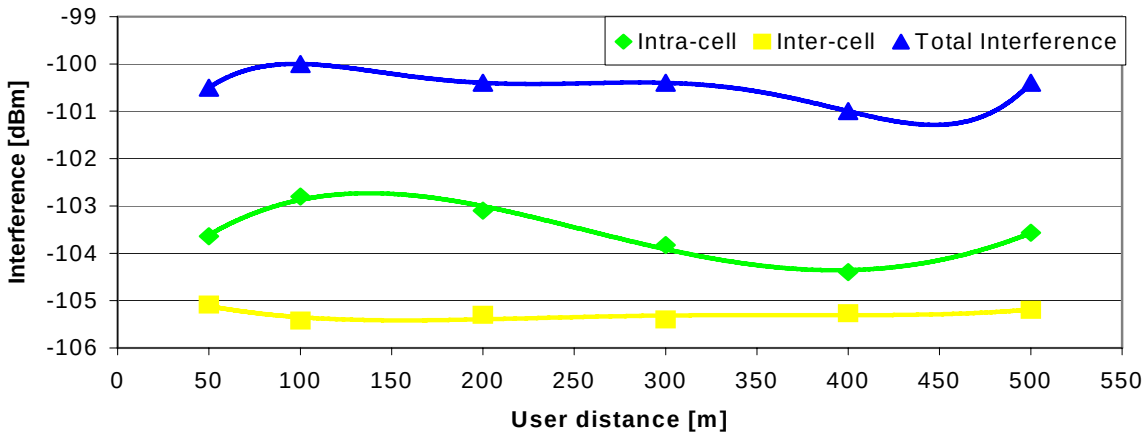

Figure H.2. UL interference, with distance, for the default scenario, in the bridge.

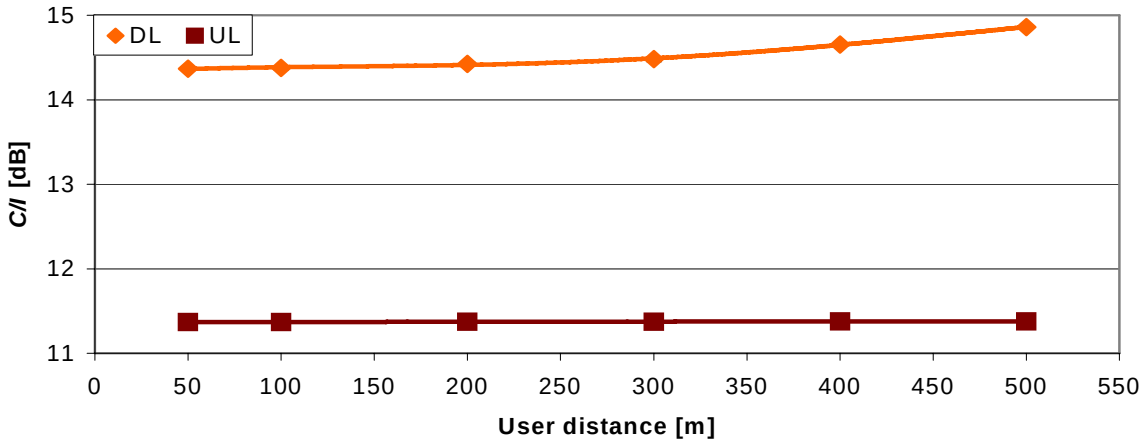

Figure H.3. C/I for the default scenario, with distance, in the bridge.

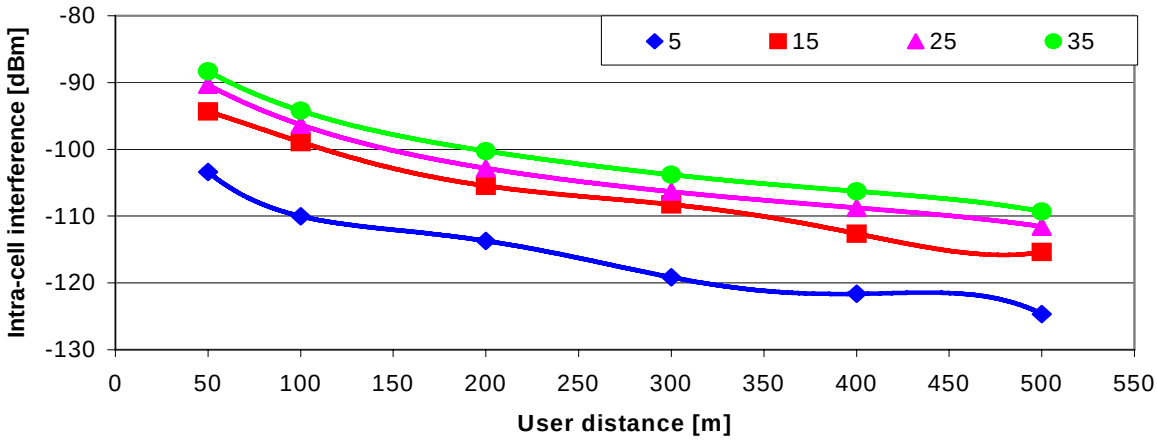

Figure H.4. DL intra-cell interferences, with distance, for different number of users, in the bridge.

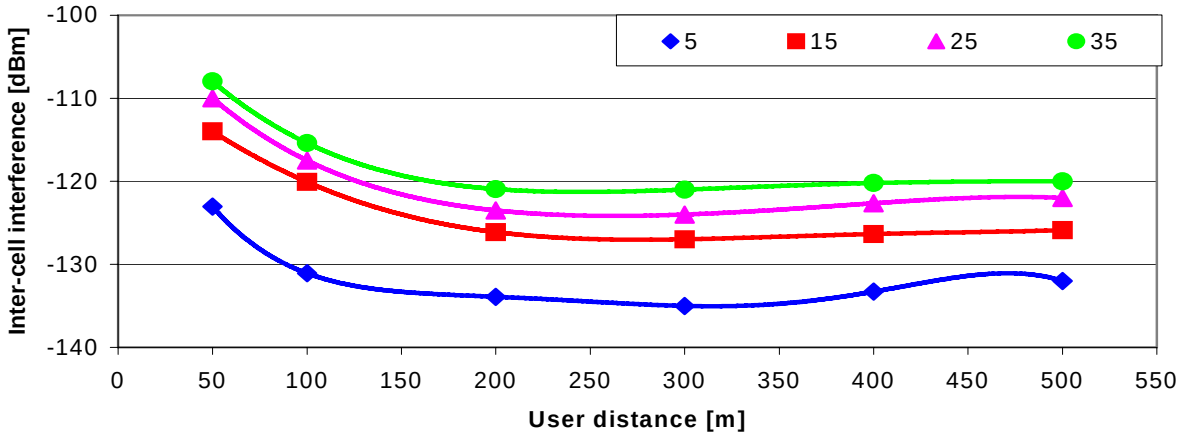

Figure H.5. DL inter-cell interferences, with distance, for different number of users, in the bridge.

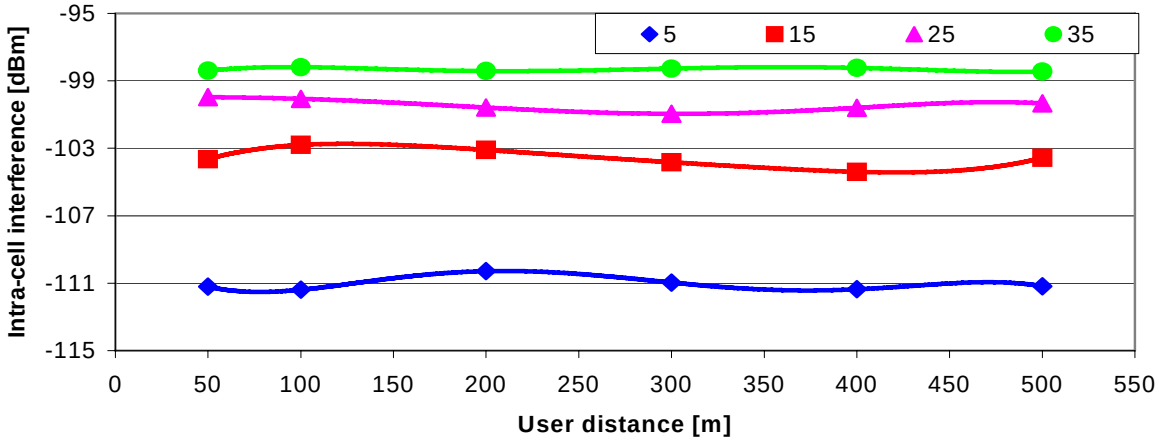

Figure H.6. UL intra-cell interferences, with distance, for different number of users, in the bridge.

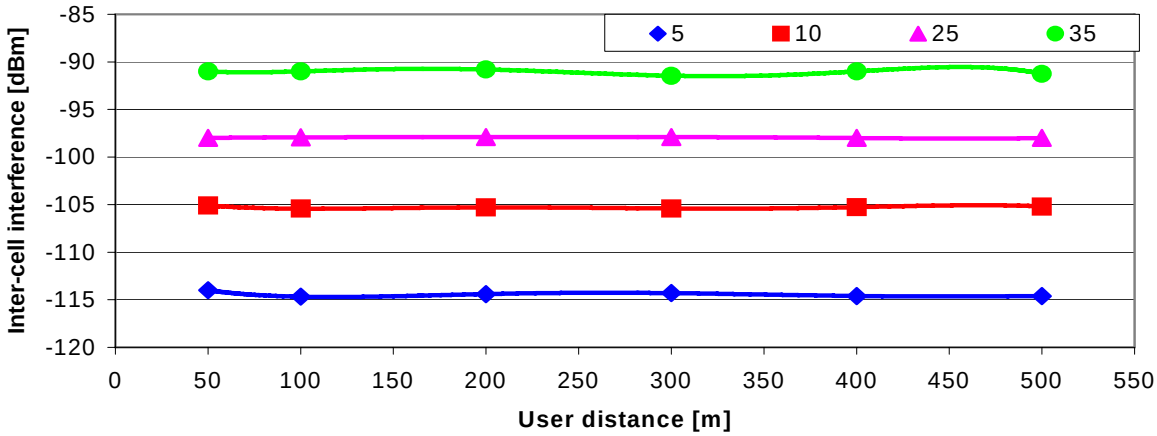

Figure H.7. UL inter-cell interferences, with distance, for different number of users, in the bridge.

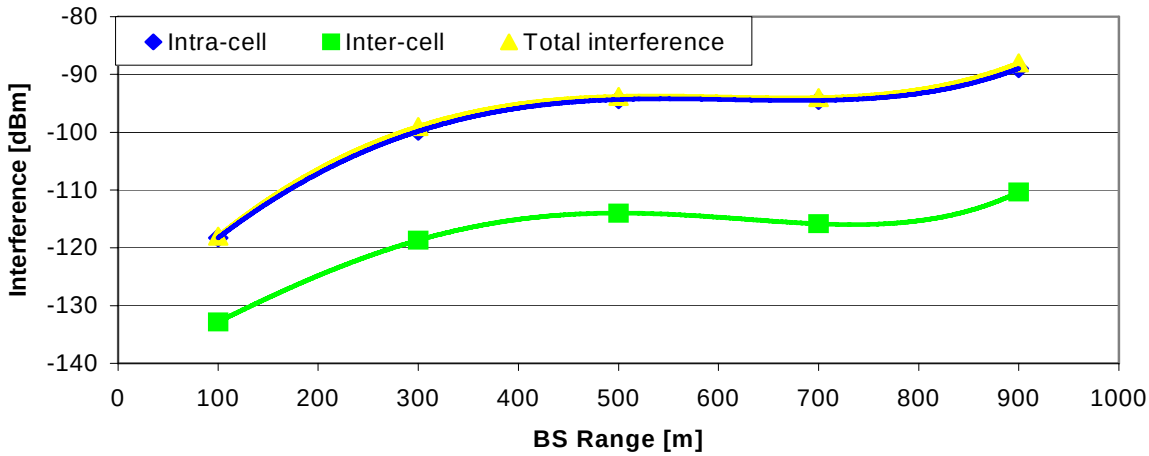

Figure H.8. DL interferences with BS range, in the bridge.

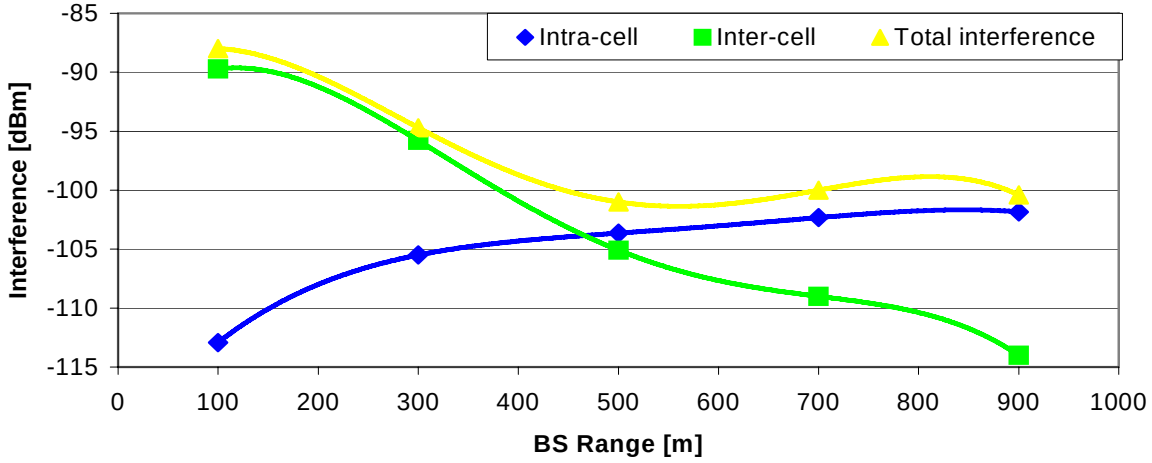

Figure H.9. UL interferences with BS range, in the bridge.

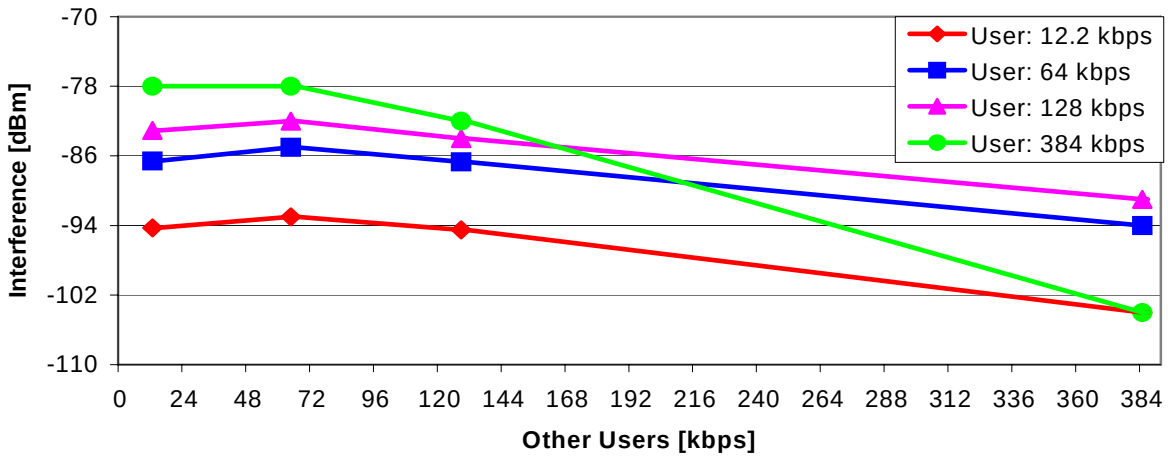

Figure H.10. Total DL interference for different services, in the bridge.

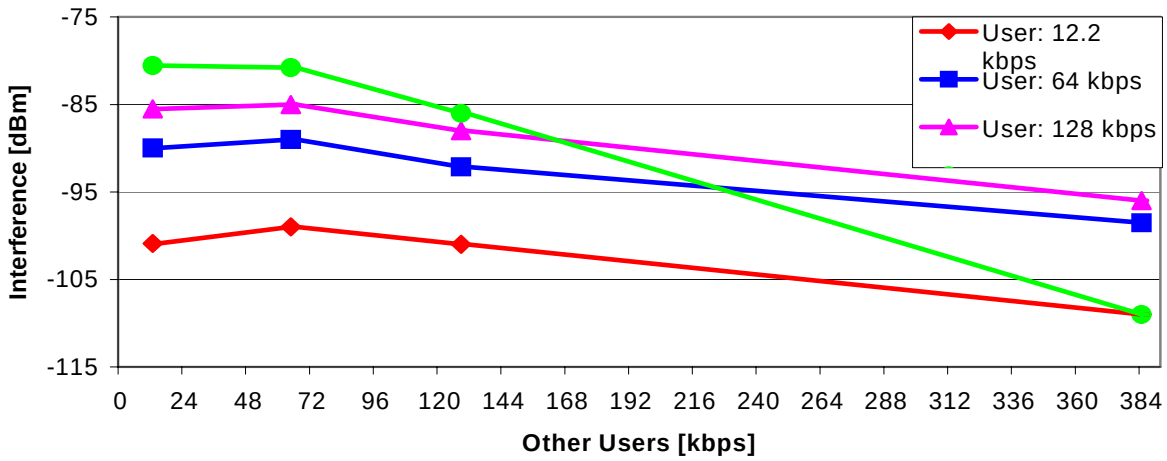

Figure H.11. Total UL interference for different services, in the bridge.

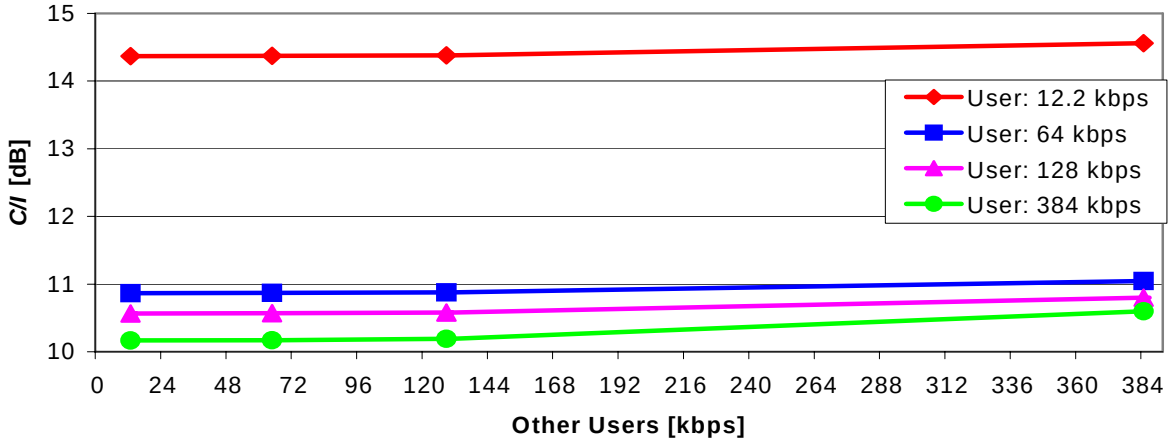

Figure H.12. DL C/I for different services, in the bridge.

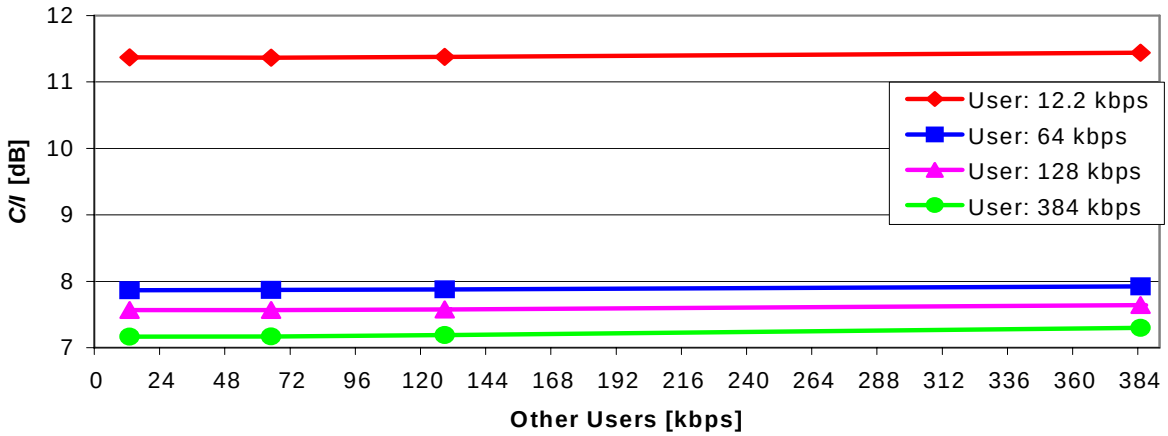

Figure H.13. UL C/I for different services, in the bridge.

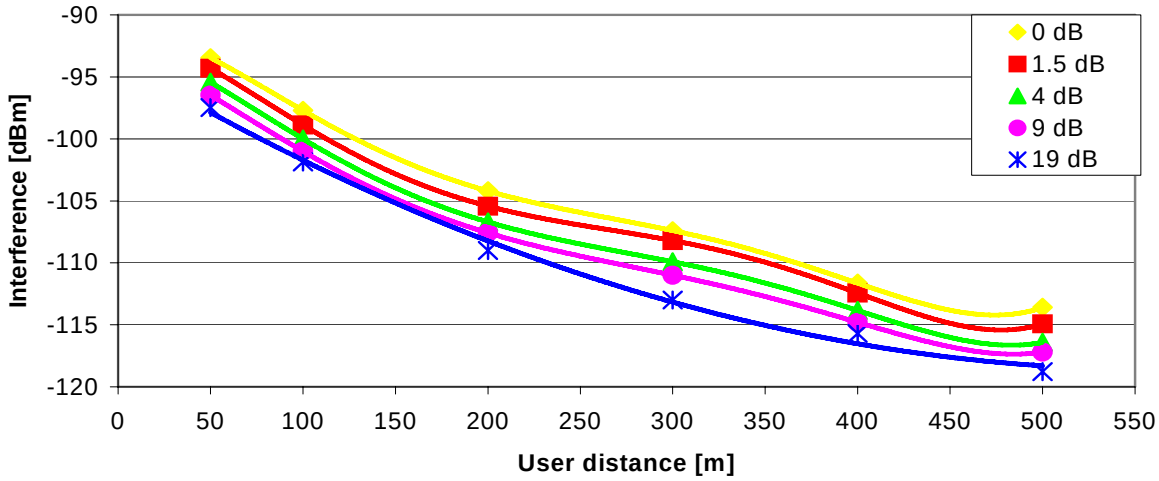

Figure H.14. Total DL interference, with distance, for different *K* parameters.

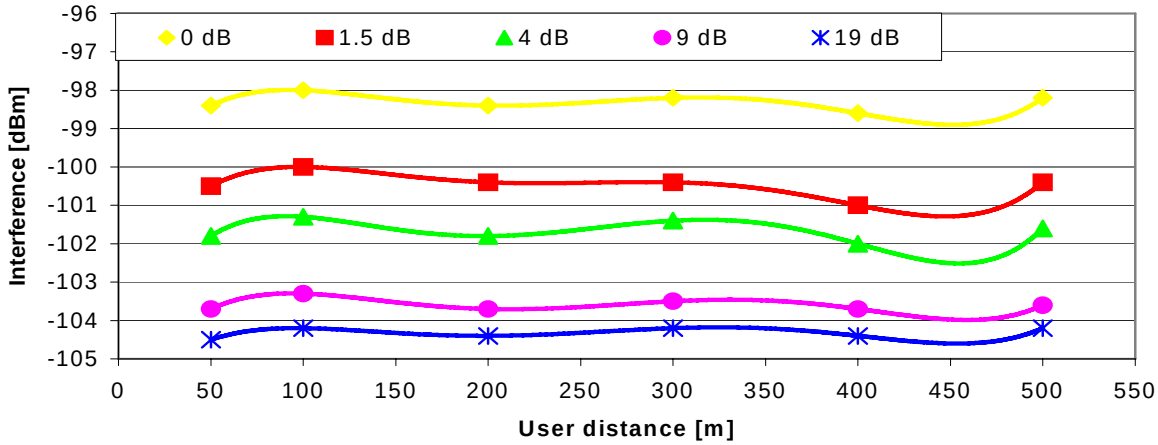

Figure H.15. Total UL interference, with distance, for different *K* parameters.

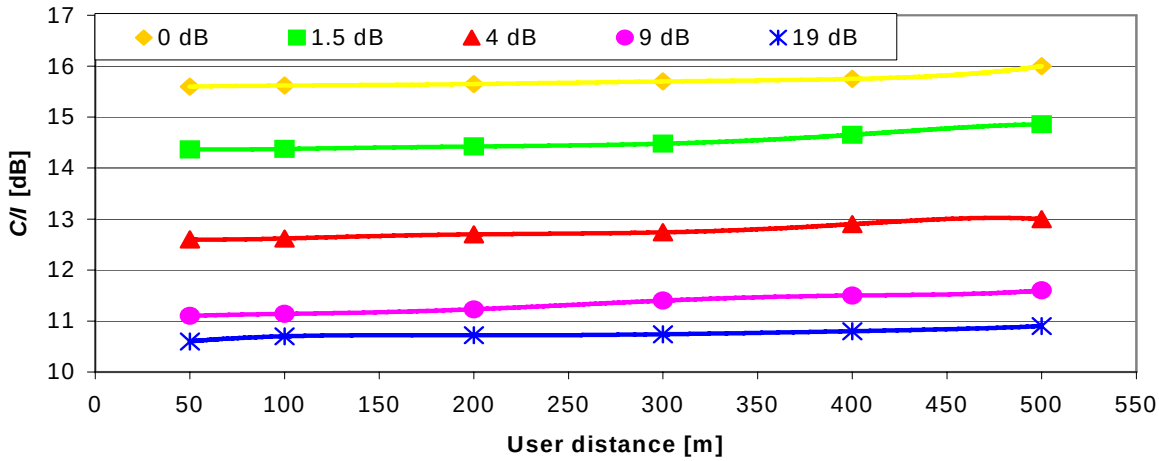

Figure H.16. DL C/I , with distance, for different *K* parameters.

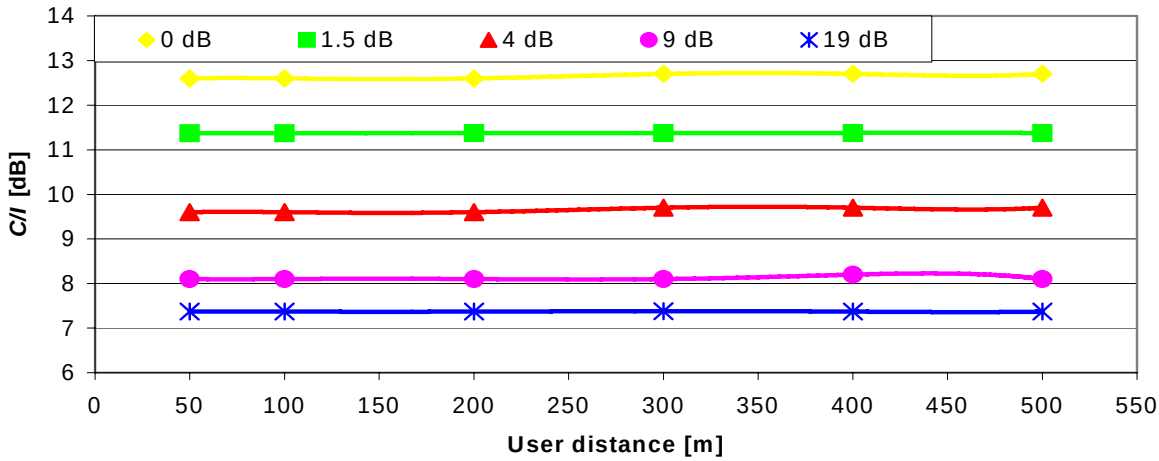

Figure H.17. UL C/I , with distance, for different *K* parameters.

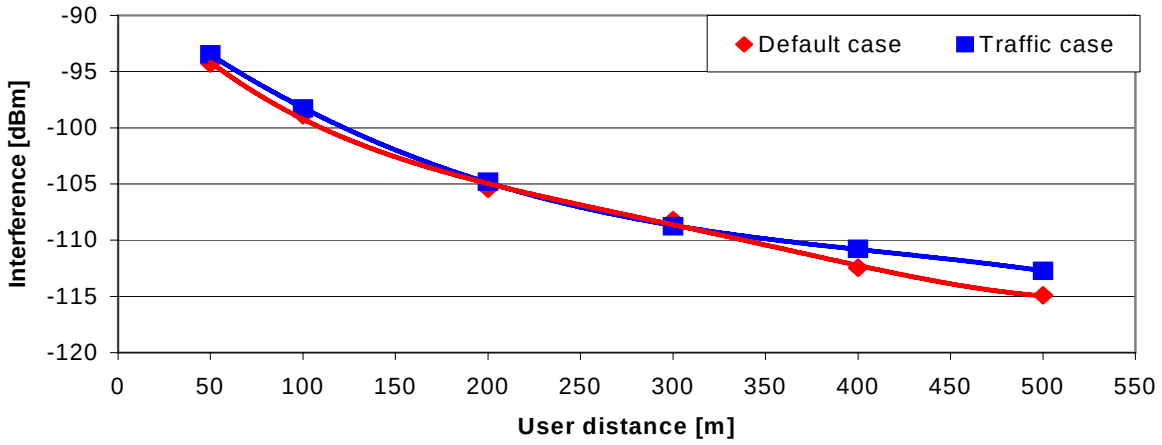

Figure H.18. Total DL interference, with distance, with and without traffic.

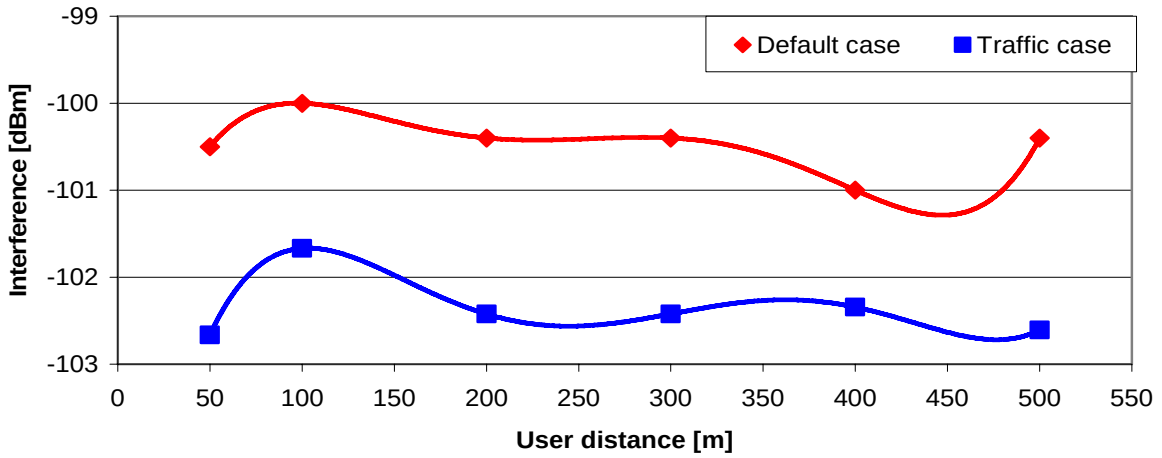

Figure H.19. Total UL interference, with distance, with and without traffic.

Annex I – Additional Results for the Rossio Tunnel Study

This annex presents some additional results obtained for the coverage study performed for the Rossio Tunnel, namely regarding interferences.

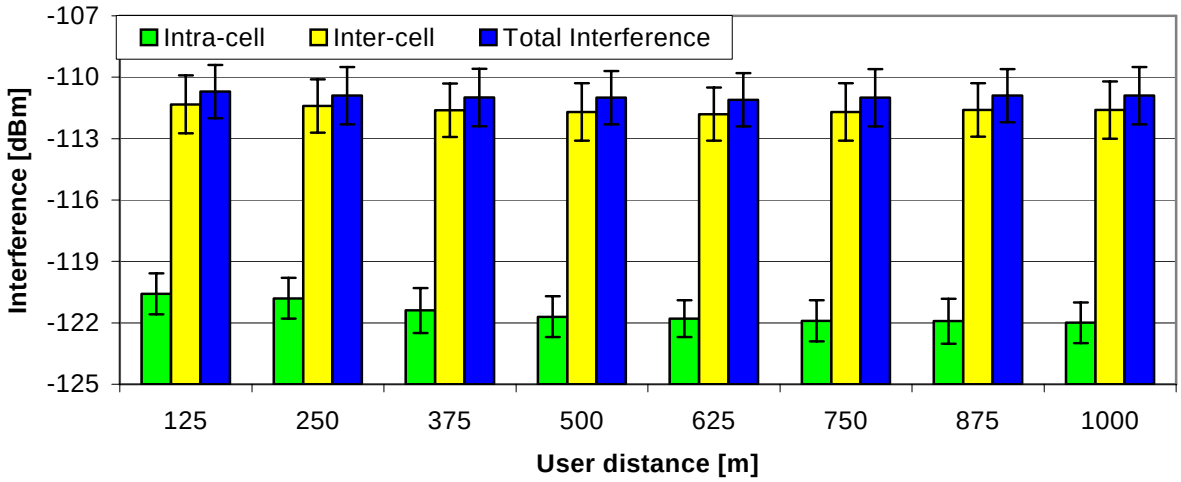

Figure I.1. DL interferences for the Rossio Tunnel, with distance.

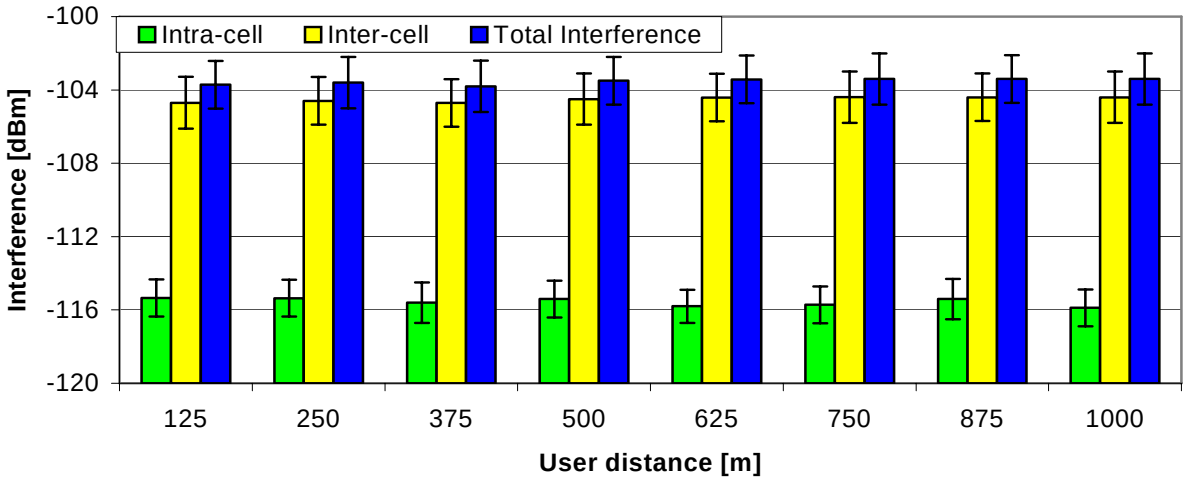

Figure I.2. UL interferences for the Rossio Tunnel, with distance.

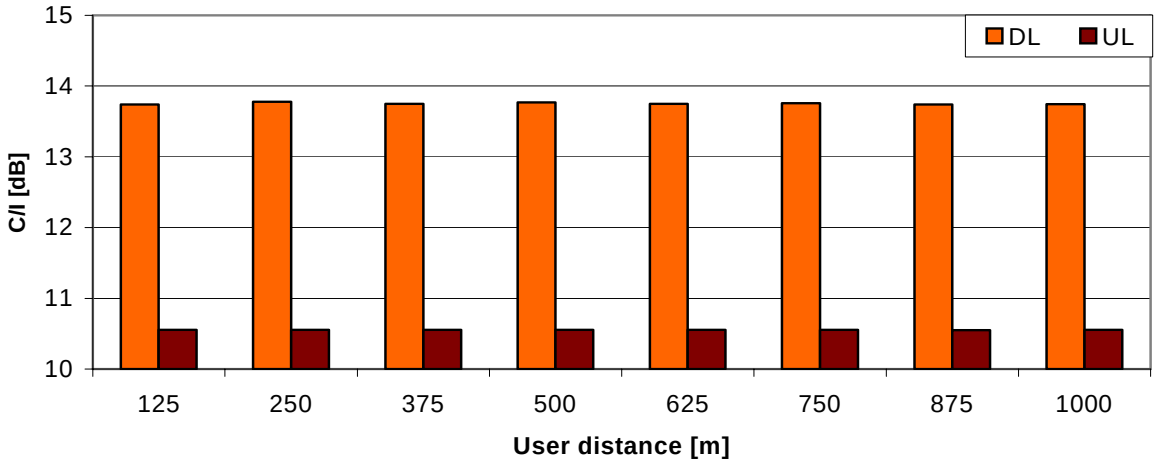

Figure I.3. C/I for the Rossio Tunnel, with distance.

Annex J – Additional Results for the Vasco da Gama Bridge Study

In this annex, the additional information regarding the interferences is presented for the study performed for the Vasco da Gama Bridge.

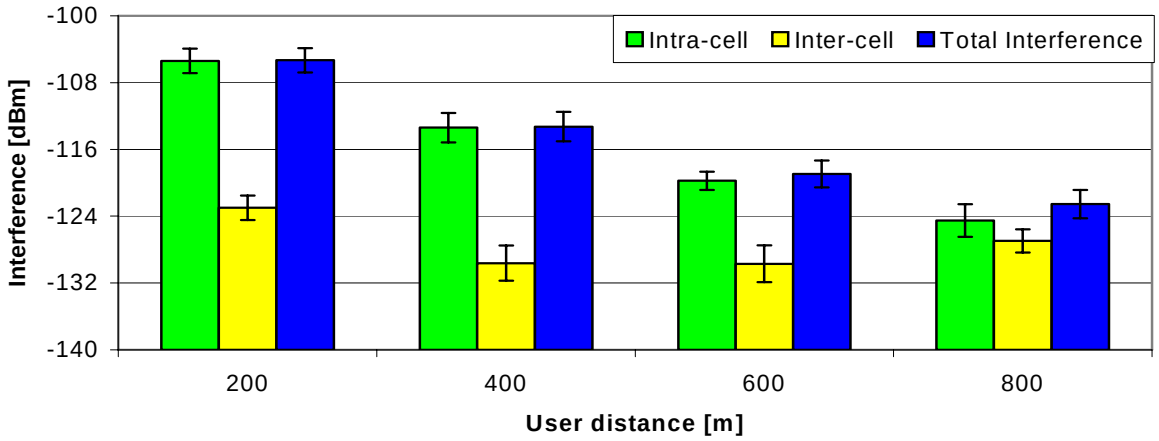

Figure J.1. DL interferences for the Vasco da Gama Bridge, with distance.

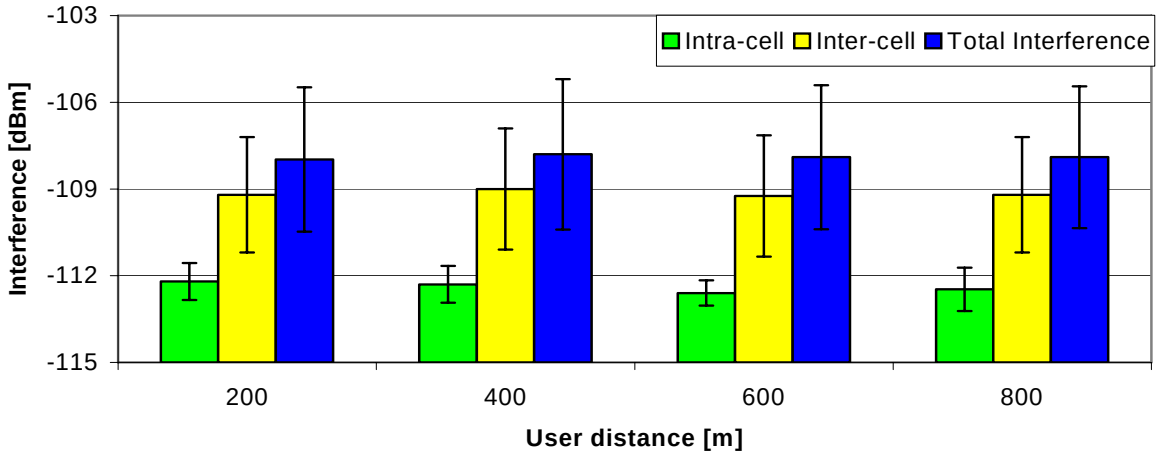

Figure J.2. UL interferences for the Vasco da Gama Bridge, with distance.

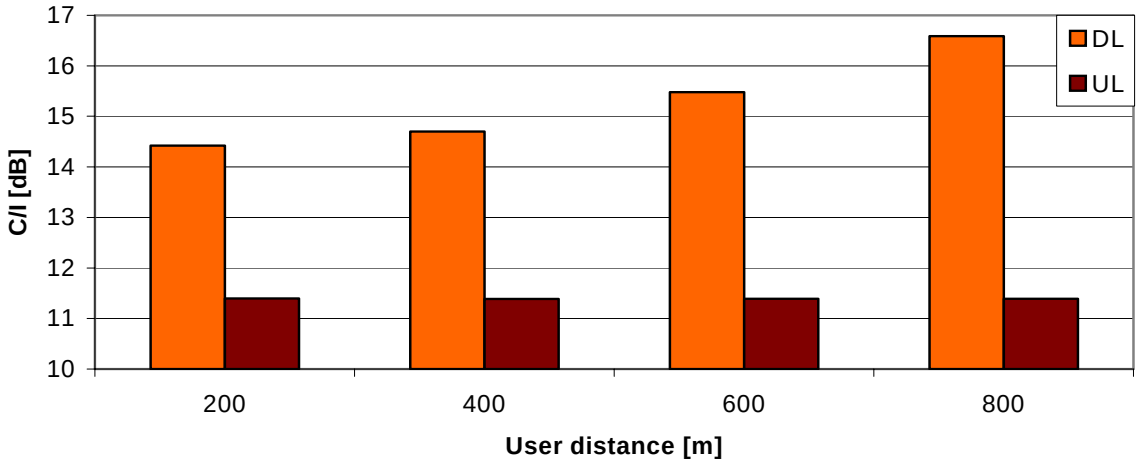

Figure J.3. C/I for the Vasco da Gama Bridge, with distance.

Annex K – Tracks Considered in the Measurements on the Underground

This annex presents, in Fig. K.1, the tracks and the stations of the Lisbon Underground where the measurements are analysed.

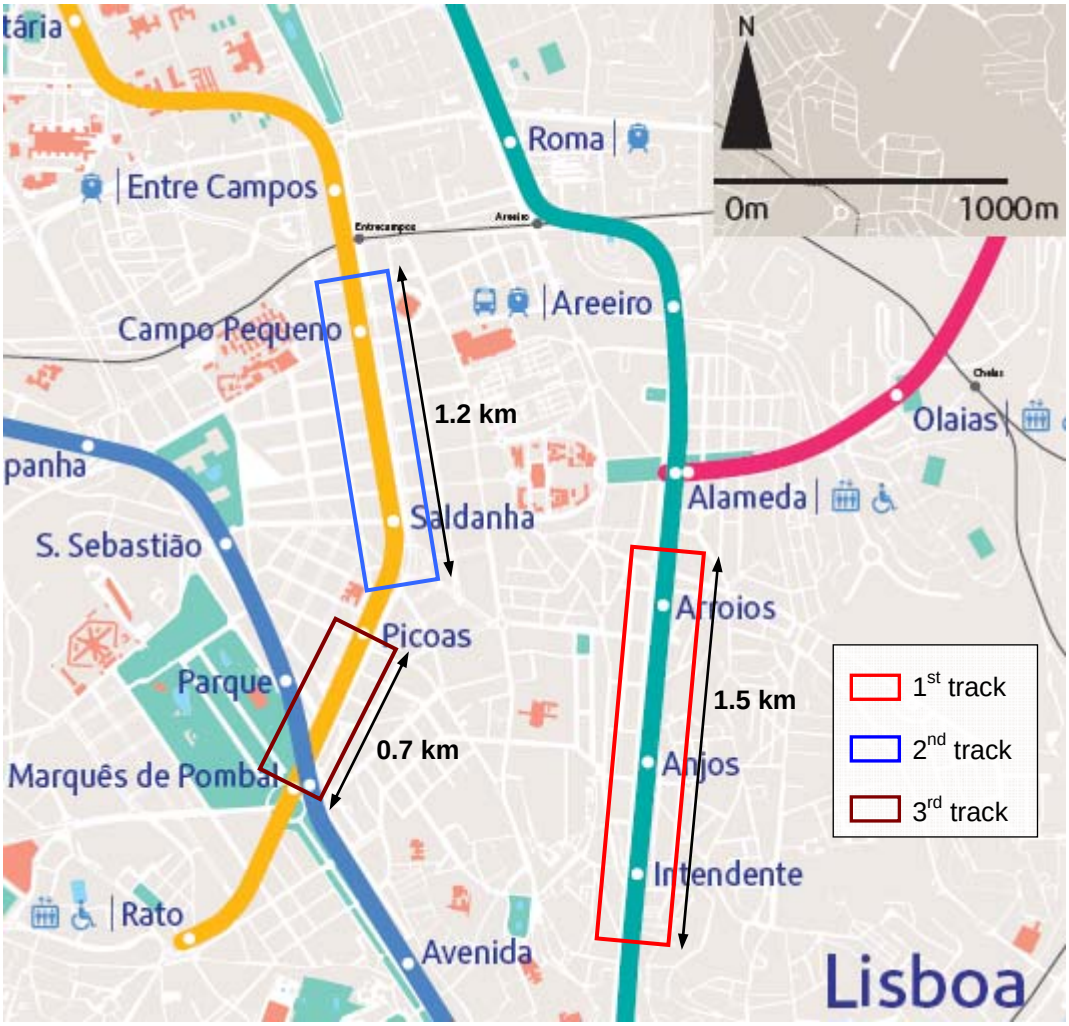

Figure K.1. Representation of the tracks, where the measurements analysis is considered, on the Lisbon Underground (adapted from [Metr08]).

Annex L – Track Considered in the Measurements on the 25 de Abril Bridge

This annex presents, in Fig. L.1, the track in the 25 de Abril Bridge where the measurements were analysed.

Figure L.1. Representation of the track, where the measurements analysis is considered, on the 25 de Abril Bridge (adapted from Google Earth software).

Annex M – Additional Results of the Measurements Performed

This annex presents some additional results, namely the variations of the transmitted and received powers, from the measurements and the simulations performed in the Lisbon Underground.

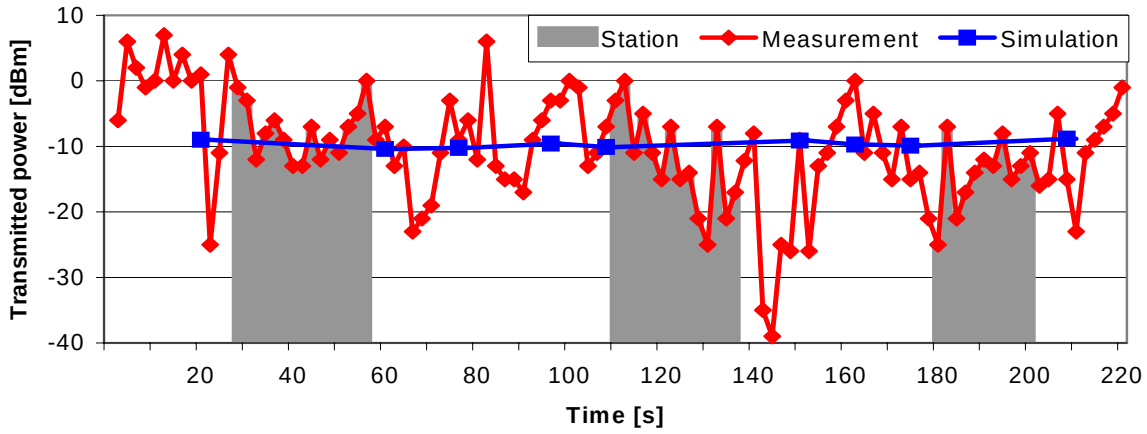

Figure M.1. MT transmitted power variation in time for the track between Intendente and Alameda.

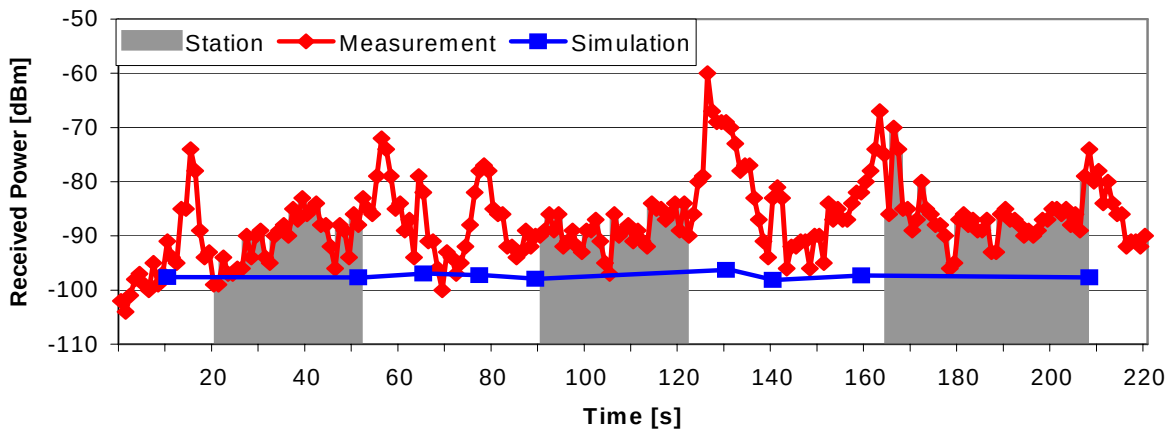

Figure M.2. MT received power variation in time for the track between Intendente and Alameda.

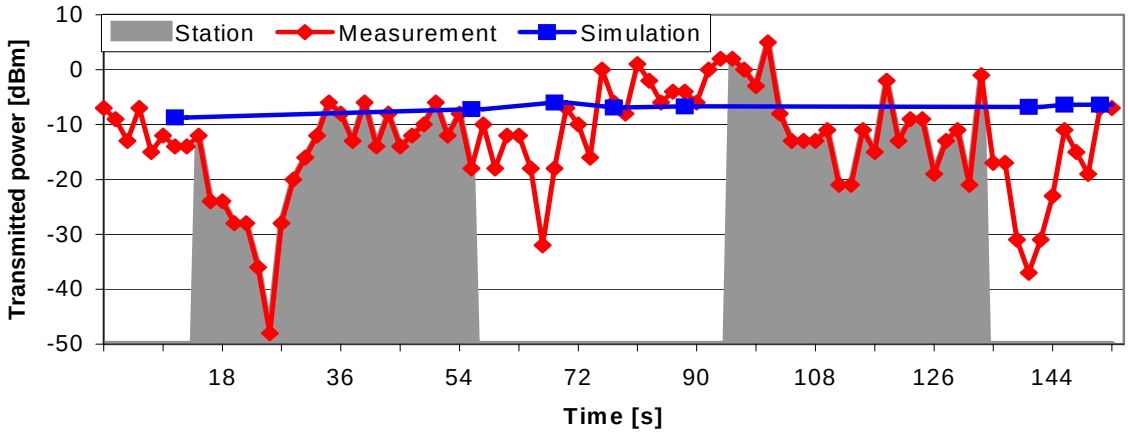

Figure M.3. MT transmitted power variation in time for the track between Campo Pequeno and Saldanha.

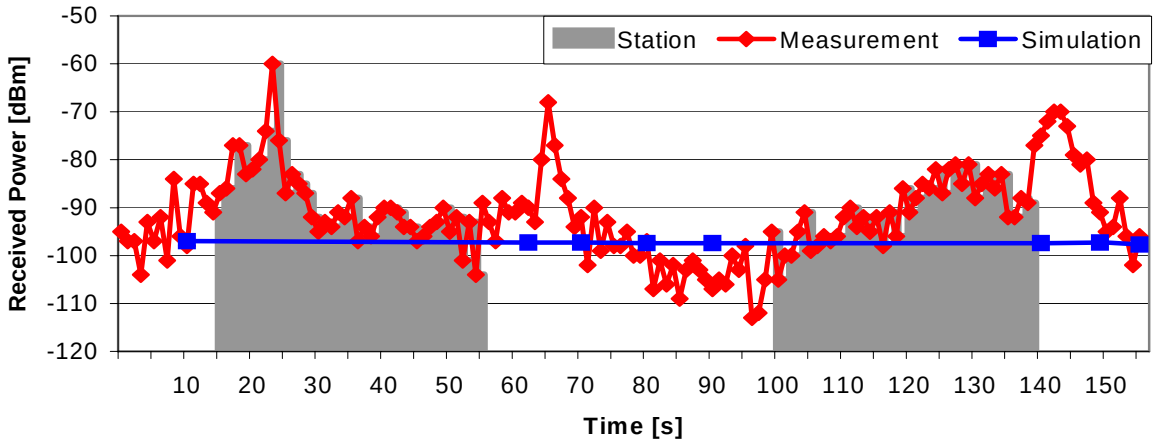

Figure M.4. MT received power variation in time for the track between Campo Pequeno and Saldanha.

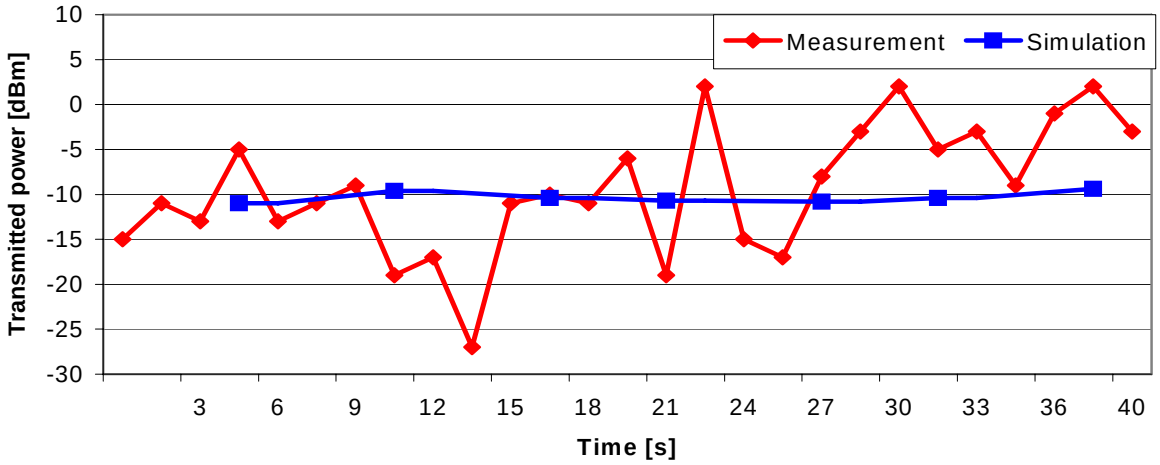

Figure M.5. MT transmitted power variation in time for the track between Picoas and Marquês de Pombal.

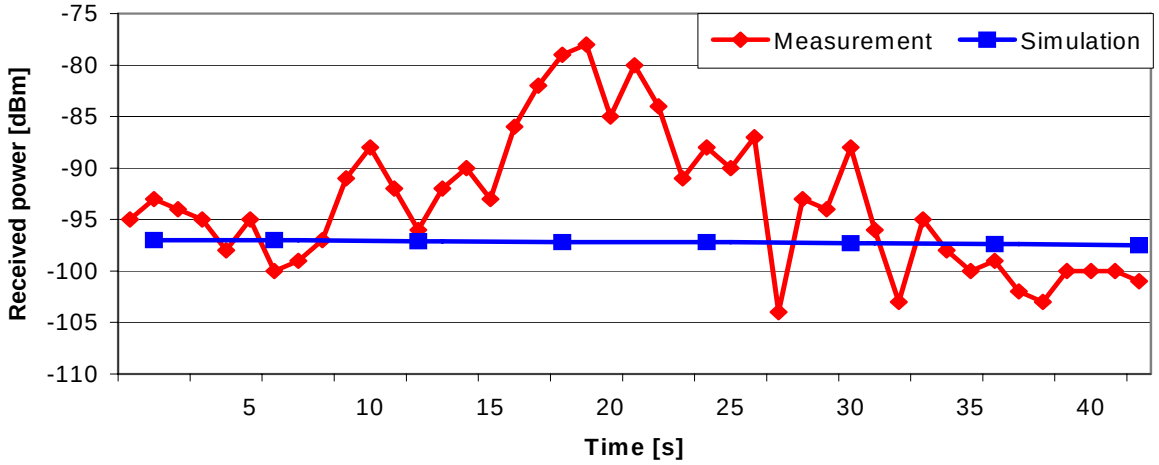

Figure M.6. MT received power variation in time for the track between Picoas and Marquês de Pombal.

References

[3GPP01] 3GPP, Technical Specification Group Services and System Aspects, *Service aspects; Services and Service Capabilities (Release 99)*, Report TS 22.105, V3.10.0, Oct. 2001 (http://www.3gpp.org/).

[Andr08] Andrew Antennas Catalogue, Sep. 2008.

[ANIT08] http://www.anite.com/nemo, June 2008.

[Bala97] Balanis,C.A., *Antenna Theory: Analysis and Design* (2nd Edition), John Wiley & Sons, New York, USA, 1997.

[Bati08] Batista,T., *Capacity Increase in UMTS/HSPA+ Through the Use of MIMO Systems*, M.Sc. Thesis, IST-UTL, Lisbon, Portugal, 2008.

[BrCA07] Briso-Rodriguez,C., Cruz,J.M. and Alonso,J.I., "Measurements and Modeling of Distributed Antenna Systems in Railway Tunnels", *IEEE Transactions on Vehicular Technology*, Vol. 56, No. 5, Sep. 2007, pp. 2870-2879.

[Cast01] Castro,J.P., *The UMTS Network and Radio Access Technology*, John Wiley & Sons, Chichester, UK, 2001.

[Chen03] Chen,Y., *Soft Handover Issues in Radio Resource Management for 3G WCDMA Networks*, Ph. D. Thesis, University of London, London, UK, 2003.

[CODE08] http://www.codegear.com, May 2008.

[Corr07] Correia,L.M., *Mobile Communications Systems Lecture Notes*, Instituto Superior Técnico, Lisbon, Portugal, 2007 (https://fenix.ist.utl.pt/disciplinas/scm-1/2006-2007/2-semestre/pagina-inicial).

[DaCo99] Damosso,E. and Correia,L.M., *Digital Mobile Radio Towards Future Generation Systems (COST 231 Final Report)*, COST Telecom Secretariat, European Comission, Brussels, Belgium, 1999.

[DLMD07] Dudley,D.G., Lienard,M., Mahmoud,S.F. and Degauque,P., "Wireless Propagation in Tunnels", *IEEE Antennas and Propagation Magazine*, Vol. 49, No. 2, Apr. 2007, pp. 11-26.

[Enge08] http://engenhariacivil.wordpress.com/2007/09/16/tunel-do-rossio-parte-i, Aug. 2008.

[EPCC06] Esteves,H., Pereira,M., Correia,L.M., Caseiro, C., *Impact of Intra- and Inter-Cell Interferences on UMTS-FDD*, in *Proc. of EW'2006 – European Wireless Conference*, Paris, France, June 2006. (http://www.ew2007.org/papers/1569014744.pdf).

[Fari99] Farinha,J.S., *Construction Works of the Lisbon Underground – Underground's Notebooks – Notebook n. 5* (in Portuguese), Metropolitano de Lisboa, Portugal, 1999.

[Fern99] Fernandes,M., *The 25 de Abril Bridge – 2nd Phase Construction – Railway Installation* (in Portuguese), REFER, Oct. 1999.

[Gast05] Gast,M., *802.11 Wireless Networks: The Definitive Guide, Second Edition*, O'Reilly Media, California, USA, 2005.

[GSMW08] http://www.gsmworld.com/news/statistics/index.shtml, Aug. 2008.

[HoTo04] Holma,H. and Toskala,A., *WCDMA for UMTS* (3rd Edition), John Wiley & Sons, Chichester, UK, 2004.

[HoTo06] Holma,H. and Toskala,A., *HSDPA/HSUPA for UMTS* (1st Edition), John Wiley & Sons, Chichester, UK, 2006.

[KALN05] Kaaranen,H., Ahtiainen,A., Laitinen,L., Naghian,S., Niemi,V., *UMTS Networks: Architecture, Mobility and Services* (2nd Edition), John Wiley & Sons, Chichester, UK, 2005.

[Kath08] Kathrein Antennas Catalogue, Sep. 2008.

[KiJL03] Kim,Y.,Jung,M.,Lee,B., "Analysis of Radio Wave Propagation Characteristics in Rectangular Road Tunnel at 800 MHz and 2.4 GHz", in *Proc. of APS'2003 – IEEE Antennas and Propagation Society International Symposium*, Columbus, Ohio, USA, June 2003.

[LaWN06] Laiho,J., Wacker,J. and Novosad,T., *Radio Network Planning and Optimisation for UMTS,* John Wiley & Sons, Chichester, UK, 2006.

[Luso08] http://www.lusoponte.pt, Sep. 2008.

[Marq08] Marques,A., *Modelling of Building Height Interference Dependence in UMTS*, M.Sc. Thesis, IST-UTL, Lisbon, Portugal, 2008.

[Metr08] http://www.metrolisboa.pt, Sep. 2008.

[MLND08] Molina-Garcia-Pardo,J.M., Lienard,M., Nasr,A., Degauque,P., "On the Possibility of

Interpreting Field Variations and Polarization in Arched Tunnels Using a Model for Propagation in Rectangular or Circular Tunnels", *IEEE Transactions on Antennas and Propagation*, Vol. 56, No. 4, Apr. 2008, pp.1206-1211.

[Moli05] Molisch,A.F., *Wireless Communications*, John Wiley & Sons, Chichester, UK, 2005.

[NiSB98] Nilsson,M., Slettenmark,J. and Beckman,C., "Wave Propagation in Curved Road Tunnels", in *Proc. of APS'1998 – IEEE Antennas and Propagation Society International Symposium*, Atlanta, Georgia, USA, June 1998.

[Shan02] Shankar,P.M., *Introduction to Wireless Systems*, John Wiley & Sons, New York, USA, 2002.

[Stae05] Staehle,D., "An Analytical Method for Coverage Prediction in the UMTS Radio Network Planning Process", in *Proc. of VTC'2005 – 61st IEEE Vehicular Technology Conference*, Stockholm, Sweden, June 2005.

[TJVM03] Tanghe,E., Joseph,W., Verloock,L and Martens,L., "Evaluation of Vehicle Penetration Loss at Wireless Communication Frequencies", *IEEE Transactions on Vehicular Technology: Accepted for future publication*, 2003.

[UMTS08] http://www.umts-forum.org/index2.php?option=com_content&do_pdf=1&id=2315, Aug. 2008.

[VAGH98] Vainikainen,P., Aikio,P., Gruber,R., Hall,M., Degauque,P., Lienard,M., Berbineau,M., Szelag,M., Mollet,F., Klingler,M., Pirard,W., Deryck,L., Verolleman,Y., "Characteristics of the 2 GHz Radio Propagation Channel in High Speed Train Environment", *ACTS Mobile Communications Summit*, Rhodes, Greece, June 1998 (http://www.ist-mobilesummit.org/acts/sesh1.doc).

[Zhan03] Zhang,Y.P., "Novel Model for Propagation Loss Prediction in Tunnels", *IEEE Transactions on Vehicular Technology*, Vol. 52, No. 5, Sep. 2003, pp. 1308-1314.

[ZhHw98] Zhang,Y.P., Hwang,Y., "Characterization of UHF Radio Propagation Channels in Tunnel Environments for Microcellular and Personal Communications", *IEEE Transactions on Vehicular Technology*, Vol. 47, No. 1, Feb. 1998, pp. 283-296.